

9. SITE 694¹

Shipboard Scientific Party²

HOLE 694A

Date occupied: 9 February 1987, 1650 local time
Date departed: 10 February 1987, 1630 local time
Time on hole: 23 hr, 40 min
Position: 66°50.829'S, 33°26.79'W
Bottom felt (m, drill pipe): 4664.4
Distance between rig floor and sea level (m): 11
Water depth (drill-pipe measurement from sea level, m): 4653.4
Penetration (m): 9.8
Number of cores: 1
Total length of cored section (m): 9.8
Total core recovered (m): 9.85
Core recovery (%): 100
Oldest sediment cored
Depth sub-bottom (m): 9.85
Nature: hemipelagic mud, fine-grained turbidites
Age: lower Pliocene

HOLE 694B

Date occupied: 10 February 1987, 1630 local time
Date departed: 14 February 1987, 1337 local time
Time on hole: 93 hr, 7 min
Position: 66°50.835'S, 33°26.826'W
Bottom felt (m, drill pipe): 4664.4
Distance between rig floor and sea level (m): 11
Water depth (drill-pipe measurement from sea level, m): 4653.4
Penetration (m): 179.2
Number of cores: 24
Total length of cored section (m): 179.2
Total core recovered (m): 67.08
Core recovery (%): 37.4
Oldest sediment cored
Depth sub-bottom (m): 179.2
Nature: diatom-bearing clayey mud, graded silt
Age: late Miocene
Measured velocity (km/s): 1.589

HOLE 694C

Date occupied: 14 February 1987, 1422 local time
Date departed: 18 February 1987, 0900 local time

Time on hole: 90 hr, 38 min
Position: 66°50.820'S, 33°26.763'W
Bottom felt (m, drill pipe): 4664.4
Distance between rig floor and sea level (m): 11
Water depth (drill-pipe measurement from sea level, m): 4653.4
Penetration (m): 391.3
Number of cores: 23
Total length of cored section (m): 212.1
Total core recovered (m): 71.7
Core recovery (%): 33.8
Oldest sediment cored
Depth sub-bottom (m): 212.1
Nature: silt, diatom claystones (cherty at base)
Age: middle middle Miocene
Measured velocity (km/s): 1.717 (sediment), 4.130 (cherty layer)

Preliminary results: Site 694, on the northern part of the Weddell Sea abyssal plain, and remote from continental areas, was occupied from 9 to 18 February 1987. Three holes were drilled: Hole 694A is a single advanced piston corer (APC) core from 0 to 9.8 mbsf; Hole 694B consists of 15 APC, 7 extended core barrel (XCB), and 2 washed cores from 0 to 179.2 mbsf; Hole 694C consists of 1 washed core from 0 to 179.2 mbsf and 22 XCB cores from 179.2 to 391.3 mbsf. The quality of the cores is good only in the uppermost part of the sequence; in other parts it is moderately to highly disturbed.

The sedimentary sequence is mostly terrigenous in origin with a minor biosiliceous component and fluctuating abundance of ice-rafted material throughout. Almost all sediments are interpreted as hemipelagic silts and clays and turbidites. The sequence ranges in age from middle middle Miocene through Quaternary. A paleomagnetic polarity stratigraphy in the topmost 20 m of Hole 694B extends from the Brunhes to lower Gilbert Chrons, but paleomagnetic stratigraphy is difficult to apply lower in the hole. Biostratigraphic ages are based on diatoms and radiolarians and are broadly defined. Four units have been recognized: seafloor to 21.1 mbsf, lower Pliocene to upper Pleistocene clay and clayey mud with minor silt, sand, and diatom-bearing clayey mud interpreted as cyclic fine-grained turbidites and hemipelagic sediments; 21.1 to 111.5 mbsf, lower Pliocene sorted lithic quartz sands, interpreted as sandy turbidites; 111.5 to 304.3 mbsf, upper middle Miocene to lowermost Pliocene varied sediments of hemipelagic and turbiditic origin, including graded silts, with or without diatoms; diatom-bearing silty and clayey muds with interbedded silts and sandy muds; and at the base, a homogeneous gravel-bearing sandy and silty mud of glacial-marine origin; 304.3 to 391.2 mbsf, middle middle Miocene diatom-bearing and diatom claystones and graded silts representing distal turbidites and hemipelagites. The base of this unit is marked by a hard silicified claystone layer that probably caused loss of the XCB. The sequence at Site 694 is similar to the middle and upper part of the section at DSDP Site 323, Leg 35, in the Bellingshausen Basin, west of the Antarctic Peninsula.

Ice-rafted debris exhibiting a wide size range was found discontinuously throughout the sequence in varying abundances, suggesting changes in the intensity of Antarctic glaciation from the middle Miocene. Dominance of sedimentary rocks in the lithic material of the turbidites and the glacial material at Site 694 suggests that the principal source area is the Antarctic Peninsula and the present-day region of the Filchner-Ronne ice shelf, rather than East Antarctica. Hence the site provides insights about the development of glaciation

¹ Barker, P.B., Kennett, J.P., et al., 1988. *Proc. Init. Repts. (Pt. A), ODP*, 113, College Station, TX (Ocean Drilling Program).

² Shipboard Scientific Party as given in the list of Participants preceding the contents.

on West Antarctica. Several observations on the sediments, neritic diatoms, and clay mineralogy suggest the development of major West Antarctic glaciation and ice-sheet formation during the late Miocene to early Pliocene. The sedimentary sequence suggests instability of this ice-sheet during the late Miocene. The most rapid deposition of turbidites (~180 m/m.y. or greater) probably occurred within an interval of only 0.5 m.y. or less during early Gilbert Chron (C3R4), before 4.8 Ma. This rapid turbidite deposition occurred during an interval marked elsewhere by major climatic cooling, increased and highly variable $\delta^{18}\text{O}$ values in foraminifer tests, and low sea level. High rates of turbidite sedimentation in this interval probably resulted from an expanding, yet unstable, West Antarctic ice-sheet. From 4.8 Ma (earliest Pliocene) to the present day, turbidite deposition virtually ceased at Site 694, indicating that the West Antarctic ice-sheet has been a permanent and stable feature since earliest Pliocene times.

BACKGROUND AND OBJECTIVES

Site 694 is located on the northern part of the abyssal plain of the Weddell Basin (Fig. 1) in 4653 m of water. The site is about 900 km north of East Antarctica and about 900 km east of the Antarctic Peninsula. This site is the deepest of 7 sites that form a depth transect in the Weddell Sea region for studies of the vertical water-mass stratification, sediment history, and bottom-water evolution during the Late Phanerozoic around the Antarctic.

A multichannel seismic reflection profile (Fig. 2A, B) indicates the presence of a relatively thick (~1-s two-way traveltime [tw]) sequence of moderately reflective, parallel-layered sediments considered to represent a sequence of interbedded hemipelagic sediments and fine-grained turbidites. A distinct seismic reflection horizon occurring at 0.45 s twt on the multichannel seismic reflection profiles may represent an unconformity and/or a change in the character of the terrigenous sediments.

Because of considerable depth of deposition at Site 694, well below the carbonate compensation depth (CCD) and in an area of relatively low siliceous biogenic productivity, as shown by the drilling at similar latitudes on Maud Rise, the sequence was expected to be almost exclusively terrigenous, with only a minor biogenic component. Site 694 is the only basin site; the others are located either on the continental margins or on Maud Rise. With these factors in mind, there were several major objectives at Site 694.

First, the sequence of fine-grained turbidites should provide a record of continental erosion during the glacial and preglacial climatic regimes of Antarctica. The dating of different sediment packages in the sequence and estimates of changing sedimentation rates should provide important information about the history of climatic change on the continent. Redeposited sediments of preglacial age derived from Antarctica may also contain spores and pollens providing a record of vegetation and climatic change on the continent.

Second, the sequence may provide data related to the history of bottom-water production in the Weddell Sea. Since Site 694 is located within Antarctic Bottom Water (AABW) and relatively close to the source of present-day production of Weddell Sea Bottom Water, past intervals of intensified bottom-water activity may have decreased sedimentation rates or formed hiatuses at Site 694 that could be detected in the stratigraphic record. The importance of AABW is global, but its history is only indirectly known and inferred from the dating of hiatuses in the ocean basins and the interpretation of oxygen isotopic stratigraphy in much shallower waters. Are the widespread hiatuses known from wide areas of the global oceanic basins (Kennett et al., 1972; Rona, 1973; Davies et al., 1975; Barron and Keller, 1982) also represented as intervals of reduced sedimentation rates or hiatuses at Site 694? Do intervals of higher rates of sedimentation at Site 694 coincide with intervals represented by hiatuses

at Site 693 located on the East Antarctic continental margin? Knowledge of the stratigraphic sequence at Site 694 should assist with the interpretations of the record at the other sites.

Rough basement topography beneath the turbidite sequence in the region of Site 694 is caused by abundant small offset fracture zones and slow spreading. The Weddell Basin was formed on the southern flank of the South American-Antarctic spreading center. The basin floor becomes younger northward, and the gross magnetic anomaly orientation is east-west. Spreading was originally north-south, but during the Late Cretaceous and Cenozoic rotated through northwest-southeast to its present east-west orientation. This rotation created the fracture zones and the rough basement topography. Site 694 was chosen to be located on ocean floor no younger than about 50 m.y. so that the presumed onset of AABW near the Eocene/Oligocene boundary could be examined.

Sediments in the Weddell Sea thicken southward and probably also to the west toward the continental areas which may be the source areas of the sediment. Piston cores recovered near Site 694 consist of interbedded turbidites and hemipelagic clays containing a relatively rare ice-rafted component. Microfossils are rare to absent. One of the problems expected at Site 694 was to establish an adequate stratigraphic framework, a traditional problem in the studies of deep-water turbiditic sequences that normally contain only rare microfossils. The interpretation of the magnetostratigraphic record may well be complicated by poor recovery and the presence of hiatuses. Nevertheless, at least a gross stratigraphy was expected to be established based upon rare microfossils contained within the hemipelagic material or occurring as reworked forms within the turbidites.

The drilling plans for Site 694 were to use the advanced hydraulic piston corer (APC) to refusal, followed by continuous coring using the extended core barrel (XCB) through as much of the remaining sequence as possible to the lower Cenozoic and, if time allowed, to the Cretaceous. Rotary drilling would be used if the deeper objectives were not obtained using the XCB. Drilling was not planned to extend to basement, because the prime targets were sedimentary and the oldest objective was some 20 to 30 m.y. younger than basement age. The site was to be logged.

OPERATIONS

Site 694 is about 800 km northwest of Site 693. As the ship steamed toward the next location, a phenomenon not seen recently was observed: "night." Near 68°S, 24°W we observed dozens of bergy bits and hundreds of growlers floating in a silent, gray sea. The beacon was dropped at 66°51'S, 33°27'W at 1650 on 9 February. Thrusters were lowered and station-keeping established. The pipe was started in the hole with the modified APC/XCB bit.

The bottom-hole assembly (BHA) consisted of the bit, long bit sub, seal bore drill collar, landing saver sub, long top sub, head sub, seven 8 1/4-in. drill collars, changeover sub (XO), a 7 1/4-in. drill collar, XO, and two stands of 5 1/2-in. drill pipe and XO. The ship was unable to move immediately to the location because of an iceberg of estimated 350,000 tons less than 1 km from the site. This iceberg was towed away by the *Maersk Master*. Another iceberg of 2 million tons also was threatening and also was removed. There were 15 icebergs in the 22-km radar range, 3 or 4 of which represented potential problems.

Hole 694A

The precision depth recorder (PDR) water depth at Site 694 is 4671.3 m and the first APC was shot 5 m above the seafloor (Table 1). Unfortunately, the now-familiar full core with no mud line was obtained.

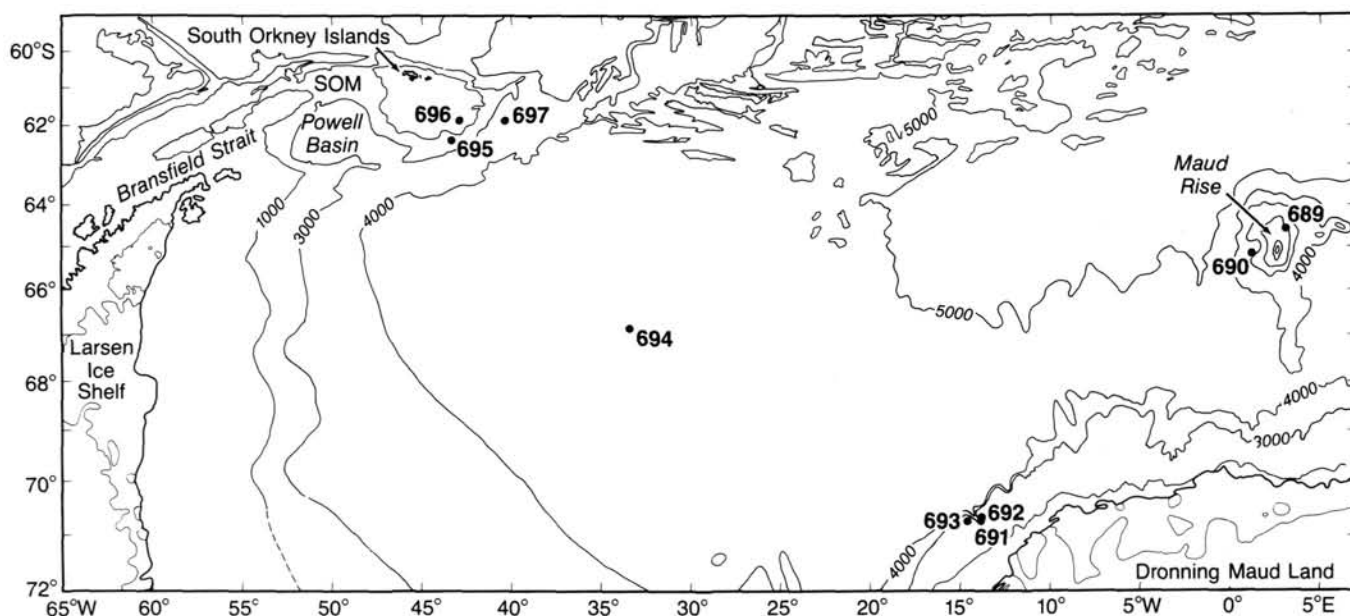


Figure 1. Location of Site 694 in the Northern Weddell Sea. SOM = South Orkney microcontinent.

Hole 694B

The bit was raised 7 m and the first core found the mud line at 4664.4 m (Table 1). APC coring continued but with poor recovery. The material being cored was mostly sand and little penetration was possible. The bit was advanced by the amount cored and overall progress was slow. The ice-management system was severely tested between 10 and 13 February. Another iceberg (#168) was routinely towed on the morning of the 11th, and there were 16 icebergs within 37 km and many growlers which had to be prop-washed. The tow of #168 was followed by a 9-hr tow of another (#165) of 2 million metric tons. While this was under tow, another iceberg (#162) that was 231 m × 163 m × 45 m in visible size and 6 million tons turned suddenly toward the ship at a distance of 5.9 km. Emergency ice-avoidance procedures were begun, the first being to suspend wireline operations and the second to pull the drill pipe to 21 m below the seafloor. The *Maersk Master* took #162 under tow when it had approached to within 4.2 km of the ship. She pulled at 95 tons, at 90° to the drift path, and at only 2.2 km from the *JOIDES Resolution* the iceberg began to divert. When it had become obvious that the iceberg would pass at a safe distance from the ship, the drill pipe was run back into the mud-filled hole.

At 0900 (local time) with the drill pipe only 18 m above the bottom of the hole, a failure occurred in the Automatic Station Keeping system (ASK). The ship drifted to a 5° offset, at which point the dynamic positioning operator gained manual control. Fortunately, the signal from the beacon was received and the drill pipe was once again pulled to just below the seafloor in case the system suffered a total failure. The fault was traced to a portion of the ASK system not actively used and repairs were complete in 2 hr. In the meantime, the *Maersk Master* was attempting to tow a small (25,000 ton) iceberg (#173) which was low, round, and smooth. The rope slipped off the iceberg four times. Finally, as a last resort, it was prop-washed. Although it was not believed possible to move such an iceberg by prop-washing, it was a complete success. Iceberg #162, which was believed to be safely behind the ship, made a 180° turn and had to be towed again for another 4 hr. Then #173 returned and had to be washed a second time. Meanwhile the bit was reamed back to the bottom in a mudless hole, since there had been insufficient time to spot it full of mud when the ASK system had failed.

Then iceberg #163 appeared. It was 328 m × 240 m × 40 m and estimated to be 12.6 million tons (about 1.6 times larger than Kyle Stadium, College Station, Texas). While it had been approaching the site it was considered untowable because of its size, but when it became obvious that it would drive the *JOIDES Resolution* from the site, it was decided to try. Forty barrels of mud were spotted in the hole and the bit was again pulled to just below the mud line.

The *Maersk Master* rigged a combination of rope with steel towing cable to provide sufficient length for a safe tow. By this time, the iceberg was only 1.1 km from the bow of the *JOIDES Resolution*. The *Maersk Master* took a 90-ton bind on the iceberg just as it had reached 0.7 km, the termination distance at which the ship would have to move off the site. For an hour, there was no discernible motion of either the *Maersk Master* or the iceberg. Slowly the colossus began to move away, and after 20.5 hr it was 3.7 km from the ship and our operation was safe. Was this the biggest object ever moved by man? Perhaps. The question is, was it actually moved? The iceberg made a 135° turn as the towing force was applied, but all the others in the area made a similar turn as the tide changed. A careful examination of the plots of icebergs in the area suggests that the path of #163 was at least influenced by the tow.

On 13 February, iceberg #163 was a safe distance from the site and the drill pipe was started back into the hole. It was necessary to wash Core 113-694B-20W from 4679 to 4805 mbsl. Coring resumed at 0000 hr on 14 February after having lost 24.25 hr in waiting for iceberg #163. Cores 113-694B-21X to 113-694B-25X were cut to 4853 mbsl where the spring stop of the latch assembly in the XCB parted. The lower portion of the XCB remained in the hole and the hole was abandoned.

Hole 694C

The ship was moved 30 m north and Hole 694C was spudded at 1422 hours, 14 February (Table 1). The first core, 113-694C-1W was a wash core from the seabed to 4843.7 mbsl or 179.2 mbsf, equal to the total depth of the Hole 694B. Hole 694C was drilled with the XCB from 4843.7 to 5055.8 mbsl or 179.2–391.3 mbsf. The formation apparently contained a large amount of sand, and core recovery was not high. At 5055.8 mbsl the inner core barrel became stuck in the outer barrel. Two wireline runs

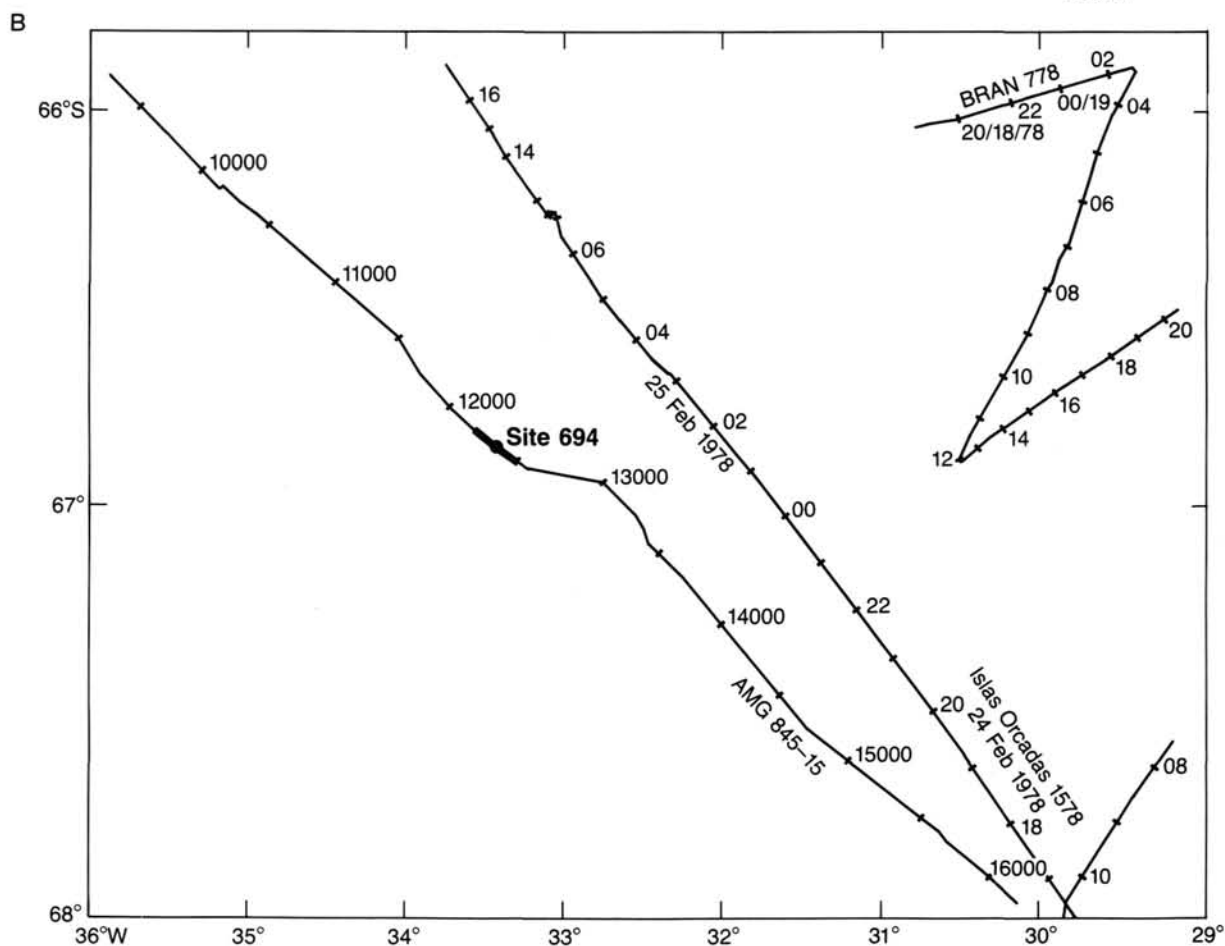
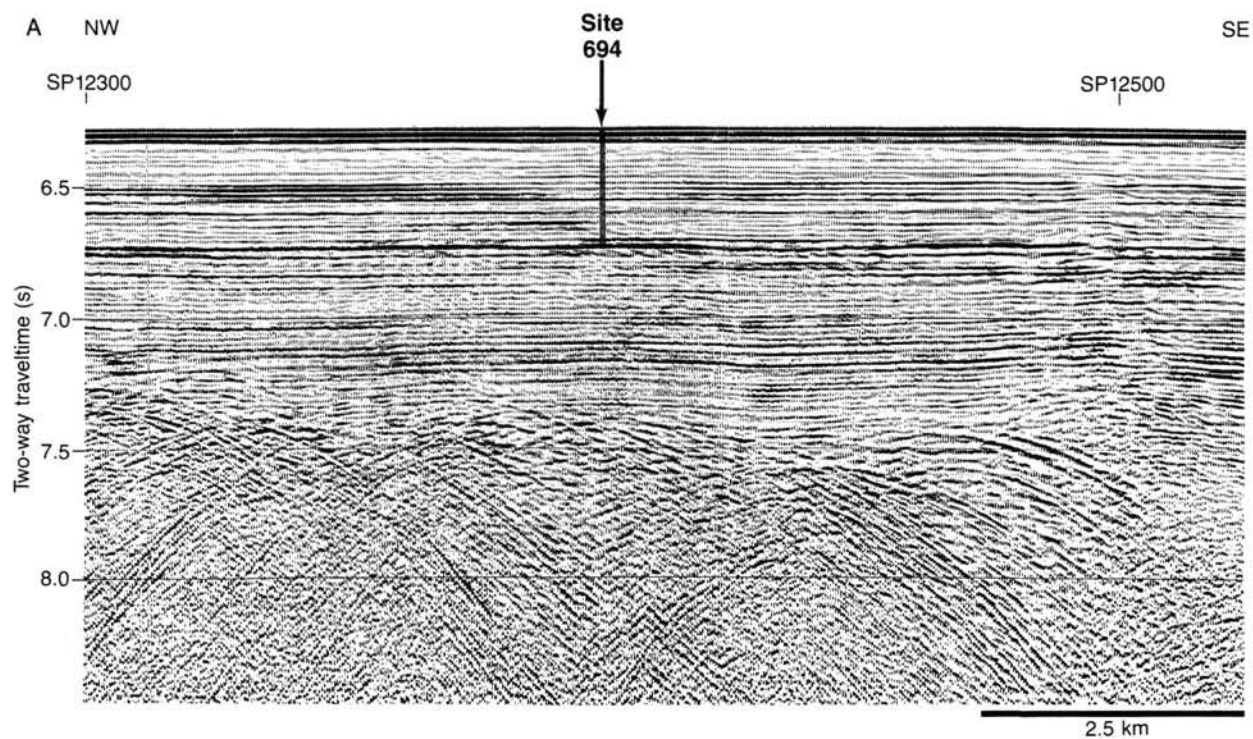


Figure 2. A. British Antarctic Survey/Birmingham University multichannel seismic reflection profile, AMG845-15, showing approximate location of Site 694 in the northern Weddell Basin, at SP 12400. B. Track chart of line AMG845-15 showing location of Site 694.

Table 1. Coring summary, Site 694.

Core no.	Date (Feb. 1987)	Time (local)	Depth (mbsf)	Cored (m)	Recovered (m)	Recovery (%)
Hole 694A						
1H	10	1645	0.0-9.8	9.8	9.85	100.0
				9.8	9.85	
Hole 694B						
1H	10	1815	0.0-5.5	5.5	5.58	101.0
2H	10	2000	5.5-15.1	9.6	9.71	101.0
3H	10	2145	15.1-24.7	9.6	9.32	97.1
4X	11	0145	24.7-34.3	9.6	2.53	26.3
5X	11	0415	34.3-44.0	9.7	2.00	20.6
6H	11	0600	44.0-53.6	9.6	4.21	43.8
7H	11	0830	53.6-63.1	9.5	0.00	0.0
8X	11	1145	63.1-72.8	9.7	0.00	0.0
9H	11	1400	72.8-82.5	9.7	0.65	6.7
10H	11	1530	82.5-92.2	9.7	2.45	25.2
11H	11	1715	92.2-101.9	9.7	0.36	3.7
12H	11	1830	101.9-107.4	5.5	0.10	1.8
13H	11	2015	107.4-111.5	4.1	1.50	36.6
14H	11	2145	111.5-121.2	9.7	2.32	23.9
15H	11	2300	121.2-122.5	1.3	1.28	98.4
16W	12	1915	0.0-122.5	N.A.	N.A.	0.1
17H	12	2100	122.5-130.9	8.4	0.10	1.2
18H	12	2215	130.9-135.9	5.0	4.50	90.0
19H	12	2330	135.9-136.9	1.0	0.32	32.0
20W	13	2345	12.5-140.8	N.A.	N.A.	1.5
21X	14	0230	140.8-150.4	9.6	0.00	0.0
22X	14	0500	150.4-160.0	9.6	3.40	35.4
23X	14	0730	160.0-169.6	9.6	8.70	90.6
24X	14	0930	169.6-179.2	9.6	6.00	62.5
				175.3	65.03	
Hole 694C						
1W	14	1915	0.0-179.2	N.A.	N.A.	0.7
2X	14	2100	179.2-188.9	9.7	3.01	31.0
3X	14	2245	188.9-198.6	9.7	9.39	96.8
4X	15	0115	198.6-208.3	9.7	0.89	9.2
5X	15	0315	208.3-217.9	9.0	3.26	36.2
6X	15	0545	217.9-227.6	9.7	7.57	78.0
7X	15	0815	227.6-236.9	9.3	1.35	14.5
8X	15	1100	236.9-246.5	9.6	2.03	21.1
9X	15	1515	246.5-256.1	9.6	1.14	11.9
10X	15	1730	256.1-265.5	9.4	2.75	29.2
11X	15	1930	265.5-275.5	10.0	3.06	30.6
12X	15	2130	275.5-285.1	9.6	2.34	24.4
13X	15	2315	285.1-294.7	9.6	2.08	21.6
14X	16	0130	294.7-304.3	9.6	9.74	101.0
15X	16	0400	304.3-314.0	9.7	2.64	27.2
16X	16	0630	314.0-323.6	9.6	0.00	0.0
17X	16	0900	323.6-333.3	9.7	0.60	6.2
18X	16	1145	333.3-343.0	9.7	0.90	9.3
19X	16	1445	343.0-352.6	9.6	4.74	49.4
20X	16	1800	352.6-362.3	9.7	2.54	26.2
21X	16	2030	362.3-372.0	9.7	1.70	17.5
22X	16	2315	372.0-381.6	9.6	7.00	72.9
23X	18	0815	381.6-391.3	9.7	3.00	30.9
				211.5	71.73	

iceberg had reached 3.7 km, the first of three wireline runs were made in an attempt to pull the stuck inner barrel. All failed to dislodge the barrel. The hole was abandoned and the drill pipe was pulled. When the BHA reached the surface it was found that the box on the XCB cutter shoe had flared to such a diameter that it could not be pulled through the outer barrel.

The thrusters and hydrophones were raised, and the voyage to Site 695 (W7) was begun on 18 February at 0900.

LITHOSTRATIGRAPHY

Introduction

Three holes were drilled at Site 694 and a total of 150 m of sediment recovered (Fig. 3). The sediments are predominantly terrigenous in origin, with a small siliceous biogenic component increasing downward, and range from middle Miocene to upper Pleistocene (Brunhes). They have been divided into four lithostratigraphic units using data from visual core descriptions and smear slides. Grain size, inferred sedimentary processes, diatom content, and degree of lithification are used to distinguish Units I-IV and five subunits within Unit III (Table 2 and Fig. 3).

Because of low recovery and variable drilling disturbance, the boundaries between units and subunits generally occur between cores. Only two boundaries (I/II and IIID/IIIE) occur within a core. One may only speculate to what extent core recovery was selective (i.e., whether we missed mainly sand or mainly mud or both), particularly in the absence of logs for this site. Sands may have been artificially graded during drilling, and sands and muds may have been stirred together in a core. Where the sediment is firm enough to form drilling biscuits, these may have been reoriented within the liner. These limitations should be borne in mind while reading the following account.

Unit I (Depth 0-21.1 mbsf; Age lower Pliocene to upper Pleistocene)

Core 113-694A-1H; depth 0.0-9.8 mbsf; thickness 9.8 m; Pliocene to Pleistocene.

Cores 113-694B-1H to 113-694B-3H-5; depth 0.0-21.1 mbsf; thickness 21.1 m; lower Pliocene to upper Pleistocene.

Unit I was recovered in Holes 694A and 694B, and data from both holes have been combined to give the vertical sequence in Figure 4. The unit consists predominantly of clay and clayey mud which shows minor to strong bioturbation, with silt, sand, and diatom-bearing clayey mud as minor lithologies.

Clay and clayey mud with graded silt laminae were recovered in Cores 113-694A-1H and 113-694B-1H and Sections 113-694B-2H-1 through 113-694B-2H-4. A typical vertical sequence is shown in Figure 5. Grayish brown (2.5Y 5/2) or light olive brown (2.5Y 5/4) silt grades up into slightly burrowed clayey mud and the intensity of bioturbation increases upward. Colors in the moderately to strongly bioturbated mud are dark grayish brown (10YR 4/2) inside the burrows and more grayish (2.5Y 5/2, 4/2) outside; the lower part of Core 113-694B-1H is mainly olive gray (5Y 5/2). Silt laminae occur singly and in groups. Minor bioturbation continues through some of the laminae.

Sections 113-694B-2H-5 through 113-694B-2H, CC, and Core 113-694B-3H contain a higher proportion of thick graded silts and sands (Fig. 4). These beds are light yellowish brown (2.5Y 6/3) to olive brown (2.5Y 4/4) and the interbedded muds, which are siltier than those at the top of the unit, are pale olive (5Y 6/3) to olive gray (5Y 5/2). The lower part of Unit I is observed to be less bioturbated than the upper part, though this may be a result of fainter color contrasts. Parallel lamination is present in most of the silt and sand beds.

Diatom-bearing clayey mud occurs as burrowed layers 1-30 cm thick in Sections 113-694A-2H-5 through 113-694B-2H-7.

were made in an attempt to free it. While pulling out of the hole with the wire on the second trip, the motor on the wireline winch began to fail. The wire was recovered and the problem was traced to an intermittent failure of a switch. While the electrician was working on the winch motor at 0830, 17 February, iceberg #183 entered the danger zone. It was identified as the former #163 which is the candidate for the largest object ever moved by man. The hole was loaded with 100 bbl of mud and for the third time the drill pipe was pulled to just below the seafloor. The *Maersk Master* took #163 under tow at a distance of 1.7 km and almost immediately it began to move without a fight. It was moved away to 3.7 km and released. As soon as the

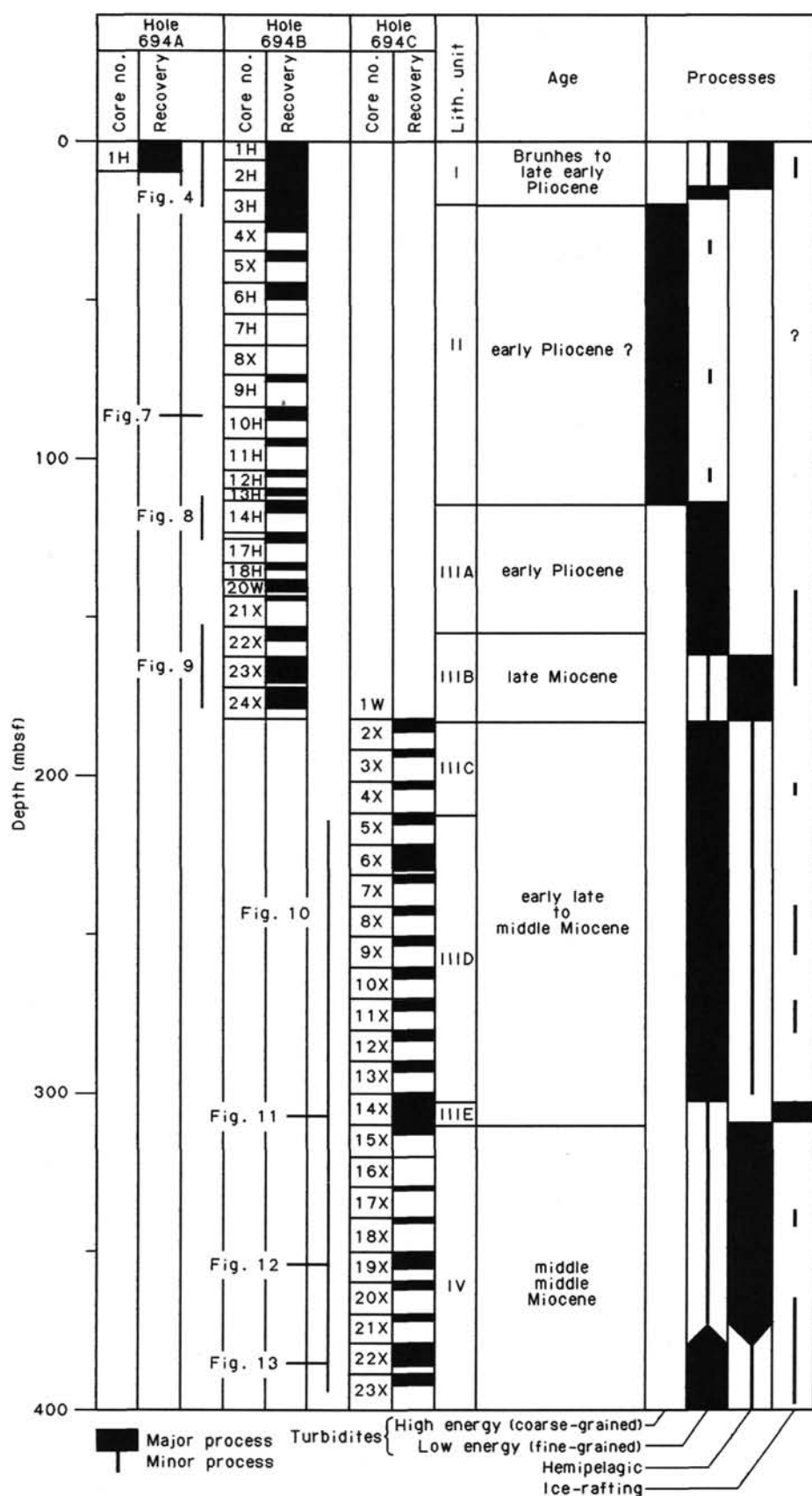


Figure 3. Age, recovery, and lithologic units and age of Site 694 cores, with locations of figures. Right-hand column shows the main sedimentary processes as they changed with time.

Table 2. Lithologic units at Site 694.

Unit	Cores	Depth (mbsf)	Major sediment types	Drilling disturbance
I	694A-1H 694B-1H to -3H-5	0–21.1	Hemipelagic muds, fine-grained turbidites.	Soupy near top, otherwise slight disturbance.
II	694B-3H-5 to -14H	21.1–111.5	Thick, coarse to fine sands.	Low recovery; some grading and sorting of sands.
III	694B-14H to -24X 694C-2X to -15X	111.5–304.3	Muds, silts, sands; some diatom-bearing.	Very low recovery.
IIIA	694B-14H to -22X	111.5–150.4	Muds, graded silts, sands; few diatoms.	Slightly disturbed.
IIIB	694B-22X to -24X	150.4–179.2	Diatom-bearing clayey muds, graded silts.	Slightly to very disturbed.
IIIC	694C-2X to -5X	179.2–208.3	Barren muds, silts, coarse sands.	Drilling biscuits. Sands concentrated in core catchers.
IIID	694C-5X to -14X-3, 45 cm	208.3–298.2	Diatom-bearing muds, silts, sands.	Gravel concentrated in core catcher.
IIIE	694C-14X-3, 45 cm to -15X	298.2–304.3	Gravel-bearing sandy and silty mud.	Drilling biscuits; some are reoriented.
IV	694C-15X to -23X	304.3–391.3	Diatom and diatom-bearing claystones, silts near base.	

These layers are light yellowish brown (2.5Y 6/4) and slightly stiffer than the surrounding mud.

Ice-rafted debris, seen as scattered sand grains when the core surface is cleaned with a glass slide, occurs in distinct layers in Core 113-694A-1H (Fig. 6). The sand fraction from the sample marked on Figure 6 (Sample 113-694A-1H-6, 103–107 cm) is very poorly sorted with lithic grains as large as 6 mm. Acid to intermediate plutonic rocks, quartz-mica schists, fine-grained chlorite-mica schists, and several large feldspars form the largest grains; the finer sand includes abundant quartz, some feldspar, and a wide variety of heavy minerals including biotite, hornblende, and garnet with rare glauconite, epidote, chlorite, and magnetite. Manganese micronodules also occur. Most grains except glauconite are angular to subangular.

Interpretation

Sequences such as that illustrated in Figure 5 are interpreted as fine-grained turbidites passing up into hemipelagic sediments. Where there is less color contrast (or more drilling disturbance) it is more difficult to distinguish turbiditic from hemipelagic clay. Unit I is cyclic in that some intervals contain abundant turbidites and others very few (Fig. 4); variations in turbidite supply and in the amount of ice-rafted material may be linked to glacial/interglacial processes. The occurrence of diatom-bearing muds in distinct layers may be related to variation in sea-ice cover.

Unit II (Depth 21.1–111.5 mbsf; Age lower Pliocene)

Cores 113-694B-3H-5 to 113-694B-14H; depth 21.1–111.5 mbsf; thickness 90.4 m; lower Pliocene.

This unit consists mainly of unconsolidated sand and is characterized by poor recovery (16%; Fig. 3). Overall the sediment becomes coarser downward from sandy mud in Core 113-694B-3H to very coarse sand in Core 113-694B-14H. Clay and clayey mud are present only as thin interbeds or as clasts within sand.

Coarse to very coarse sand forms the whole of Cores 113-694B-11H and 113-694B-13H and the lowest 60 cm of Core 113-694B-10H. Its dark gray color results from the high proportion (about 70%) of lithic grains. In Cores 113-694B-11H and 113-694B-13H the sand is well-sorted with subangular to subrounded grains. Lithic fragments are fine-grained sedimentary rocks with

rare plutonic and volcanic rocks. Quartz forms about 25%, with small amounts of feldspar; opaque minerals and garnet are the most prominent accessories.

Coarse sand also forms the bases of thick graded beds in Core 113-694B-4X (whole core), and Samples 113-694B-9H, 20–65 cm, and 113-694B-10H, 0–125 cm. These beds are graded to fine sand at the top. The finer sand contains more quartz and fewer lithic fragments than the very coarse sand described above, and is lighter in color (grayish brown 2.5Y 4/2 to dark gray 5Y 4/1).

Most of the remainder of Unit II consists of fine to medium sand and sandy mud. Original bed thickness is not known because of poor recovery. Colors include pale olive (5Y 6/3), gray (5Y 5/1), and dark gray (N 4/1). Sorting is moderate to poor and the beds are not graded.

Clay, clayey mud, and silty mud occur as subrounded to angular clasts 1–3 cm across (rarely 5–6 cm) within coarse to very coarse sand (Fig. 7). They come in a wide variety of colors from gray through olive to greenish gray (see barrel sheets). Clasts commonly form 5%–10% of the sequence. Clay also occurs in place in Cores 113-694B-5X and 113-694B-9H in layers 10–40-cm thick. The 10-cm core-catcher sample representing Core 113-694B-12H contains dark greenish gray (5GY 4/1) silty and clayey mud.

No ice-rafting record is discernible for this unit.

Interpretation

The sands in Unit II are the products of high-energy turbidity currents. Mud clasts may have been added to the beds either during erosion of the seafloor nearer the source, or (more likely) during the coring process. Possible sources for the lithic grains are the Mesozoic and Paleozoic sedimentary rocks of the southern Antarctic Peninsula and Ellsworth Mountains.

Unit III (Depth 111.5–304.3 mbsf; Age upper middle Miocene to lower Pliocene)

Cores 113-694B-14H to 113-694B-24X, and 113-694C-2X to 113-694C-15X; depth 111.5–304.3 mbsf; thickness 192.8 m; middle Miocene to lower Pliocene.

Unit III is a varied group of sediments lying below the massive sands of Unit II and above the partly lithified diatom claystones of Unit IV. A convenient lower boundary is the base of a

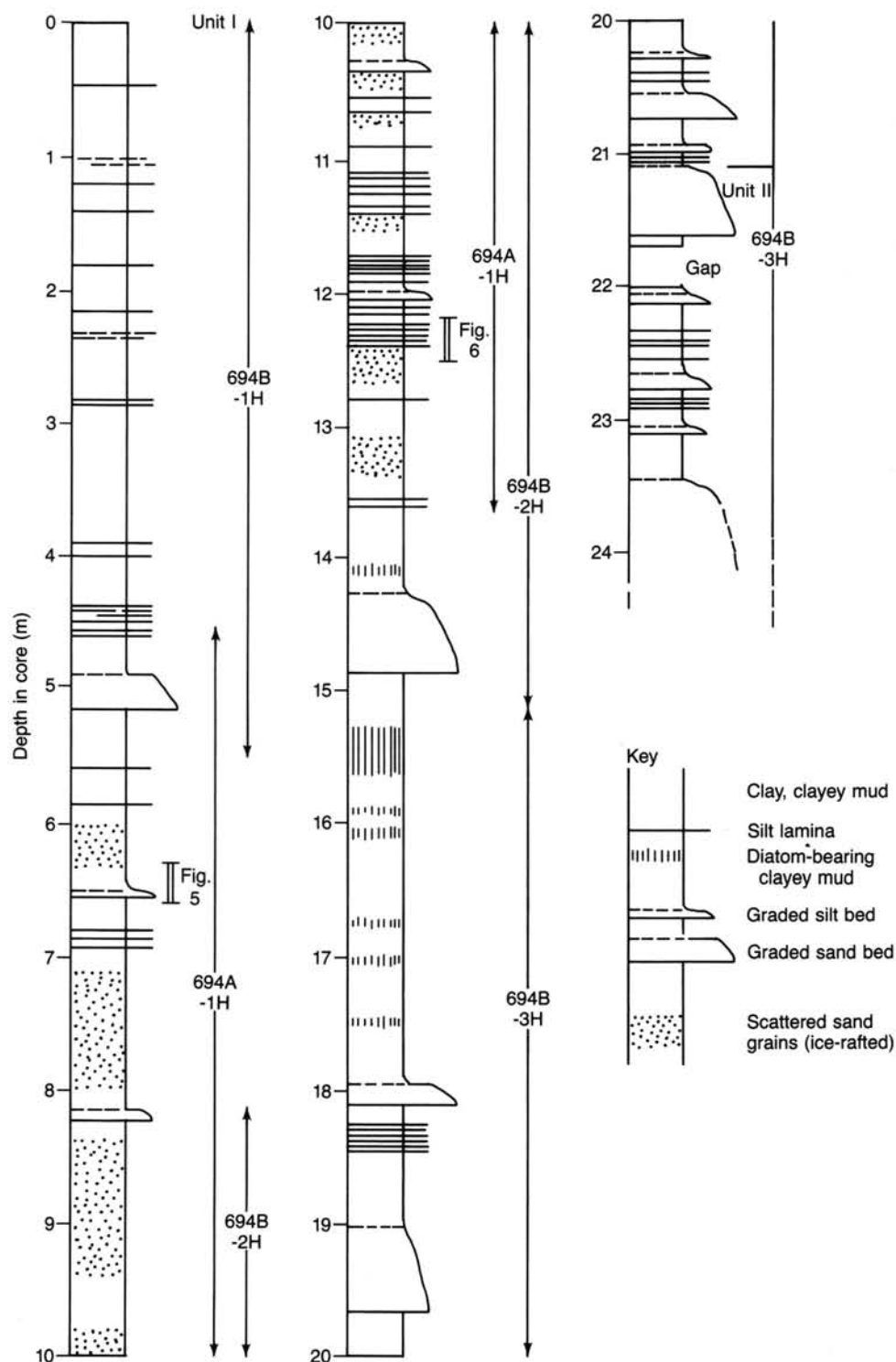


Figure 4. Lithologic section showing occurrence of graded silts and sands, ice-rafted debris, and diatom-bearing layers; in Unit I and upper part of Unit II. Detailed correlation with Hole 694A shows that there is a 2-m gap between Cores 113-694B-1H and 113-694B-2H. The details of this sequence are very well defined by *P*-wave logger velocities ("Physical Properties" section, this chapter).

thick, gravelly mud sequence in Core 113-694C-14X. The five subunits are defined using the proportion of diatoms (Subunits IIIA, B, C, D) and grain size (Subunit IIIE); Table 2.

Subunit IIIA (depth 111.5–150.4 mbsf)

Cores 113-694B-14H to 113-694B-22X; thickness 38.9 m; lower Pliocene(?) (by default).

This subunit contains a total of only 4 m of sediment in four coherent cores, (113-694B-16W and 113-694B-20W are wash cores, 113-694B-17H contains only a trace of sediment, and the nominal 4.5 m of Core 113-694B-18H consists largely of drilling mud (Wyoming bentonite). Figure 8 shows the sequence of graded fine sands, silts, and clays in Cores 113-694B-14H and 113-694B-15H. The thick sand in Core 113-694B-14H is dark

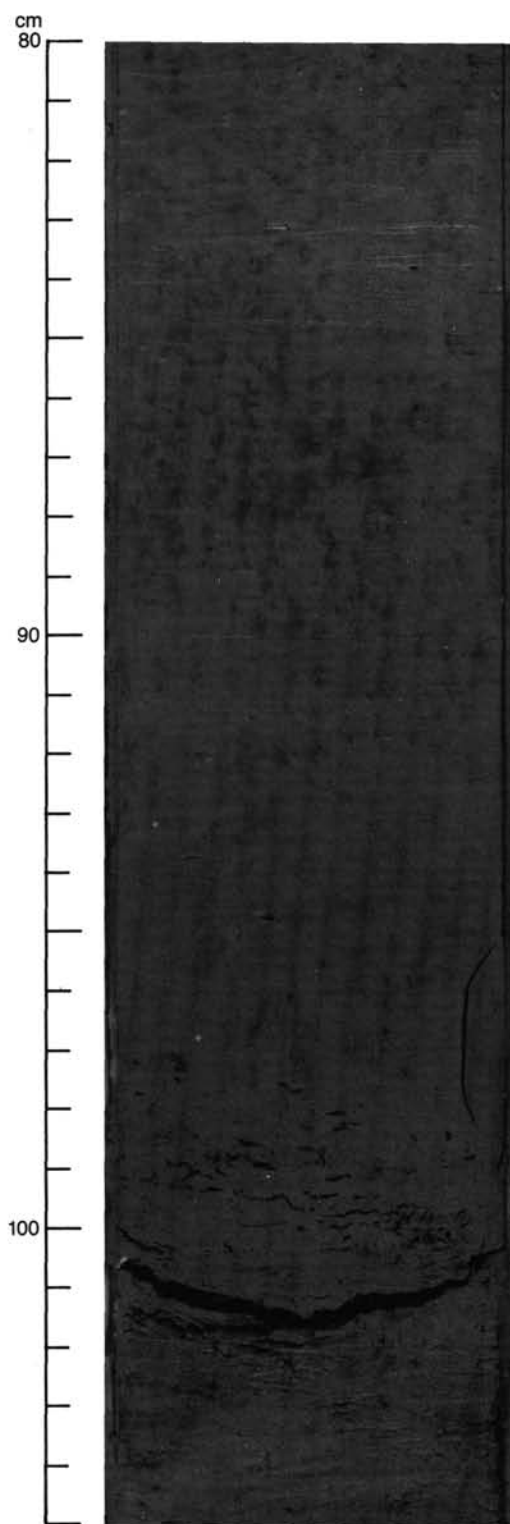


Figure 5. Graded silt (interpreted as turbiditic) grading up into burrowed clayey mud (interpreted as hemipelagic); in Unit I; 694A-1H-2, 80–105 cm; location shown in Figure 4.

greenish gray (5GY 4/1), fine-grained and moderately sorted with coarse tail-grading in the lowest 50 cm. Thinner sands and silts are dark gray (5Y 4/1), well-sorted, and show very few sedimentary structures apart from grading. Composition of the sands is predominantly quartz with some feldspar including fresh albite-twinned plagioclase. Among the accessory minerals hornblende, garnet, and opaque minerals are equally abundant.

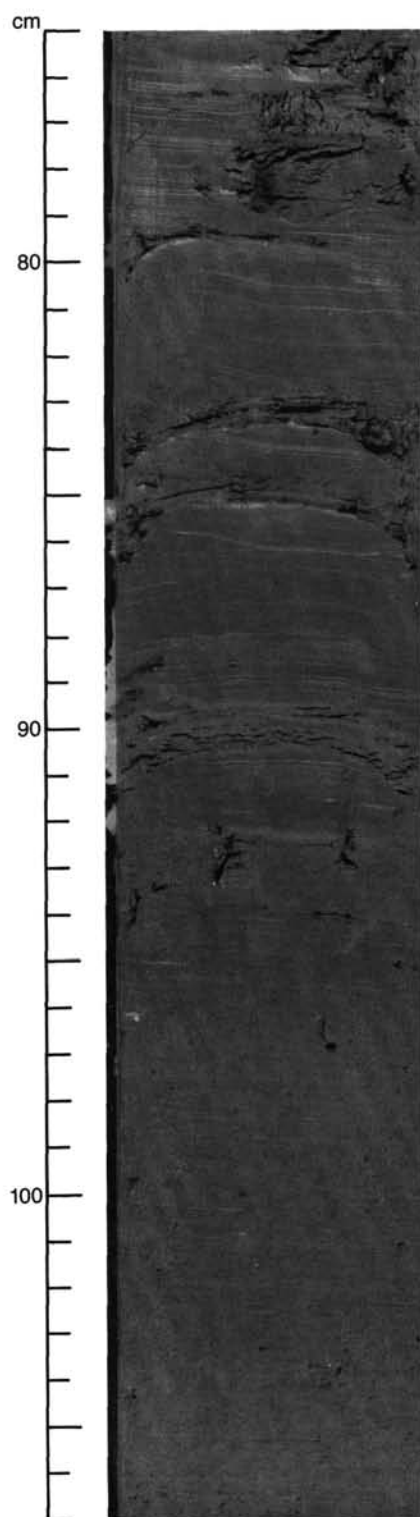


Figure 6. Graded silt laminae overlain by clays (interpreted as fine-grained turbidites); in Unit I; Sample 113-694A-1H-6, 75–105 cm. Below 96 cm, clayey mud containing scattered sand grains is interpreted as hemipelagic with ice rafting. Sample 113-694A-1H-6, 103–107 cm, is described in text. Location shown in Figure 4.

Interbedded clayey muds are dark greenish gray (5GY 4/1) to very dark gray (5Y 3/1). Those in Core 113-694B-14H contain 5%–20% diatoms; those in Core 113-694B-15H are barren and moderately bioturbated. The remainder of Subunit IIIA comprises lumps of dark gray (5Y 4/1) sand and mud and grayish

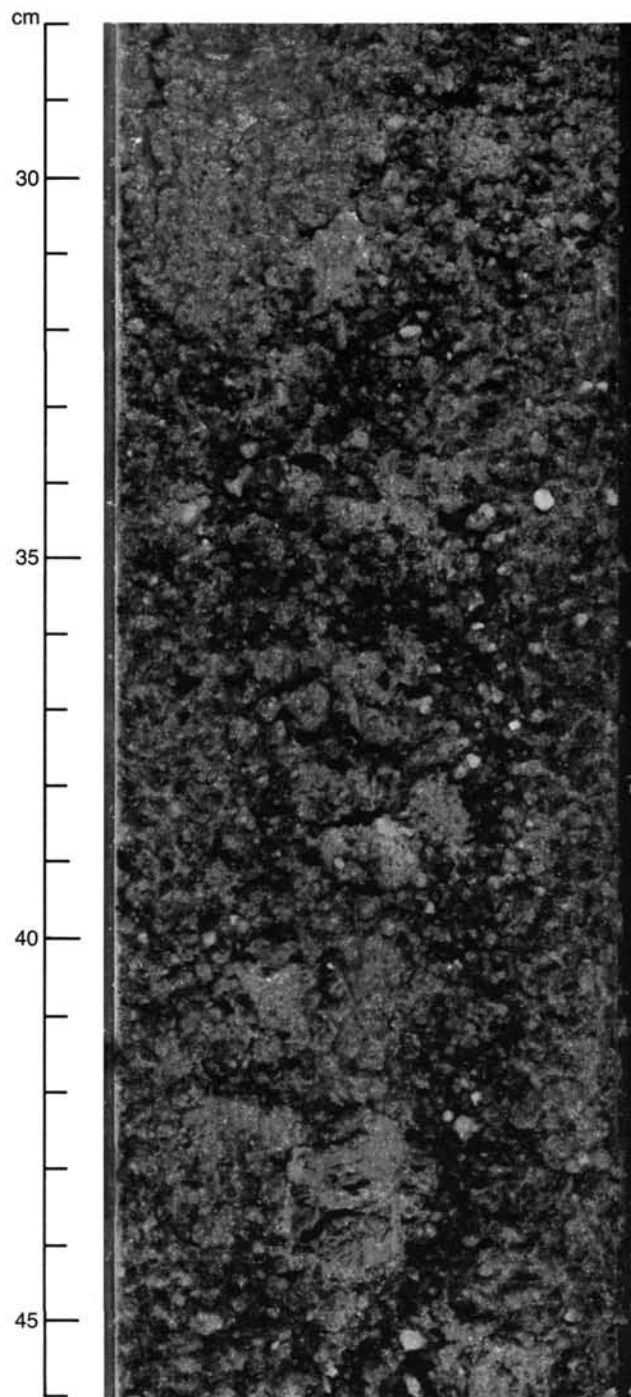


Figure 7. Very coarse sand with subrounded to subangular grains and small mud clasts; in Unit II; Sample 113-694A-10H-2, 28–46 cm.

brown (2.5B 4/2) clay in Core 113-694B-18H, totalling about 10 cm; dark bluish gray (5B 4/1) clay with a disturbed 10-cm silt bed in Core 113-694B-19H; and dark greenish gray (5BG 4/1) clay in Core 113-694B-21X.

Interpretation

The graded sand/silt layers are interpreted as turbidites, all rather fine grained except for the thick sand in Core 113-694B-14H. Bioturbation in the muds in Core 113-694B-15H may indicate a longer interval between turbidity flows than in the rest of the subunit, but there is little evidence for hemipe-

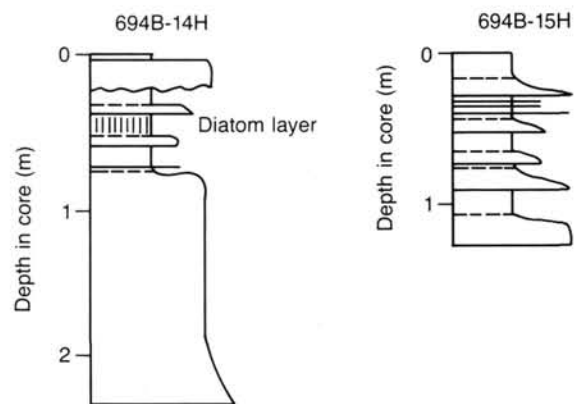


Figure 8. Lithologic sections for Cores 113-694B-14H and 113-694B-15H; in Subunit IIIA. Key same as Figure 4.

lagic deposition. The occurrence of hornblende and fresh plagioclase in the sands suggests a source area with some volcanic rocks.

Subunit IIIB (Depth 150.4–179.2 mbsf)

Cores 113-694B-22X through 113-694B-24X; thickness 28.8 m; upper Miocene.

This subunit includes similar graded silts to those in Subunits IIIA and IIIC, but the interbedded clayey muds contain diatoms (Fig. 9A). Graded silt beds 1–15 cm thick form some 30% of Core 113-694B-22X and 15% of Cores 113-694B-23X and 113-694B-24X (example in Fig. 9B). Parallel lamination was observed rarely in the silts.

The clays, clayey and silty muds, and diatom-bearing clayey and silty muds which make up the rest of Subunit IIIB are mainly dark greenish gray (5BG 4/1) and greenish gray (5GY 5/1) in Core 113-694B-22X and gray (5Y 5/1) in the upper part of Core 113-694B-23X; below this the predominant colors are light brownish gray (2.5Y 6/2) and light olive gray (5Y 6/2), with olive gray (5Y 5/2) and olive (5Y 5/3) toward the base of Core 113-694B-24X. This systematic color change is not accompanied by obvious compositional changes in the smear slides. Color contrasts between silts and muds are minimal, but silts tend to be more olive or brown than the surrounding mud. Moderate bioturbation occurs in most of Core 113-694B-24X; in each burrowed layer the amount of bioturbation increases upwards away from graded silt (e.g., Fig. 5).

Ice-rafted debris is abundant in Core 113-694B-23X, with the muds in most of Sections 113-694B-23X-2 through 113-694B-23X-4 containing sand grains and granules. Dropstones occur in Core 113-694B-22X and scattered sand grains occur at the top of Section 113-694B-24X-3.

Interpretation

Subunit IIIB is a mixture of fine-grained turbidites and hemipelagic sediments. The graded silts and directly overlying muds are turbidites, while thick burrowed mud units and intervals with abundant ice-rafted debris are likely to be hemipelagic.

Subunit IIIC (Depth 179.2–208.3 mbsf)

Cores 113-694C-2X to 113-694C-5X; thickness 29.1 m; middle to lower upper Miocene.

This thin subunit, affected by severe drilling disturbance, lacks diatoms. Core 113-694C-2X consists of graded silts 3–80 cm thick interbedded with clays showing minor to moderate bioturbation. Thin silt layers are gray (5Y 5/1) and thicker ones dark gray (N 4/0) or dark greenish gray (5GY 4/1); clays are dark greenish gray (5BG 4/1). Cores 113-694C-3X and 113-

A

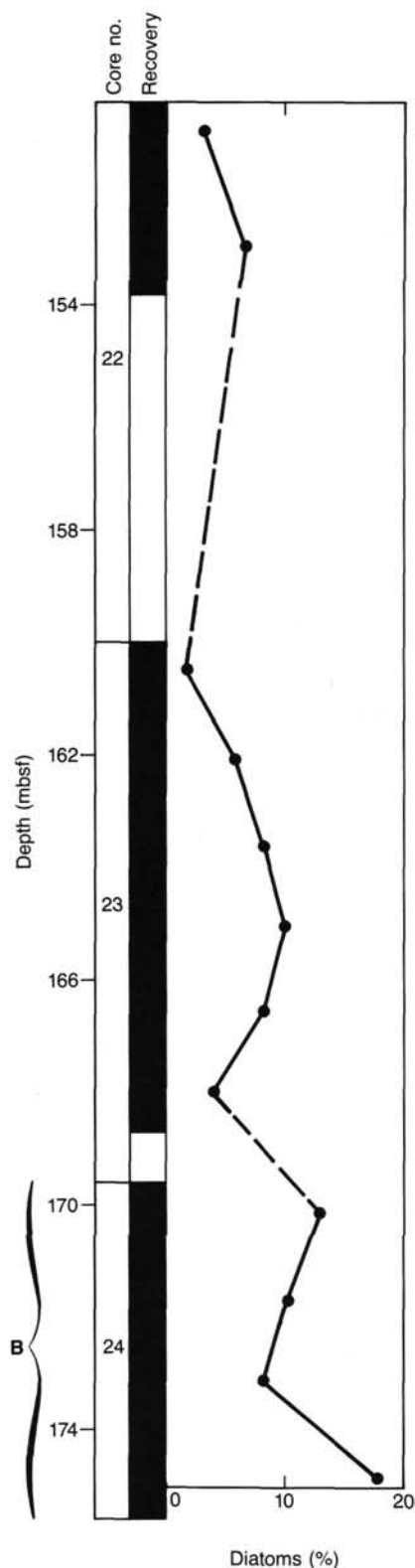
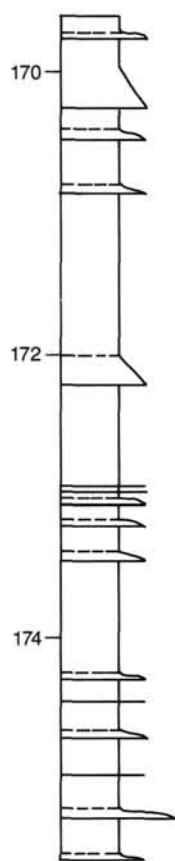


Figure 9. A. Proportion of diatoms in mud (i.e., graded silts and sands omitted); in Subunit IIIB. Values were measured by point-counting smear slides. Possible cyclicity indication. B. Lithologic section in Core 113-694B-24X showing occurrence of graded silt beds; in Subunit IIIB. Key same as Figure 4.

B



694C-4X each contain disturbed greenish gray (5G 5/1) muds, with coarse sands in the core catchers. The only ice-rafted debris is some sand (possibly uphole contamination) in 113-694C-2X-1, 121-150 cm.

Interpretation

Graded bedding in Core 113-694C-2X indicates deposition as turbidites, and moderate bioturbation in the lower part of Core 113-694C-3X may indicate hemipelagic deposition.

Subunit IIID (Depth 208.3–298.2 mbsf)

Cores 113-694C-5X to 113-694C-14X-3, 45 cm; thickness 89.9 m; middle to lower upper Miocene.

This subunit includes a variety of diatom-bearing silty and clayey muds, with interbedded silts and sandy muds. Compositional data for the muds are shown in Figure 10. The muds are various shades of dark greenish gray (5G 4/1, 5GY 4/1, 5BG 4/1, N 4/0), and the dark color may result partly from the high proportion of opaque and heavy minerals. Some minor bioturbation is observed in Cores 113-694C-5X, 113-694B-8X, 113-694B-9X, and 113-694B-12X, but most of the mud intervals lack primary sedimentary structures. The mud is firm and biscuited.

Graded sands or sandy muds, locally diatom-bearing, occur in all cores in this subunit except 113-694C-7X, 113-694C-9X, and 113-694C-13X and total 14% of recovered sediment. Colors are dark gray (N 4/1) (mainly) or dark greenish gray (5G 4/1). They range from 20 to 100 cm thick and have sharp or erosional bases and graded silty tops with some parallel lamination. Several core catchers, notably Section 113-694C-12X, CC, appear to have been plugged with sand which prevented further entry of sediment into the core barrel. Sands from the bases of the coarsest beds are moderately sorted lithic quartz sands with subrounded to subangular grains. The lithics are sedimentary rocks with a few metamorphic and volcanic rocks. The larger quartz grains are rounded and polished.

In addition, thin (less than 10 cm) silt and sand layers (classified as silty and sandy muds) occur throughout this subunit, and form about 5% of the sequence. They have sharp or erosional bases and gradational or sharp tops, and many beds are parallel laminated. Some are diatom-bearing. At the base of Core 113-694C-6X there is a 1-cm-thick pinkish gray (5YR 7/2) vitric ash containing pristine glass shards.

Ice-rafted debris is generally very sparse in Subunit IIID. No dispersed sand grains were recorded, and the dropstones found at the tops of Cores 113-694C-8X, 113-694C-11X, and 113-694C-12X may not be in place. There are three very weathered dropstones in Core 113-694C-9X. In Core 113-694C-14X sand- and gravel-sized dropstones become more abundant down to the gradational base of the subunit in 113-694C-14X-3, 45 cm.

Interpretation

Subunit IIID represents alternating turbiditic and hemipelagic deposition, with a higher proportion of diatoms than in the younger subunits. Core recovery and shipboard sampling intervals are not adequate to determine whether the fluctuations in diatom abundance (Fig. 10) are cyclic. Turbidite sands were derived from an area of mainly sedimentary rocks and the subrounded to subangular grain shape suggests that some subaqueous transport and rounding occurred prior to redeposition in deep water. Ice-rafting appears to have been unimportant during the time represented.

Subunit IIIE (Depth 298.2–304.3 mbsf)

Cores 113-694C-14X-3, 45 cm, to 113-694C-15; thickness 6.1 m; upper middle Miocene

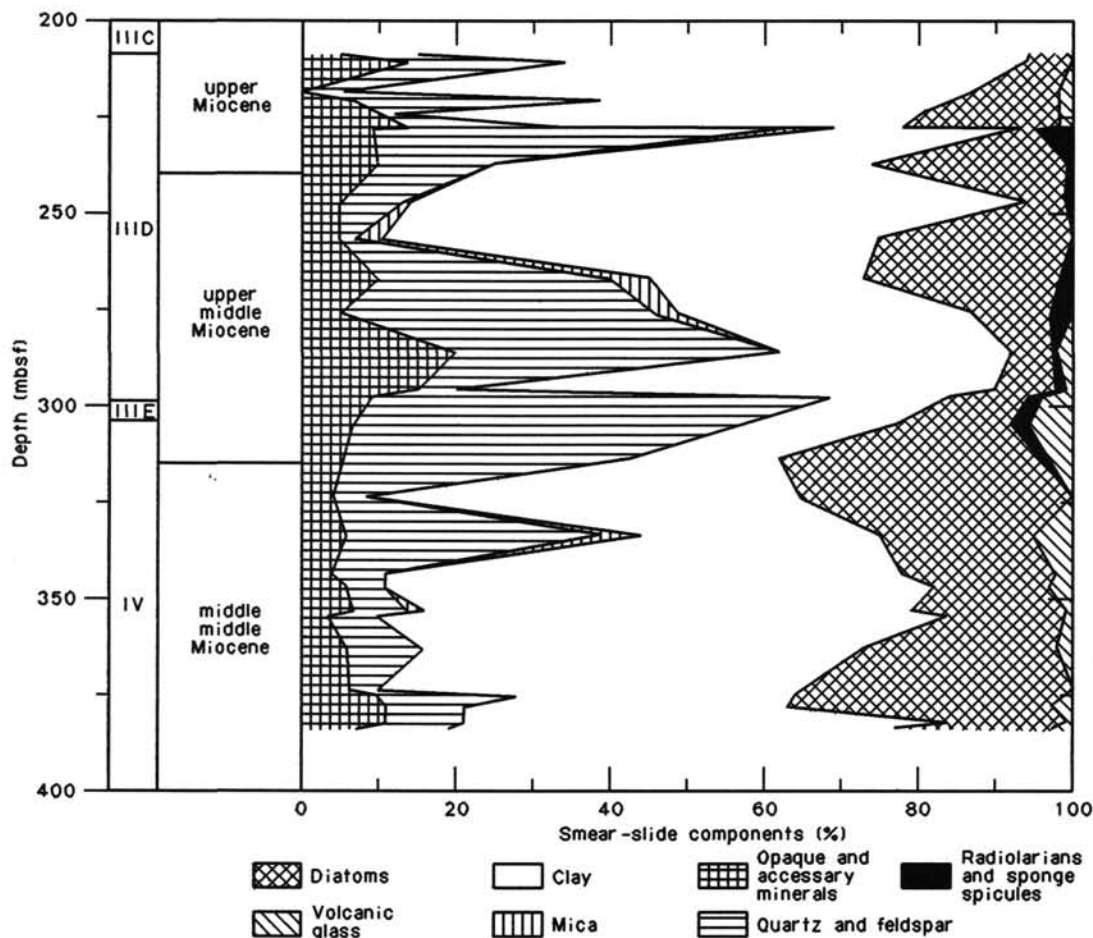


Figure 10. Composition of sediments in lithologic Units III (Subunits IIIC, IIID, and IIIE) and IV based on smear-slide data from Hole 694C. Graded silts and sands omitted.

This subunit consists of gravel-bearing sandy and silty mud, mainly dark bluish gray (5B 4/1), forming a massive interval. The sediment contains about 10% granules and small pebbles (vein quartz and sedimentary lithic fragments with rare volcanic lithic fragments) in a matrix of poorly sorted sandy or silty mud containing as much as 5% of diatoms (Fig. 11). The matrix becomes finer downward (sand:silt:clay is 40:40:20 in 113-694C-14X-3, 90 cm, and 15:45:40 in 113-694C-14X-6, 90 cm; from smear slides) but the gravel content remains constant except in the core catcher, where the lowest 15 cm contains gravel with very little matrix. This may be an artifact of drilling. A thin layer of greenish gray (5GY 6/1) diatom-bearing silt occurs in Section 113-694C-14X-4. Although disturbed, it appears to be a bed rather than a large clast: it grades into the sandy mud above and below through a gray (5Y 5/1) interval some 10 cm thick.

Interpretation

Two origins are possible for a thick, homogeneous, poorly-sorted sediment such as this: (1) debris flow; (2) ice-rafting, i.e., glaciomarine. The latter is favored because of the very distal setting of Site 694, and the lack of size grading of the coarser clasts.

Unit IV (Depth 304.3–391.3 mbsf; Age middle middle Miocene)

Cores 113-694C-15X through 113-694C-23X; thickness 87.0 m; middle Miocene.

The major sediment types in Unit IV are diatom-bearing and diatom clayey and silty mudstones, becoming more lithified downward. Recovery is poor at the top of the unit (Fig. 3) and all cores contain drilling biscuits; nevertheless, primary sedimentary structures are widespread. Sediment composition is shown in Figure 10.

Sand, excluding ice-rafted debris, is almost absent from Unit IV except for a 30-cm graded diatom-bearing sandy mud bed near the top of Core 113-694C-15X. Diatom silty to clayey muds/mudstones in Cores 113-694C-15X to 113-694C-20X are dark gray (N 4/0) to dark greenish or bluish gray (5G 4/1, 5GY 4/1, 5B 4/1) with some faint lamination. The only bioturbation in the unit occurs in Core 113-694C-19X where there are abundant *Chondrites* burrows (Fig. 12). The burrows in some biscuits appear to bifurcate upward rather than downward, suggesting that biscuits have been inverted. Similarly, lamination in biscuits in Core 113-694C-20X dips at high angles, but this is attributed to drilling disturbance rather than synsedimentary deformation. From the base of Core 113-694C-19X to 113-694C-22X there is a color change to black (5Y 2.5/1) or very dark gray (5Y 3/1), and the mudstone exhibits faint color banding on a millimeter to centimeter scale. The diatom content is somewhat lower in this interval (Fig. 10). In Cores 113-694C-22X and 113-694C-23X color returns to dark gray (N 4/1) or dark greenish gray (5BG 4/1, 5G 4/1). The mudstone near the base of Core 113-694C-23X is laminated.

A few silt laminae occur in Cores 113-694C-20X and 113-694C-21X, and Cores 113-694C-22X and 113-694C-23X contain

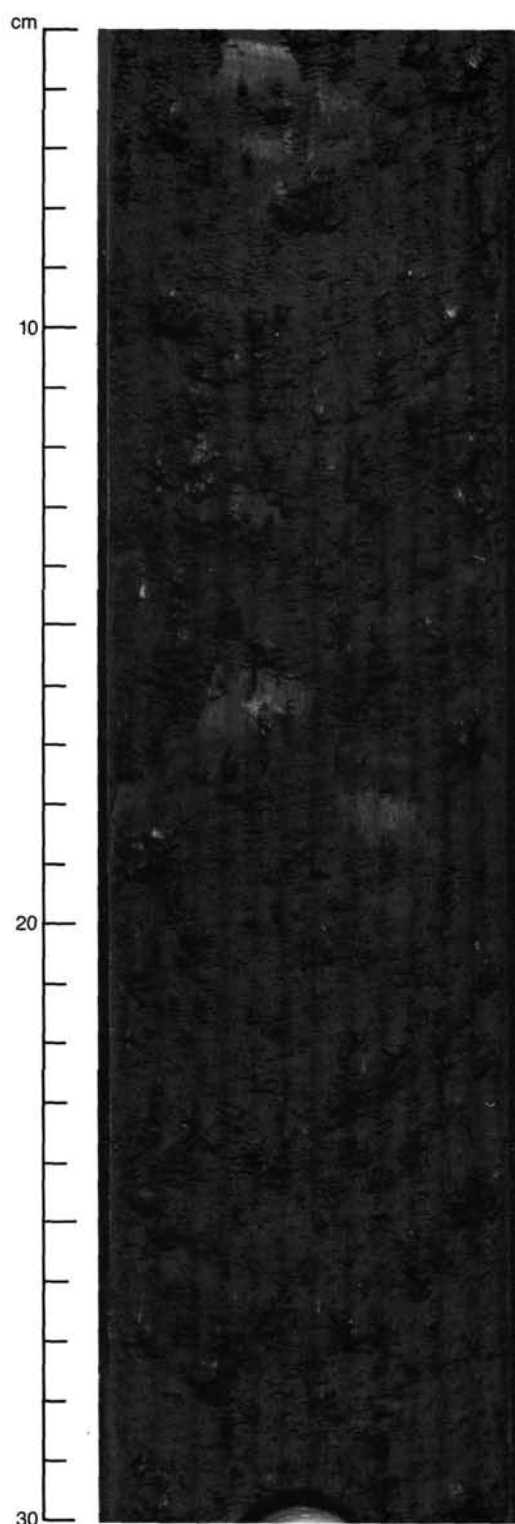


Figure 11. Gravel-bearing silty mud, Sample 113-694C-14X-6, 5–30 cm; Subunit IIIIE. Granules, small pebbles, and mud clasts (lighter patches) occur throughout and the sediment has a random fabric. Compare sorting with Figure 7.

graded silt beds commonly 5–10 cm thick, constituting some 10% of the sequence (Fig. 13). The silt beds are gray (5Y 5/1), sharp-based and very well-laminated (Fig. 14). Petrographically, they are unusual, containing 8%–10% of sponge spicules.

Ice-rafted debris occurs in sharply-defined intervals in this unit totalling 95 cm in Core 113-694C-19X, 58 cm in Core 113-694C-20X, 12 cm in Core 113-694C-22X, and 9 cm in Core 113-694C-23X. Although concentrations of coarse sand have evidently been reworked during the drilling process (Fig. 15), their occurrence in only certain thin horizons suggests that the sand is not a contaminant from further uphole. The 9-cm interval in Core 113-694C-23X is inversely graded. A sample from Core 113-694C-22X is well-sorted fine quartz sand with about 5% feldspar and rare garnet, chlorite, staurolite, and glauconite. Approximately 5% of grains are black, angular, and polished and are thought to be iron/manganese-coated grains.

Interpretation

The graded silts in Unit IV are fine-grained turbidites but it is not known how much of the diatom-bearing and diatom mudstone is turbiditic in origin. The burrowed interval in Core 113-694C-19X is almost certainly hemipelagic. Ice-rafting does not appear to have been continuously active. The occurrence of well-sorted sand and iron/manganese-coated grains in at least one of the sandy layers indicates a period of very slow sedimentation with winnowing by bottom currents.

Conclusion

The relative importance of different sedimentary processes (high- and low-energy turbidity currents, hemipelagic deposition from a nepheloid layer, and ice-rafting) has changed with time at Site 694. These processes are summarized in the right-hand column of Figure 3.

Clay Mineralogy

X-ray diffraction analyses were completed on 36 samples from Holes 694A, 694B, and 694C (Fig. 16). The objectives of clay mineral studies at Site 694 are (1) to identify the major paleoenvironmental changes as expressed by clay associations (using a sampling interval of one per core), (2) to examine the cyclic variations of clay associations in relation to slight lithologic changes expressed by the changing color of the sediment (using a sampling interval of one per section), and (3) to compare the clay associations with those recognized at other Leg 113 sites in the Weddell Sea.

Results

The clay minerals identified include chlorite, vermiculite, illite, kaolinite, and smectite (Fig. 16). Based on the relative abundances of the various clay species, four clay units (C1–C4) were recognized for Site 694.

Unit C1 extends from the seafloor to 160 mbsf, is Pleistocene to late Miocene and consists of illite (abundant to very abundant), chlorite (rare to abundant), kaolinite (rare to common), and smectite (absent to abundant). The clay minerals are generally well crystallized.

Unit C2 extends from 160 to 256 mbsf, is late Miocene and consists of illite (abundant to very abundant), kaolinite (rare to common), smectite (absent to abundant), chlorite (absent to abundant), and vermiculite (absent to common). Clay minerals are moderately crystallized.

Unit C3 which extends from 256 to 380 mbsf has a clay association of abundant to very abundant illite, common to abundant chlorite, and rare kaolinite, sporadically associated with rare to common smectite. Clay minerals are well crystallized. This unit ranges in age from the middle to the early late Miocene.

Unit C4 extends from 380 mbsf to the terminal depth at 391 mbsf and consists of abundant chlorite and illite. Clay minerals are well crystallized. This unit is middle Miocene in age.

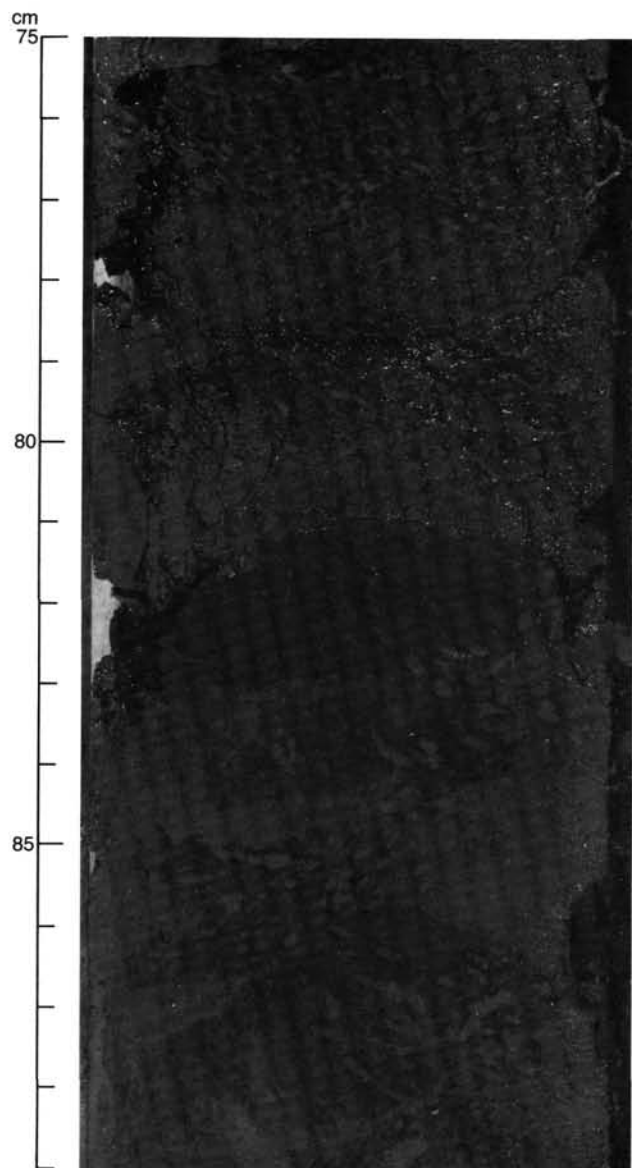


Figure 12. Chondrites burrows in dark mudstone. Sample 113-694C-19X-2, 75–89 cm; Unit IV.

Natural and heated slides display similar intensities of chlorite 001 and 002 reflections in Unit C4. In Units C1–C3, chlorite 001 peaks increase and 002 peaks disappear after heating. The structure of chlorite becomes unstable during heating if most of its octahedral interlayers consist of Fe: the 001 peak increases, while the 002 peak decreases progressively above 500°C. The disappearance of the mineral reflections around 600°C indicates the collapse of the chlorite structure. The structure of chlorite is more stable, and mineral reflections persist until around 800°C, if the octahedral interlayers consist primarily of Mg (Brindley and Brown, 1984). We infer that chlorite is mainly magnesium-rich in Unit C4, and iron-rich in the other clay units.

Paleoenvironmental Interpretation

Unit C4 (middle Miocene) is characterized by abundant magnesium-rich chlorite, which is derived from recrystallization during diagenetic and metamorphic processes. Chlorite and illite contents increase progressively with increasing diagenetic processes (mainly a consequence of pressure and heat-flow effects), and both minerals form a single clay association into late diage-

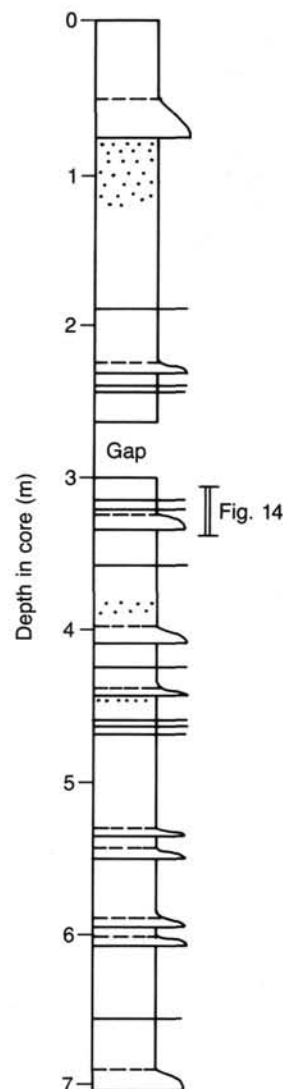


Figure 13. Lithologic section in Core 113-694C-22X showing occurrence of graded silts and thin layers of scattered sand grains; Unit IV. Key same as Figure 4.

netic and metamorphic environments (Dunoyer de Segonzac, 1969). As a consequence, well-crystallized clay minerals in Unit C4 result possibly from physical erosion of metamorphosed Antarctic terrains.

Iron-rich chlorite appears in Unit C3 (middle to early late Miocene). This mineral can be formed from both diagenesis and chemical weathering. In some modern Antarctic soils, iron liberated through weathering forms amorphous oxides, later incorporated within crystalline materials which often lead to chlorite formation. Other soils are dominated by mica-illite (Ugolini and Jackson, 1982). As a consequence, the clay associations of Unit C3 (and the upper Units C1 and C2) probably contain clay particles derived from weathering processes on Antarctica.

The East Antarctic ice-sheet developed prior to deposition of Unit C3, preventing pedogenesis in most continental areas, and chlorite could have been derived partially from the removal of Antarctic relict soils and of sediments deposited earlier on the East Antarctic margin. Chlorite could also have originated from pedogenesis on West Antarctica, where an ice-sheet developed during the late Miocene (Ciesielski et al., 1982).

Smectite and kaolinite probably resulted from the removal of sediments outcropping on and around Antarctica, as was the

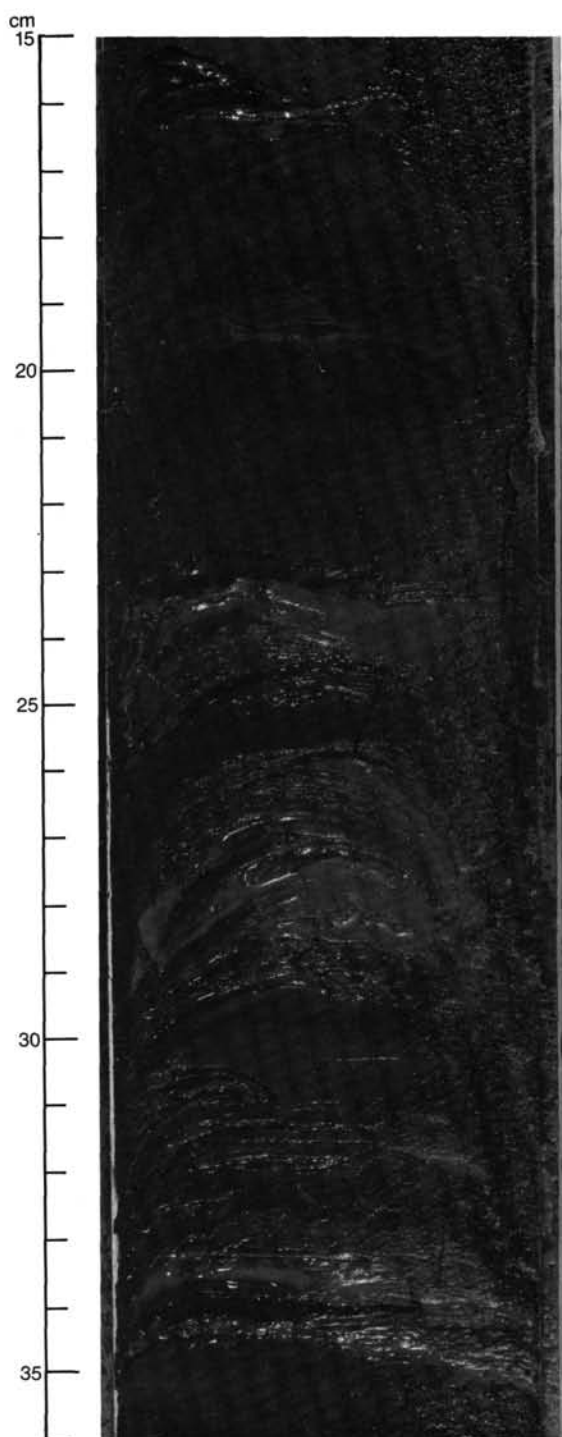


Figure 14. Laminated silt bed, Sample 113-694C-22X-3, 15–36 cm; Unit IV. Location is shown in Figure 13. Curved edges of drilling biscuits may cut across originally parallel lamination to produce pseudocross-lamination (e.g., at 31 cm).

case on Maud Rise (Sites 689 and 690) and on the Antarctic margin (Site 693). The appearance of iron-rich chlorite, kaolinite, and smectite in Unit C3 suggest that a change in the detrital supply at Site 694 occurred during the middle Miocene.

Increased abundances of smectite and kaolinite in Unit C2 reflect an increased removal of ancient sediments, starting during the early late Miocene. This mineralogic change probably

occurred as ice-volume increased on Antarctica around 10 Ma ago (Kennett and Von der Borch, 1985).

Moderate crystallinity of clay minerals and replacement of chlorite by vermiculite in the upper part of the unit probably reflect a slight intensification of weathering in the source area, which favored the removal of chemical elements from the soils. Vermiculite occurs in modern soils from Antarctic regions (Ugolini and Jackson, 1982) and is common in the alpine and northern regions of Europe (Millot, 1964).

Clay mineral data suggest increased influences of erosion of ancient terrain followed by more intense weathering culminating in the upper part of the unit. This unit corresponds stratigraphically to Unit C2 at Site 693, where increased chlorite content was interpreted as a consequence of more intense weathering on Antarctica. All these mineralogic changes probably occurred during a relatively warm period evidenced in the middle late Miocene around 7–8 Ma ago (Kennett and Von der Borch, 1985).

Alternating olive, olive-gray, and grayish-brown sediments were studied in Sections 113-694B-24X-2 and 113-694B-24X-4. Variations of the clay association are not related to the color of the sediment. However, vermiculite occurs in olive to olive-gray diatom-bearing clayey mud, suggesting that most of these sediments were deposited during warmer intervals.

Unit C1 (Pleistocene to late Miocene) is characterized by increased content of chlorite and kaolinite, and a better crystallinity of the clay minerals. This unit stratigraphically corresponds to the lower part of Unit C1 at Site 693, but chlorite and kaolinite are more abundant, and illite is less abundant at Site 694, reflecting the influence of different source areas. However, clay associations at Site 694, on the Antarctic margin (Site 693) and on Maud Rise (Sites 689 and 690) became rather similar during the lower Pliocene, when extensive glaciation, possibly associated with increased circulation, favored the homogenization of the detrital supply in the Weddell Sea.

Lithostratigraphy Appendix: Ice-Rafted Dropstones, Holes 694B and 694C

Eight dropstones were recovered from Holes 694B and 694C. Only pebbles 1×1 cm or larger were sampled for petrographic study (Table 3).

The dropstones are subangular to subrounded, range in size from 1×1 cm to 6×6 cm, and one specimen, a gneiss, (113-694B-2H-7, 35–37 cm) shows slight oxidation. Based on their lithology, the dropstones are grouped into basic volcanic and metamorphic rocks. Petrogenetically, the basic volcanic rocks are pyroxene tholeiite, and the metamorphic rocks are gneiss, hornfels, and schist.

The tholeiite is aphyric, but the random distribution of small chlorite patches indicates that the chlorite may be replacing pyroxene phenocrysts. The blebby chlorite is speckled with epidote and sphene.

The metamorphic rocks show alteration from the upper amphibolite facies (presence of diopside poikiloblasts) to the greenschist facies metamorphism (biotite). In the hornfels and schist, quartz predominates, whereas in the gneiss, quartz is subordinate to the feldspars. Sillimanite and kyanite are common in both the hornfels and the schist, and amphibole poikiloblasts are common in the gneiss.

The dropstones are randomly distributed within the stratigraphic column, and they do not appear to concentrate at any particular depth (Fig. 3). The age of the sediments containing the pebbles ranges from the middle middle Miocene to the late Pliocene.

Dropstones in Holes 694B and 694C are relatively few. Their lithology (volcanic and metamorphosed sedimentary rocks) suggest the Antarctic Peninsula as the source area.

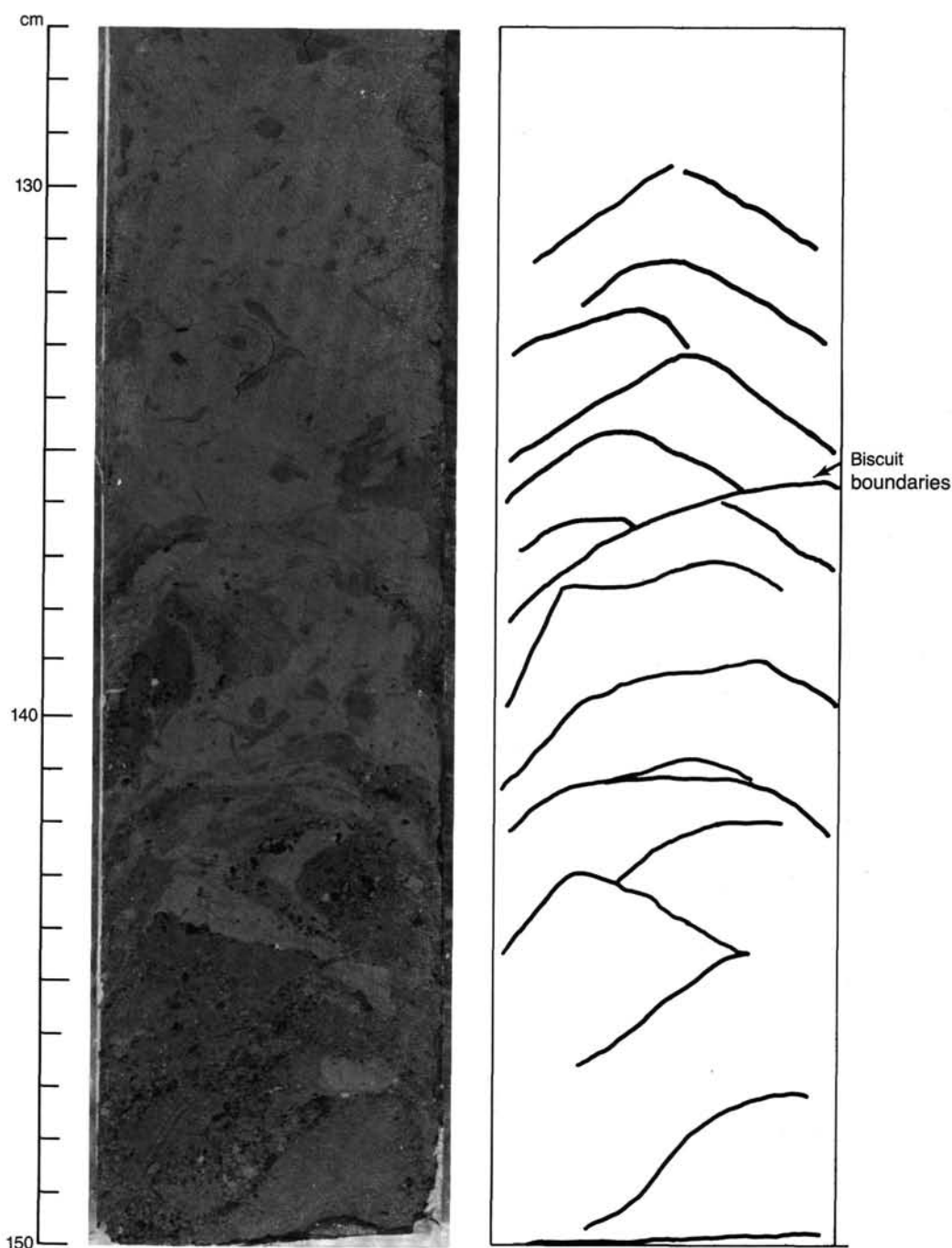


Figure 15. Interval of coarse sand interpreted as ice-rafted debris, Sample 113-694C-19X-1, 127-150 cm; also showing *en echelon* drilling biscuits.

PHYSICAL PROPERTIES

Introduction

The objectives of the physical-properties program at Site 694 were to help characterize the physical properties of high-latitude continental margin, abyssal-plain siliceous sediments, and provide an important link between geophysical data and the geological realities of the materials that constitute the sedimentary section described by shipboard stratigraphers and sedimentologists.

The physical-properties program consisted of obtaining the following measurements: (1) Index properties—gravimetric de-

terminations of bulk density, porosity, water content, and grain density; (2) Vane Shear Strength—a relative measure of the resistance of the sediment to loads and a measure of its cohesive-ness; (3) Compressional Wave Velocity—the speed of sound in the sediments; and (4) Thermal Conductivity—the ability of the sediment to transport heat.

Index Properties

Two methods of determining the bulk densities and porosities of the sediments were used for Site 694. Bulk density, porosity, and water content were determined at discrete points within

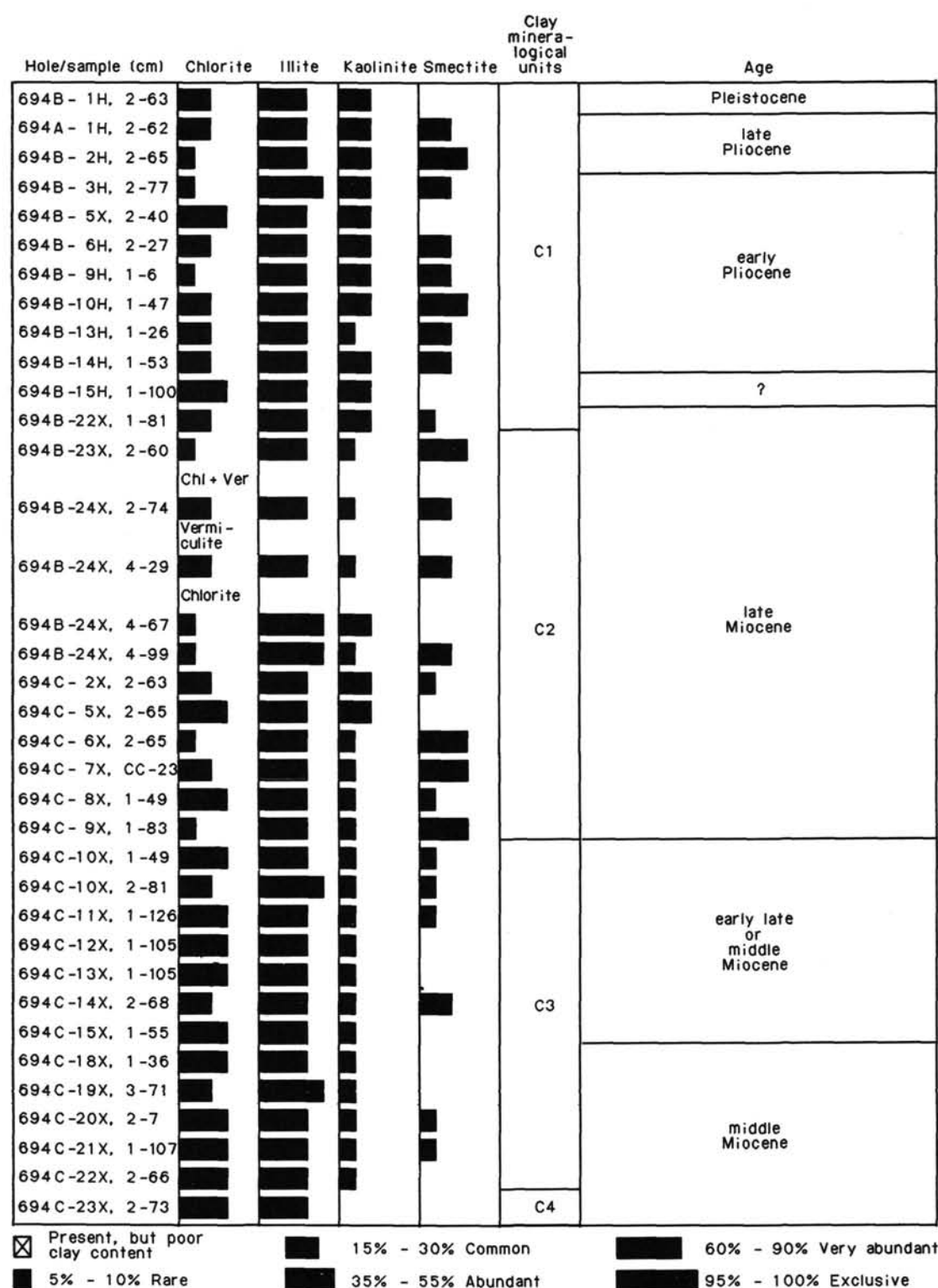


Figure 16. Clay mineralogy, Site 694.

the cores by gravimetric determination in addition to the bulk density and porosity obtained from GRAPE (Gamma Ray Attenuation Porosity Evaluation) scanning of whole-round core sections (Boyce, 1976). All core sections from Site 694 were logged on the GRAPE unit, from which bulk density and porosities are computed assuming a grain density of 2.75 g/cm³.

Index properties measured on samples selected from the most intact portions of cores are listed in Table 4. Profiles of bulk density, water content (dry basis), and grain density are illustrated in Figure 17. A profile of porosity is illustrated in Figure 18.

Due to the disturbed conditions of the sediments cored and the abundance of coarse-grained material at Site 694 there are

Table 3. Petrographic description of dropstones from Site 694.^a

Rock number: 113-694B-2H-7, 35–37 cm

Name: pyroxene-amphibole gneiss

Size: 2 × 2 cm

Depth: 14.85 mbsf

Shape: subrounded

Weathering: slight oxidation

Major minerals	%	Accessory minerals	Comments
Plagioclase	30	Actinolite	Upper amphibolite metamorphism; diopside poikiloblasts. Retrograde metamorphism; actinolite rims pyroxene. Fe-rich biotite is dark red.
Quartz	20	Sericite	
Diopside	20		
Hornblende	20		
Biotite	5		
K-feldspar	5		

Rock number: 113-694B-23X-4, 101–104 cm

Name: biotite hornfels

Size: 5 × 6 cm

Depth: 165.51 mbsf

Shape: subrounded

Weathering: none

Major minerals	%	Accessory minerals	Comments
Quartz	80	Magnetite	Granoblastic texture. Iron-rich biotite occurs in random orientation. Sillimanite are fibrous bundles or square cross-sections. Some iron stain after magnetite.
Biotite	10	Plagioclase	
Sillimanite	5		

Rock number: 113-694B-23X-4, 105–107 cm

Name: kyanite, sillimanite schist

Size: 4 × 4 cm

Depth: 165.55 mbsf

Shape: subrounded

Weathering: none

Major minerals	%	Accessory minerals	Comments
Quartz	65	Kyanite	Intermediate between biotite schist and hornfels. There is a slight alignment of biotite, but texture is mostly granoblastic. Biotite is red, iron-rich.
Biotite	15	Sillimanite	
Magnetite	10	Apatite	

Rock number: 113-694C-4X-1, 7–8 cm

Name: amphibole-biotite gneiss

Size: 3 × 3 cm

Depth: 198.67 mbsf

Shape: subangular

Weathering: none

Major minerals	%	Accessory minerals	Comments
Quartz	20	Carbonate	Dark green biotite and amphibole; biotite predates amphibole, and both poikilitically enclose quartz. Strong pleochroic halo occurs around zircon.
Plagioclase	50	Sphene	
Orthoclase	10	Sericite	
Amphibole	10	Zircon	
Biotite	7		

Rock number: 113-694C-21X-CC, 2–6 cm

Name: pyroxene tholeiite

Size: 6 × 6 cm

Depth: 363.82 mbsf

Shape: subrounded

Weathering: none

Major minerals	%	Accessory minerals	Comments
Augite	30	Epidote	Aphyric basalt. Chlorite patches indicate phenocryst replacement and vesicles. Sphene and epidote occurs in chlorite pools. Clinopyroxenes are granular and unaltered.
Plagioclase	30	Sphene	
Pigeonite	10	Sericite	
Chlorite	25		

^a If the major mineral percentage does not equal 100, the accessory minerals make up the additional component.

Table 4. Index properties, water content, porosity, bulk density, and grain density measured on samples from Site 694.

Core, section, top (cm)	Depth (mbsf)	Water content		Porosity (%)	Bulk density (g/cm ³)	Grain density (g/cm ³)
		(% wet weight)	(% dry weight)			
113-694A-						
1H-7, 5	9.1	44.33	79.63	69.02	1.59	2.57
1H-7, 24	9.2	44.80	81.15	69.98	1.60	2.59
1H-7, 44	9.4	45.39	83.13	71.90	1.62	2.75
113-694B-						
1H-3, 92	3.9	44.57	80.41	70.10	1.61	2.51
2H-2, 111	8.1	42.80	74.84	69.74	1.67	2.54
2H-4, 111	11.1	45.70	84.15	71.01	1.59	2.71
2H-6, 111	14.1	43.65	77.47	69.94	1.64	2.90
3H-2, 122	17.8	39.70	65.83	68.23	1.76	2.74
3H-2, 130	17.9	43.38	76.61	68.53	1.62	2.31
5X-1, 91	35.4	34.93	53.67	62.98	1.85	2.45
19H-1, 13	136.2	29.74	42.32	56.22	1.94	3.03
22X-1, 122	151.6	30.50	43.89	56.36	1.89	2.88
22X-2, 106	153.0	38.03	61.37	63.85	1.72	2.83
23X-1, 130	161.3	35.67	55.45	60.85	1.75	2.64
23X-2, 130	162.8	35.23	54.40	60.22	1.75	2.68
23X-3, 84	163.8	27.75	38.40	51.88	1.92	2.98
23X-5, 138	167.4	27.63	38.17	52.25	1.94	2.86
24X-1, 97	170.6	32.18	47.45	56.94	1.81	2.80
24X-3, 85	173.5	25.38	34.01	49.11	1.98	2.73
113-694C-						
2X-1, 86	180.1	28.62	40.09	55.43	1.98	3.00
2X-CC, 10	181.9	20.02	25.03	40.84	2.09	2.73
3X-1, 12	189.0	20.93	26.47	40.91	2.00	2.59
5X-1, 103	209.9	29.92	42.69	55.94	1.92	3.00
5X-2, 80	211.2	13.97	16.25	30.32	2.22	2.69
5X-CC, 52	212.1	26.11	35.34	50.64	1.99	2.79
6X-1, 0	217.9	29.59	42.03	46.86	1.62	2.79
6X-1, 132	219.2	27.60	38.13	52.50	1.95	2.74
6X-4, 53	222.9	31.79	46.61	55.57	1.79	2.66
6X-CC, 20	225.2	30.83	44.58	60.90	2.02	2.93
8X-1, 17	237.1	27.19	37.34	54.16	2.04	2.95
9X-1, 76	247.3	28.53	39.92	53.43	1.92	2.72
10X-2, 75	258.4	35.92	56.05	61.84	1.76	2.71
11X-1, 121	266.7	28.64	40.13	54.41	1.95	2.78
11X-CC, 3	268.3	34.92	53.66	59.75	1.75	2.40
12X-1, 18	275.7	26.54	36.13	50.73	1.96	2.83
12X-CC, 31	277.7	9.92	11.01	23.11	2.39	2.69 Sand
13X-1, 55	285.7	31.49	45.96	57.15	1.86	2.71
14X-1, 77	295.5	33.14	49.56	58.16	1.80	2.66
15X-1, 19	304.5	26.46	35.98	49.57	1.92	2.56
17X-CC, 20	329.3	29.79	42.43	54.01	1.86	2.59
18X-1, 60	333.9	30.69	44.27	59.63	1.99	3.01
19X-3, 91	346.9	27.88	38.67	54.64	2.01	2.94
20X-CC, 7	354.9	25.83	34.83	52.33	2.08	2.91
21X-1, 16	362.5	29.06	40.95	55.48	1.96	2.85
22X-CC, 20	378.6	29.18	41.20	54.19	1.90	2.74
23X-1, 7	381.7	29.99	42.83	57.82	1.98	2.57

insufficient physical-property data to characterize the site in detail. There are, however, sufficient data to assign specific geotechnical properties to the four major and five minor lithostratigraphic units (Fig. 3, Table 2).

The range and average values of the index properties, bulk density, water content, grain density, and porosity in lithostratigraphic Unit I (0–21.1 mbsf) are as follows:

	range		
	low	high	average
bulk density (g/cm ³)	1.59	1.76	1.64
water content (%)	65	80	76.5
grain density (g/cm ³)	2.31	2.71	2.61
porosity (%)	68	71	70

In general the hemipelagic sediments of Unit I are marked by high water content, high porosity, and a fluctuating grain density. The rate of increase (gradient) for bulk density, from 0 to 179.2 mbsf, (Unit 1-Subunit IIIB) is $0.0016 \text{ g/cm}^3/\text{m}$. The water content decreases $0.19\%/ \text{m}$ over the same interval and porosity decreases $0.086\%/ \text{m}$.

Only one sample was measured in lithostratigraphic Unit II and Subunit IIIA (Table 4).

Lithostratigraphic Subunit IIIB (150.4–179.2 mbsf) consists of sediments with the following geotechnical characteristics:

	range		
	low	high	average
bulk density (g/cm^3)	1.72	1.99	1.84
water content (%)	34	61	46
grain density (g/cm^3)	2.64	2.98	2.80
porosity (%)	49	64	56

The rate of increase and decrease with depth (gradients) of the index properties in lithostratigraphic Subunit IIIB is similar to the values obtained for Unit I.

Sediments of lithostratigraphic Subunit IIIC (179.2–208.3 mbsf) have the lowest water content and porosity and the highest bulk density of all sediments at Site 694. A summary of the geotechnical characteristics are as follows:

	range		
	low	high	average
bulk density (g/cm^3)	2.00	2.00	2.00
water content (%)	25	27	26
grain density (g/cm^3)	2.59	2.73	2.66
porosity (%)	41	41	41

The largest number of geotechnical tests were made on sediments from Lithostratigraphic Subunit IIID (208.3–298.2 mbsf). A summary of the results are as follows:

	range		
	low	high	average
bulk density (g/cm^3)	1.62	2.04	1.88
water content (%)	36	56	43
grain density (g/cm^3)	2.40	3.00	2.76
porosity (%)	47	61	55

The gradients of the index properties of this unit are essentially zero or slightly positive for water content and porosity, and zero to slightly negative for bulk density.

The geotechnical properties of lithostratigraphic Unit IV (304.3–391.3 mbsf) are summarized as follows:

	range		
	low	high	average
bulk density (g/cm^3)	1.86	2.03	1.96
water content (%)	35	44	40
grain density (g/cm^3)	2.56	3.01	2.77
porosity (%)	50	60	55

The gradients of porosity and water content are slightly positive and bulk density slightly negative.

Discussion

The geotechnical nature of the various lithostratigraphic divisions of Site 694 has been described. A large decrease in porosity and water content is exhibited at 150 mbsf. From that depth to the total depth drilled (391.3 mbsf), the geotechnical

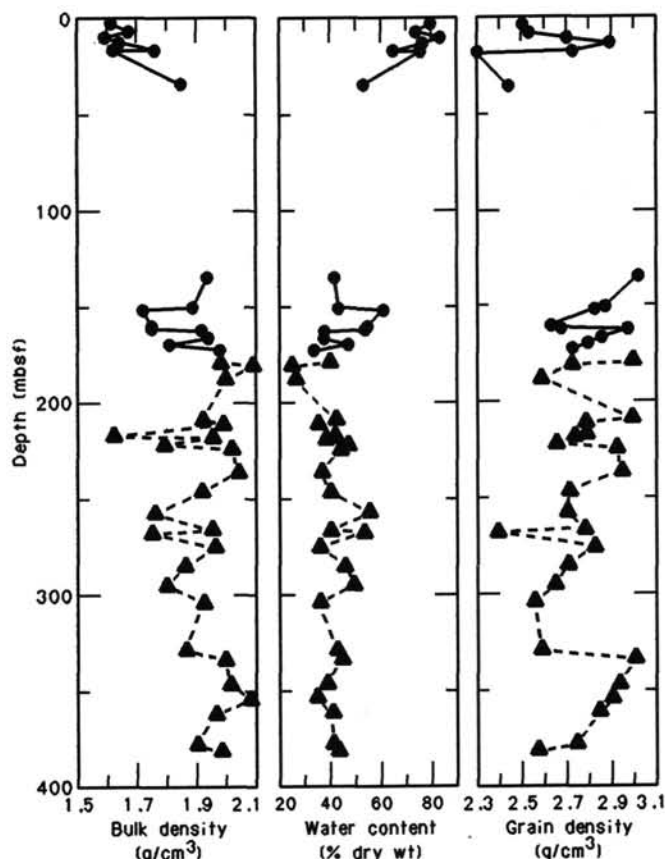


Figure 17. Profile of bulk density, water content, and grain density, Site 694. Dots = Hole 694B sediments; triangles = Hole 694C.

properties, except within Subunit IIIC, remain essentially constant. The bulk density increases only slightly with increasing depth. Stationary conditions or increasing water content and porosity with depth may reflect an increase in the siliceous biogenic character of the sediments that override part of the compacting effect of the overburden. The increase in water content and porosity with depth are associated with a decrease in grain density, which, in this area, usually reflects increasing diatom content.

Shear Strength

The undrained shear strength of the sediment was determined using the ODP Motorized Vane Shear Device. Standard 1.2-cm equidimensional miniature vanes were used with the device. Its operation and calculations follow procedures outlined in the ODP Physical Properties Handbook. Strength measurements were made on the least disturbed sections of the cores.

The shear strengths determined for Site 694 are listed in Table 5 and illustrated in Figure 19. Few strength measurements were made due to the disturbed conditions of the core. The line of best fit through the strength data (Fig. 19) translates into a shear strength gradient of 0.56 kPa/m .

Compressional Wave Velocity

Sonic velocity (V_p) in sediments are measured using two methods. First, a continuous measurement of V_p was made through the unsplit core using a P -Wave Logger (PWL) installed next to the GRAPE source and detector. Second, measurements were made on individual samples removed from the core with one measurement from every other core section. Velocity was mea-

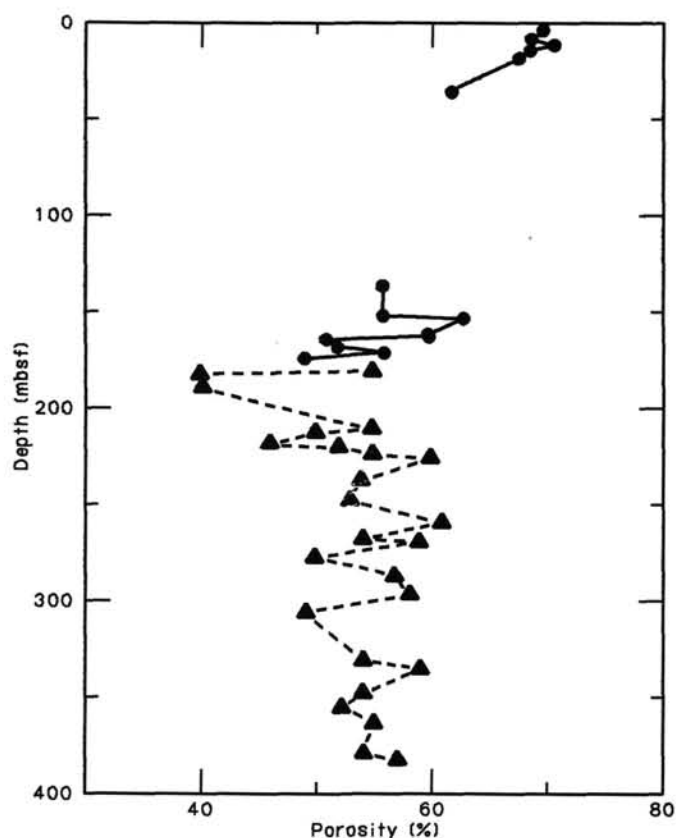


Figure 18. Profile of porosity, Site 694. Dots = Hole 694B; triangles = Hole 694C.

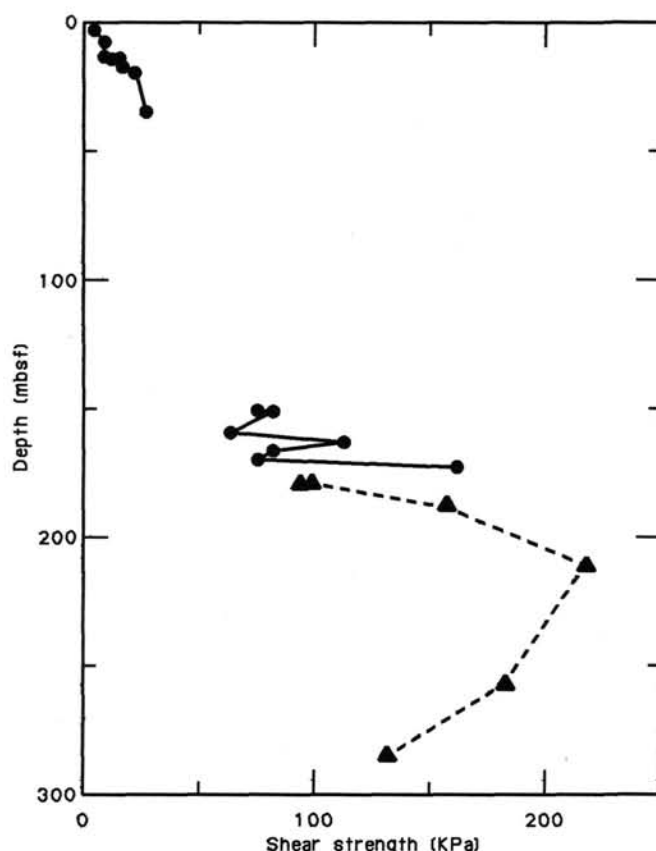


Figure 19. Undrained shear strength profile, Site 694. Dots = Hole 694B sediments; triangles = Hole 694C.

Table 5. Undrained shear strengths determined on samples from Site 694.

Core, section, top (cm)	Depth (mbsf)	Shear strength (kPa)
113-694B-		
1H-3, 82	3.8	3.7
2H-2, 121	8.2	8.1
2H-2, 130	8.3	8.1
2H-6, 105	14.1	8.1
2H-CC, 2	14.8	14.7
2H-CC, 8	14.9	11.6
2H-CC, 10	14.9	8.6
3H-2, 141	18.0	16.3
3H-2, 142	18.0	16.1
3H-4, 95	20.6	21.6
5X-1, 83	35.8	26.3
22X-1, 122	151.6	74.5
22X-2, 18	152.1	81.4
23X-1, 34	160.3	62.8
23X-3, 94	163.9	111.7
23X-5, 115	167.2	81.4
24X-1, 101	170.6	74.5
24X-3, 90	173.5	160.6
113-694C-		
2X-1, 90	180.1	97.7
2X-1, 134	180.5	93.1
3X-1, 16	189.1	155.9
5X-CC, 6	211.9	216.4
10X-2, 57	258.2	181.5
13X-1, 83	285.9	130.3

sured in only one direction, usually horizontal to the long axis of the core.

The results of velocity measurements made on the Hamilton Frame are listed in Table 6 and illustrated in Figure 20. The average velocity of the sediments in the various lithostratigraphic units are as follows:

Lithostratigraphic	Unit I	1483 m/s
	Unit II	1532 m/s
	Subunit IIIB	1550 m/s
	Subunit IIIC	1610 m/s
	Subunit IIID	1620 m/s
	Unit IV	1666 m/s

Velocity at Site 694 increases with depth, in a more or less constant fashion, and has a gradient of 0.61 m/s/m. The highest mudstone velocities measured are 2481 m/s at 295.5 mbsf and 1717 m/s at 381.7 mbsf. Sandstone (dropstone) velocity measured 4290 m/s. The siliceous siltstone recovered at the very base of Hole 694C had a velocity of 4130 m/s.

An analysis of the PWL data shows close agreement with velocities measured with the Hamilton Frame. A detailed examination of the PWL data was not undertaken, but preliminary examinations indicate that the data are excellent. The PWL results for Core 113-694A-1H (Fig. 21). It shows that the near-sea-floor muds have velocities less than that of sea water (~1500 m/s). The high velocities in the figure are associated with sand layers. Within the upper 9.5 m of Hole 694A, the velocity gradient is 3.7 m/s/m, six times the average gradient for Site 694.

Table 6. Compressional wave velocities (Hamilton Frame) measured on samples from Site 694.

Core, section, top (cm)	Depth (mbsf)	Velocity (m/s)	Remarks
113-694B-			
1H-3, 92	3.9	1485	
2H-2, 111	8.1	1485	
2H-4, 111	11.1	1482	
2H-6, 111	14.1	1500	
3H-2, 122	17.8	1490	
3H-2, 130	17.9	1460	
5X-1, 91	35.4	1532	
22X-1, 122	151.6	1574	
23X-1, 130	161.3	1514	
23X-3, 130	162.8	1478	
23X-3, 84	163.8	1584	
23X-5, 138	167.4	1565	
24X-1, 97	170.6	1546	
24X-3, 85	173.5	1589	
113-694C-			
2X-1, 86	180.1	1581	
3X-1, 12	189.0	1640	
5X-1, 103	209.9	1564	
5X-2, 80	211.2	1788	
6X-1, 0	217.9	1552	
6X-2, 134	220.7	1588	
6X-4, 53	222.9	1597	
6X-CC, 20	225.2	1738	
8X-1, 17	237.1	1654	
10X-2, 75	258.4	1570	
13X-1, 55	285.7	1536	
14X-1, 77	295.5	2481	Mudstone
15X-1, 19	304.5	1712	
17X-CC, 20	329.3	1628	
18X-1, 2	333.3	4290	Sandstone
19X-3, 91	346.9	1698	Mudstone
22X-CC, 20	378.6	1575	
23X-1, 7	381.7	1717	
23X-2, 137	384.5	4130	Siliceous siltstone

Thermal Conductivity

As mentioned in the "Explanatory Notes" chapter (this volume), the thermal conductivity is measured by the needle-probe method (Von Herzen and Maxwell, 1959). A needle probe was inserted through a drill hole in the core liner so that the probes were orientated perpendicular to the core axis. If there was not sufficient time to allow the core to come to thermal equilibrium, due to the necessity of splitting the cores to examine for gas, etc., "oblique" and "end" insert methods were used on the split cores. "Oblique" insert method means that the probe was inserted obliquely from the surface of the split core. "End" insert method means that the probe was inserted into the end of the core, so that the probes were oriented parallel to the core axis. Results of the thermal conductivity measurements are listed in Table 7.

The results of the thermal conductivity range from 1.099 to 1.379 W/m-k. We could not identify significant differences among the test methods. Furthermore, the difference between what we call "normal" and "end" methods is within 5% (Suess, von Huene, et al., 1988, "Physical Properties" section).

Summary

The characteristics of the physical properties at Site 694 are rather poorly defined due to the disturbed nature of the cores and the abundance of sandy sediments. There are, however, sufficient data to assign a characteristic geotechnical profile for the various lithostratigraphic units of Site 694.

Lithostratigraphic Unit I contains high water content, high porosity, and low bulk-density sediment with compressional

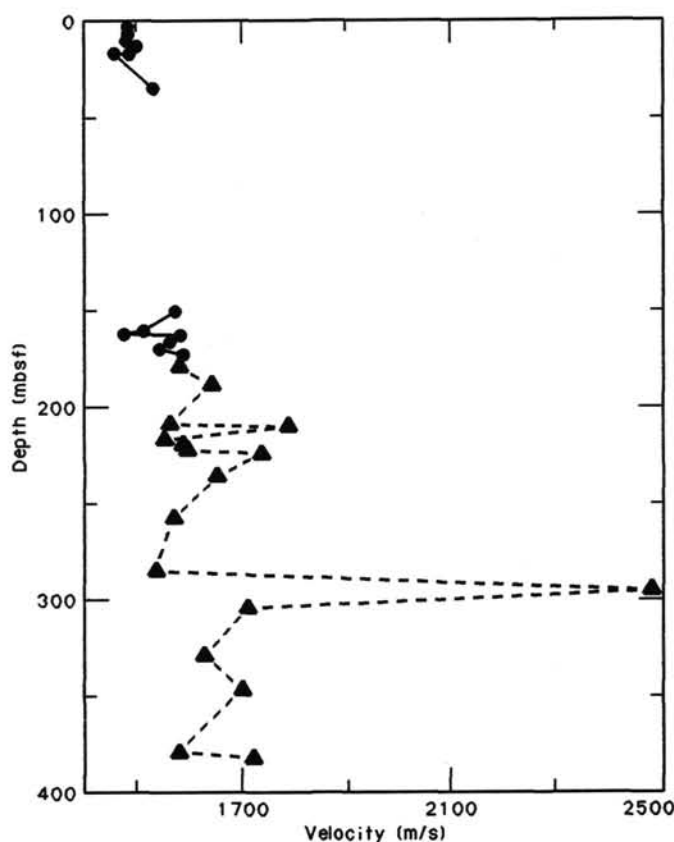


Figure 20. Compressional wave velocity (Hamilton Frame) for Site 694. Dots = Hole 694B; triangles = Hole 694C.

wave velocities less than that of seawater. Lithostratigraphic Unit II was not sampled due to its high sand content. Lithostratigraphic Subunit IIIB consists of a diatom-bearing mud with an average porosity of 56% and an average velocity of 1550 m/s. Lithostratigraphic Subunit IIIC contains muds, silty-muds, and silt with an average porosity of 41% and an average velocity of 1610 m/s. This unit exhibits the lowest porosity of Site 694. Lithostratigraphic Subunit IIID, a diatom-rich mud, contains a sediment with a porosity of 56% and an average velocity of 1620 m/s. Lithostratigraphic Subunit IV is a diatom-rich semilithified sediment with an average porosity of 55% and an average velocity of 1666 m/s. In Lithostratigraphic Subunit IIID and Unit IV, the porosity and water content increased slightly with depth. This increase probably reflects an increase in diatom content and the disturbed conditions of the cores. The shear strength at Site 694 increased at an average rate of 0.56 kPa/m. The average thermal conductivity in the upper 16 mbsf of the site is 1.294 W/m-k.

SEISMIC STRATIGRAPHY

The seismic stratigraphic aspects of drilling at Site 694 are straightforward, if only because less than half of the planned penetration was achieved, recovery was low, and none of the holes were logged.

The site was originally located on multichannel seismic reflection profile AMG845-015 (British Antarctic Survey/University of Birmingham), at shotpoint (SP) 12400 (Fig. 2A). It lies in an area of moderately elevated, 90-m.y.-old basement. The site was located thus because the bedding is to some extent draped over the the basement topography, so that the depth to any particular reflector is reduced over a basement high. Since the drill-

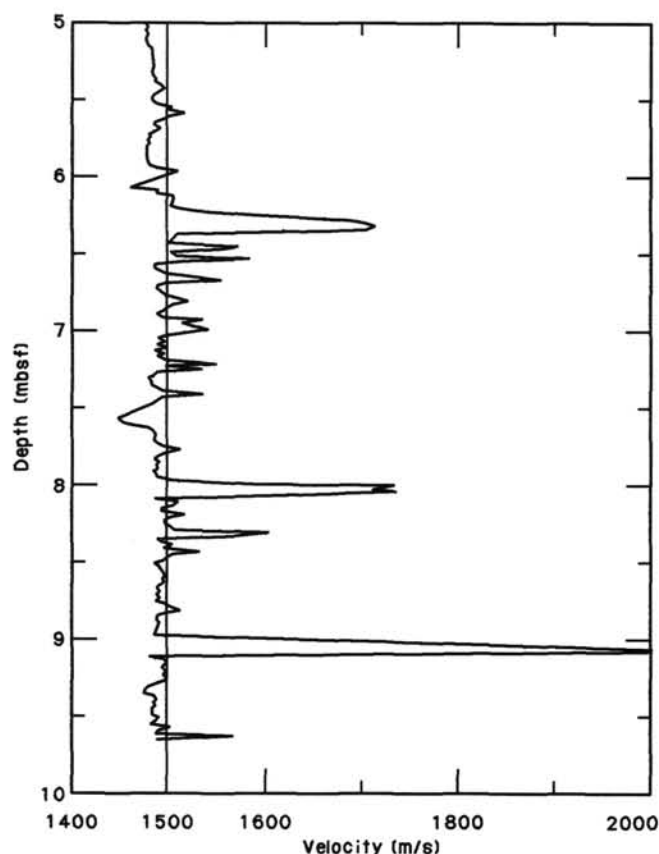


Figure 21. Velocity profile from *P*-wave logger data for Core 113-694A-1H.

ing targets all concerned sediments significantly younger than basement, some beneficial reduction in the total drilling depth seemed likely to accrue. The draping is considered to be an effect of differential compaction of mixed hemipelagic and turbiditic sediments, rather than an indication of pelagic deposition.

JOIDES Resolution's approach to Site 694 was made without benefit of Global Positioning Satellite (GPS) navigation, and the beacon was dropped about 1.8 km north of the chosen site. The single-channel water-gun record (Fig. 22) obtained during the approach did not show oceanic basement, but did show

some doming of the deeper sediments, suggesting that the basement high lay beneath them. For that reason, and because oceanic basement reflectors at a total depth of about 7.5 s twt are not precisely imaged by nonmigrated two-dimensional sea-surface profiling, it was considered sufficiently close to offset 450 m south of the beacon (1350 m north of the original site location).

The lithologies sampled at Site 694 included hemipelagic clays and muds with ice-rafted detritus, fine-grained turbidites, and very coarse to coarse sand turbidites. Recovery was poor, possibly because of the thick, coarse beds. The cored sediments were often disturbed. PWL data reflected this situation, being reduced in both quantity and reliability. Measured velocities in the clays and muds were mainly lower than those predicted by the velocity-depth curve of Carlson et al. (1986), and other physical properties were similarly indicative of sediment disturbance during the coring process (see "Physical Properties" section, this chapter). However, velocities in the sandy basal sections of turbidites were typically as much as 200 m/s higher than in the surrounding hemipelagic sediments, reflecting the low porosity of a well-sorted sand (see, for example, Fig. 23). Thus, it was difficult to establish with confidence a valid velocity-depth model. An unknown but probably large part of the sediment not recovered was high-velocity well-sorted sand, whereas measured clay and mud velocities were probably lower than *in-situ* values. A sonic log of the deepest hole would have resolved all of these uncertainties, but this was prevented by the XCB jamming in the bit, causing the hole to be abandoned.

A velocity was assigned to each unit or subunit (depth intervals averaged) on the basis of the PWL measurements and subjective judgments as to the degree of disturbance seen and the nature of the unit, as follows:

Unit	Depths (mbsf)	Velocity (m/s)
I	0–20	1520
II	20–110	1700
IIIA	110–150	1700
IIIB	150–180	1600
IIIC	180–250	1640
IIID	250–295	1700
IIIE	295–305	1800
IV	305–380	1700

The velocity-depth and consequent time-depth model derived from these imperfect data are as much as 4% faster than the model of Carlson et al. (1986) down to 150 m, as a result of the well-sorted sand turbidites in Units II and IIIA, but converge upon that model at greater depths and virtually coincide at the base of the hole. This derived model has an uncertainty of 2% or 3% at least, but the result is reasonable compared with previous Leg 113 sites, which were slightly slower than the model of Carlson et al. (1986) but lacked the sands found at Site 693.

Figure 24 shows the lithologic units compared with the *JOIDES Resolution* profile approaching the site. The comparison is surprisingly close, with many of the lithologic units having distinctive reflection characteristics and with unit boundaries coinciding with changes in reflection character. The multi-channel seismic profile was not used because of the 1.35-km offset of the site, but it shows similar features, with a barely perceptible difference in depth.

The model predicts a two-way traveltime of 460 ms to the base of the recovered sediment at 391.3 mbsf. Hole 694C was abandoned when the XCB could not be recovered. It had failed as a result of drilling several meters through a much harder sediment than had been encountered previously. When the BHA came on deck, a thin silicified claystone lay at the bottom of the section recovered. If this is representative of one or more thicker

Table 7. Thermal conductivities of sediments from Site 694.

Core, section, top (cm)	Depth (mbsf)	K (W/m-K)	Remarks (direction, heating time)
113-694A-			
1H-7, 0	9.0	1.134	End method 4 min #1
1H-7, 10	9.1	1.119	Oblique 4 min #2
1H-7, 0	9.0	1.203	Oblique 4 min #3
1H-7, 10	9.1	1.133	Same as #1 #4
1H-7, 0	9.0	1.215	End method 4 min #5
			Slightly different position
1H-7, 20	9.2	1.211	Oblique 4 min #6
1H-7, 40	9.4	1.114	Oblique 6 min #7
1H-7, 50	9.5	1.099	Oblique 6 min #8
113-694B			
1H-3, 86	3.9	1.351	
1H-3, 90	3.9	1.206	
2H-3, 90	9.4	1.379	
3H-1, 90	16.0	1.241	

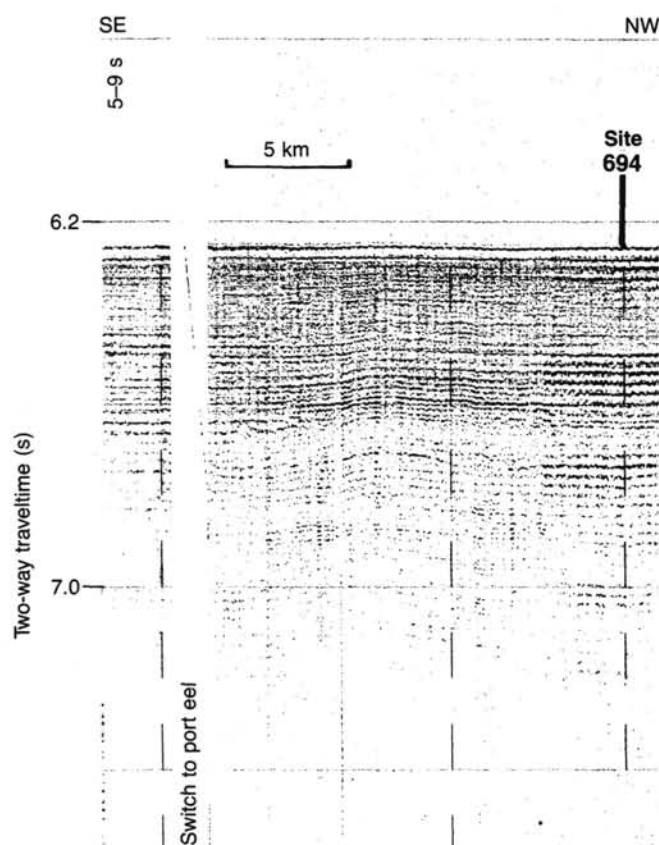


Figure 22. Single-channel seismic profile obtained by JOIDES Resolution during approach to Site 694.

beds, then they coincide with the strong reflector at 460 ms. This reflector is the strongest in the entire seismic section near the site, and is of regional extent, so its identification should prove useful for regional investigations. Also, if this identification is correct, then the time-depth model is also reasonably accurate, and the times to the other lithologic boundaries are known.

The seabed reflector is weak, which is reasonable for the low density and velocity of the mainly hemipelagic Unit I. It does contain thin graded beds with higher velocities (Fig. 23) but, being thin, these are not well-imaged at the much longer wavelengths of the water-gun system. Stronger reflectors occur beneath 26 ms, at the top of and within the massive sand turbidite sequence of Unit II. After 70 ms (56 mbsf), there are no further strong reflections before 216 ms, the top of Subunit IIIC. Although these units are poorly recovered, the progressive change in their nature is clear; the massive, coarse sandy turbidites of Unit II give way to more fine-grained turbidites in IIIC and to the more hemipelagic Subunit IIIB. Essentially these changes may be in the fine-scale structure, with thin graded sands and silts still abundant, so that the gross physical properties do not vary greatly.

Subunits IIIC, IIID, and IIIE between 216 and 366 ms are much more reflective. Reported bulk densities (see "Physical Properties" section, this chapter) vary more within this interval than elsewhere, so there may be compositional changes (diatom content perhaps) or changes in fine-grained turbidite abundance, of a sufficiently long wavelength to interact with the seismic source, but not capable of precise definition with the recovery obtained. Subunit IIIE, a curious, thin, poorly-sorted glacio-marine sequence, with a high seismic velocity, has its own sepa-

rate reflection. The reflectivity of the overlying unit does not extend into Unit IV, which is mainly hemipelagic except at the base.

The degree of coincidence between lithologic units (independently arrived at) and the reflectivity is remarkable. The precise explanation for that reflectivity, however, seems to lie in characteristics beyond our grasp with this recovery, such as the cyclicity or wavelength of a compositional or structural variation, rather than the nature of any one or other component. This will be the case particularly for those sediments having high inherent variability, such as mixed turbidite and hemipelagic sequences. This being so, we might expect the reflectivity to be different for seismic sources of different frequency ranges, and to change along a profile as, for example, proximity to a source changes. Such variations could be interesting to pursue.

BIOSTRATIGRAPHY

Site 694 was drilled in the Weddell Sea abyssal plain in 4664 m of water to examine the Cenozoic history of bottom-water fluctuations, especially the development and subsequent history of the Weddell Sea Bottom Water. The uppermost part of Hole 694B recovered Quaternary and Pliocene hemipelagic muds and turbidites. Recovery in Holes 694B and 694C was approximately 30%, and the sediments were commonly very disturbed. The poor recovery and sediment conditions are attributed to the type of sediments encountered (turbiditic sequences with medium- to coarse-grained sands and hemipelagic clays, and occasional dropstones). Hole 694B was abandoned at 179.2 mbsf after reaching the upper Miocene (*Denticulopsis hustedtii* Zone). Hole 694C was washed down to 179.2 mbsf and then cored to 391.3 mbsf, with basal sediments dated as middle Miocene (*Nitzschia grossepunctata* Zone).

Biostratigraphic age assignments are based on siliceous microfossils (diatoms, silicoflagellates, and radiolarians). No calcareous microfossils or unreworked palynomorphs were recovered.

All depths referred to in meters are sub-bottom depths (mbsf) and, unless otherwise stated, samples are from the core-catcher section. On the summary biostratigraphic chart (Fig. 25), the age or biostratigraphic zone assigned to a given core catcher is extrapolated to the midpoint of the overlying and underlying core. The section is always described from the top down.

Planktonic Foraminifers

No planktonic foraminifers were recovered at this site.

Benthic Foraminifers

All core-catcher samples from Hole 694B, Sections 113-694C-2X, CC, through 113-694C-8X, CC, and 113-694C-23X, CC, were processed and residues examined for benthic foraminifers; all samples were barren. No carbonate-rich intervals were found in the cores. Core-catcher samples from the lower cores in Hole 694C (except Section 113-694C-23X, CC) were not received in the on-board paleontology laboratory. A few samples from turbidites were examined but did not contain benthic foraminifers.

The absence of calcareous and arenaceous benthic foraminifers from all samples from Site 694 (water depth 4653 m) is in agreement with the results from DSDP Sites 322 through 325 (water depths 3700–5000 m, Bellingshausen abyssal plain), where middle Miocene or younger sediments (the interval recovered at Site 694) were barren. Arenaceous benthic foraminifers were found only in sediments dated as Oligocene?–early Miocene and older (Roegl, 1976), and rare calcareous benthic foraminifers were found only in turbidites at the shallowest site (Site 325 at 3700 m).

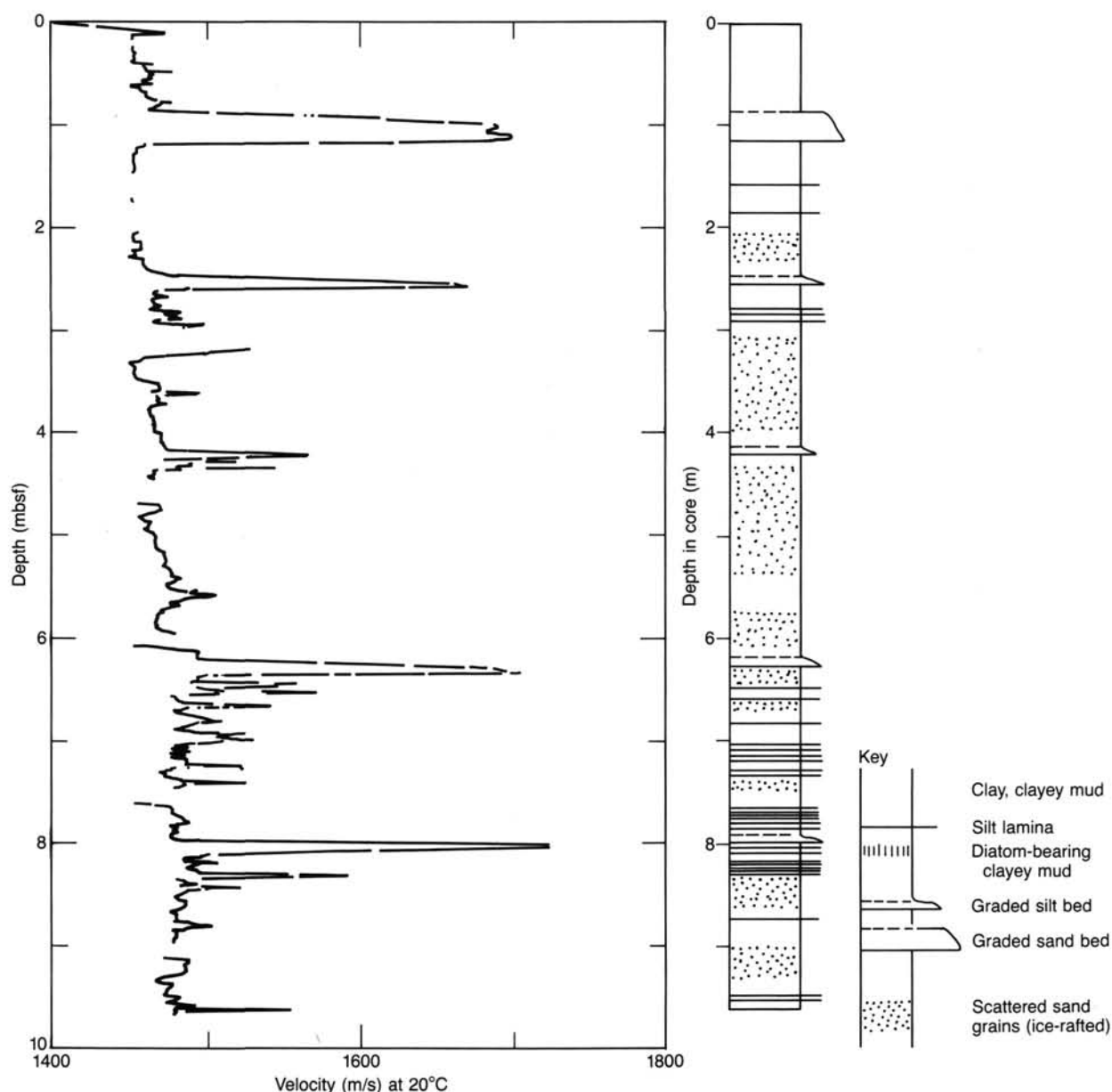


Figure 23. Comparison of *P*-wave logger sediment velocities and observed lithology in Core 113-694A-1H, showing high velocities in sandy intervals.

Calcareous Nannofossils

All core-catcher samples plus a generous number of samples taken within cores from this site were examined for calcareous nannofossils. All samples were barren. The results are incorporated in the "Biostratigraphic Summary" at the end of this section, and they compare quite favorably with those obtained by Haq (1976) for sediments of comparable age from the Belling-shausen abyssal plain where a similar sedimentary sequence was encountered (Sites 322 and 323).

Diatoms

Hole 694A

Hole 694A was abandoned after recovery of the first core because the sediment/water interface was not sampled. Section 113-694A-1H, CC, contains common, moderately preserved dia-

toms. The sample is placed in the lower Pliocene *Nitzschia angulata*/*N. reinholdii* Zone based on the joint occurrence of *Nitzschia praeinterfrigidaria* and *N. angulata*. In addition, *Thalassiothrix frauenfeldii*, *T. longissima*, *Rhizosolenia barboi*, fragments of *Ethmodiscus rex*, *Rouxia heteropolara*, and rare specimens of *Nitzschia angulata* (O'Meara) Hasle (compare taxonomic note in the "Biostratigraphy" section, "Site 689" chapter, this volume), *Denticulopsis hustedtii*, and *Thalassiosira torokina* are present. A number of samples taken from levels above the core catcher are barren of diatoms.

Hole 694B

Cores 113-694B-1H through 113-694B-15H sampled a 122.5 m thick, largely turbiditic sequence. Recovery was continuous only in the topmost three cores and dropped considerably below that because of the occurrence of medium- to coarse-grained sands.

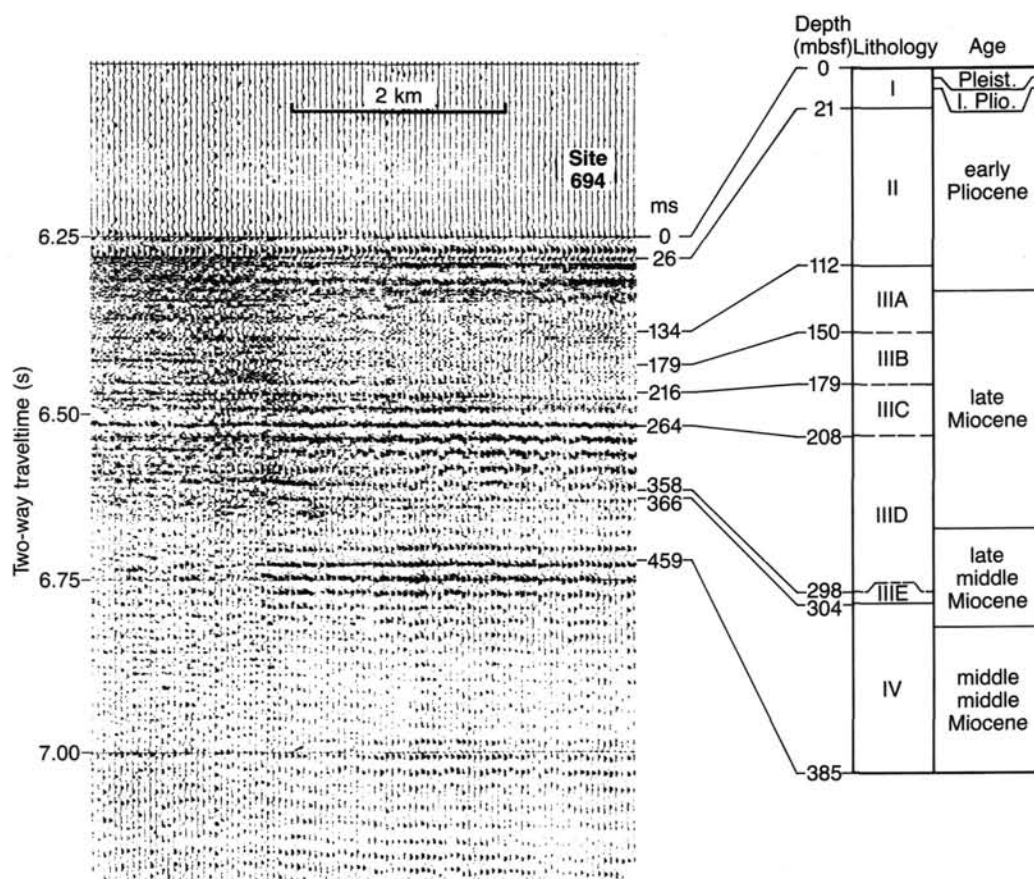


Figure 24. Comparison of lithologic units at Site 694 with digital playback of profile obtained on *JOIDES Resolution's* approach.

Within the upper 122.5 m of Hole 694B only two short sediment intervals contain moderate to well-preserved diatom assemblages. At 113-694B-2H-5, 37 cm (13.37 mbsf), an assemblage similar to that recovered in Section 113-694A-1H, CC, indicates an early Pliocene age (*Nitzschia angulata*/*N. reinholdii* Zone). This age is compatible with the magnetostratigraphy, which places this interval within the upper portion of Chron C3.

The second diatom-bearing interval is at 113-694B-14H-1, 30 cm (112 mbsf), and contains *Denticulopsis hustedtii*, *D. dimorpha* (very rare and probably displaced), *Thalassiosira torokina*, *Cosmiodiscus intersectus*, *Nitzschia angulata*, *N. praeinterfrigidaria* (very rare), and *Cosmiodiscus insignis* forma *triangula*. This assemblage indicates an age just above the Miocene/Pliocene boundary. *T. torokina* ranges within the lowermost Pliocene (middle and lower portion of the C3 Chron; Brady, 1977) whereas *C. insignis* f. *triangula* straddles the Miocene/Pliocene boundary (lowermost Chron C3 to lower C3A Chron; Ciesielski, 1983).

Within the interval from 122.5 to 179.2 mbsf of Hole 694B, moderately preserved diatoms were found only in Core 113-694B-24X. The cores above this level are barren of diatoms, or have rare to few and poorly preserved diatoms. The occurrence of *Denticulopsis hustedtii* places Cores 113-694B-22X through 113-694B-24X within the upper Miocene *D. hustedtii* Zone. In Sample 113-694B-24X-4, 75 cm, to Section 113-694B-24X, CC (174.8–179.2 mbsf), a *Denticulopsis dimorpha* acme occurs. In previous sites of Leg 113 a similar acme occurs in the lower part of the *D. hustedtii* Zone. Other species in the latter interval include *D. praedimorpha*, *Nitzschia claviceps*, *Trinacria excavata*, *Actinocyclus ingens*, *Stellarima microrias*, and very rare *Denticulopsis lauta*.

Hole 694C

Hole 694C was washed down to 179.2 mbsf. The core catcher of 113-694C-1W contains a diatom assemblage rich in *Denticulopsis dimorpha*, similar to the assemblage encountered in the lower portion of Core 113-694B-24X. Most of the fine-grained (clay-silt) sediment intervals recovered in Hole 694C (179.2–391.3 mbsf) contain rare to common, poor to moderately preserved diatoms. Indeed, it is difficult to assign established southern-high-latitude diatom zones (Weaver and Gombos, 1981) to the recovered sediment interval because of rare and scattered occurrences of key Miocene biozonal marker species such as *Denticulopsis lauta*, *D. maccollumii*, *Nitzschia denticuloides*, and *N. grossepunctata*. We can only make preliminary age assignments because the stratigraphic ranges of some species are still not well understood and because the patterns of occurrence of some species are not consistent. For this reason, it is difficult to resolve problems related to the displacement of diatom marker species via turbidity currents or bottom water activity. Displacement of diatoms is apparent by the occurrence, in many samples, of neritic species (e.g., *Actinocyclus senarius*, *Melosira* spp., and benthic species) or Paleocene species.

Two species consistently occur in the diatom-bearing samples: *Denticulopsis hustedtii* and *Actinocyclus ingens*. *D. hustedtii* is more abundant in the upper part of the cored interval (Cores 113-694C-6X through 113-694C-11X), whereas *A. ingens* is abundant in the middle part (Cores 113-694C-10X through 113-694C-18X). The occurrence of *D. hustedtii* indicates a possible age range for the entire sequence drilled in Hole 694C of upper Miocene to middle middle Miocene (including the lowermost *D. hustedtii* Zone, the *D. hustedtii*/*D. lauta* Zone, the

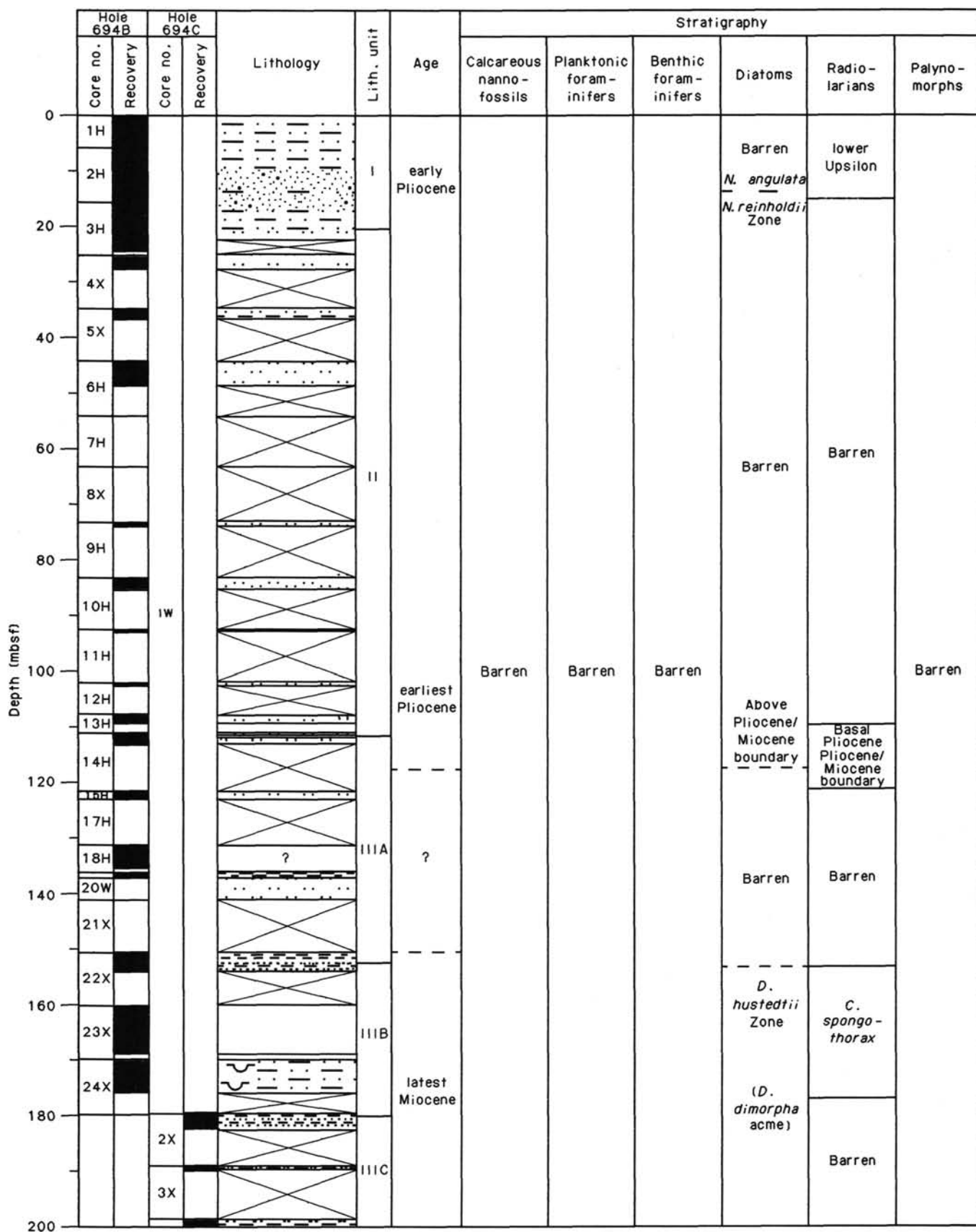


Figure 25. Biostratigraphic summary, Site 694.

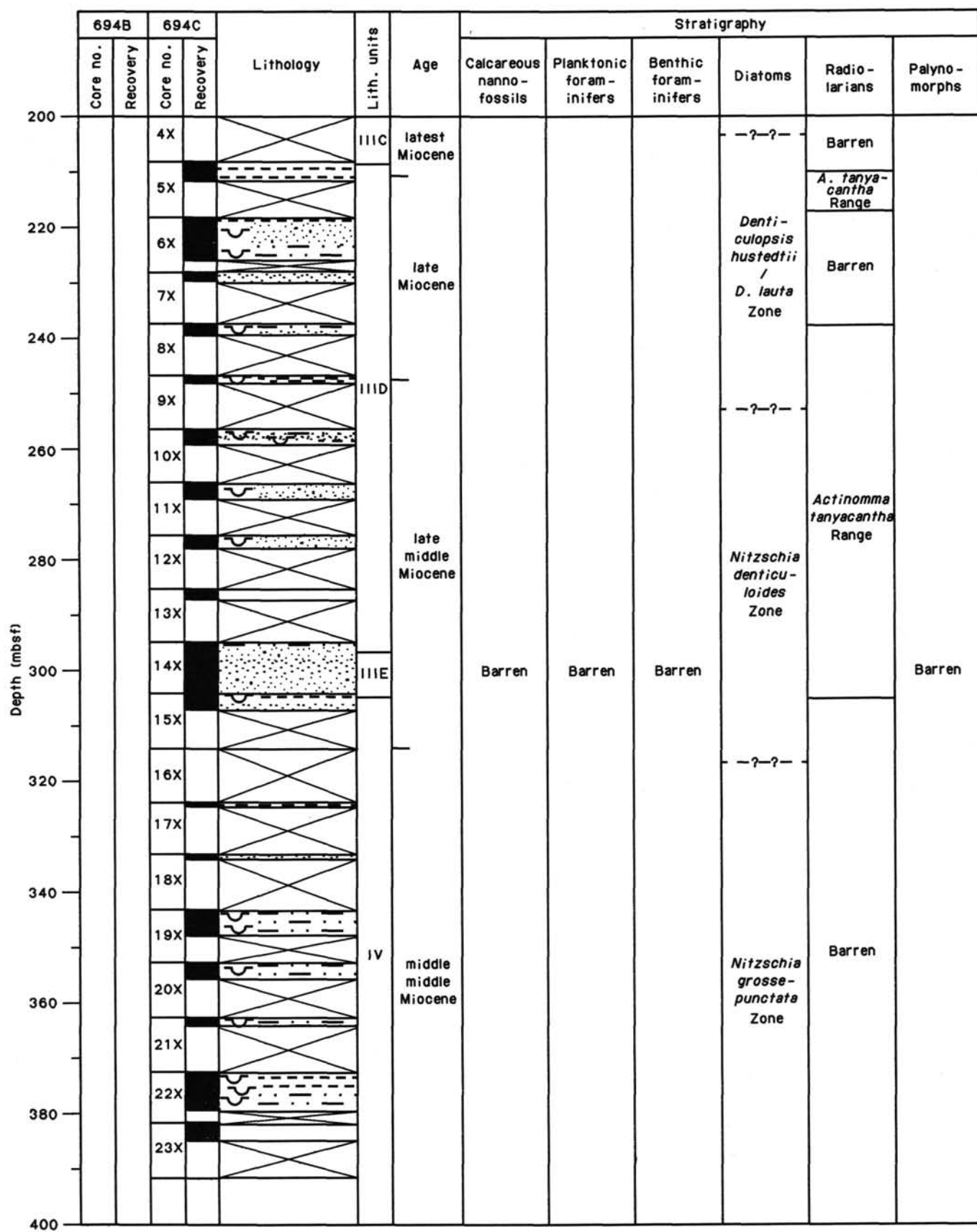


Figure 25 (continued).

Nitzschia denticuloides Zone, and the upper part of the *N. grossepunctata* Zone).

We assume that Cores 113-694C-2X through 113-694C-4X represent an interval within the lowermost *D. hustedtii* Zone (below the *D. dimorpha* acme). The sediment interval from 113-694C-5X through 113-694C-15X is placed in the *Denticulopsis hustedtii*/*D. lauta* and the *N. denticuloides* Zones (lower upper Miocene to upper middle Miocene) based on the occurrence of *Denticulopsis punctata*, *Nitzschia denticuloides*, *Crucidentacula nicobarica*, and *Rouxia* sp. 2 of Schrader (1976), the latter two species being very rare. Ranging concurrently with this is an acme of *A. ingens* which was also encountered at Sites 689 and 690 on Maud Rise.

Consequently, the lowermost part of Hole 694C (Cores 113-694C-17X to 113-694C-23X) is tentatively placed in the middle middle Miocene *Nitzschia grossepunctata* Zone, an assignment supported by rare occurrences of the nominate species (Cores 113-694C-22X and 113-694C-23X) and *Denticulopsis maccollumii* (Cores 113-694C-18X and 113-694C-21X).

Summary

At Site 694 we penetrated a 391.3-m-thick Quaternary to middle Miocene sediment sequence. The Pleistocene sediments (dated with magnetostratigraphy) are barren of diatoms, but two short diatom-bearing sections, separated by an approximately 90-m-thick sandy interval, were dated as middle early Pliocene and earliest Pliocene, respectively.

The Miocene sediments at Site 694 consistently contain poor to moderately preserved diatoms. Because several of the key Miocene biostratigraphic markers occur only rarely and inconsistently, the established diatom zonation can be assigned only tentatively. We need to obtain more information on the stratigraphic ranges of undescribed or little-known species in order to establish more reliable age assignments for Site 694 sediments. Such information may be provided by detailed stratigraphic studies of other sites drilled during Leg 113. We can address questions surrounding the principal objectives of this hole only after the stratigraphic questions have been resolved. Additional comments on diatom taxonomy and stratigraphy are made in the "Biostratigraphy" sections "Site 689" and "Site 697" chapters (this volume).

Radiolarians

At Site 694 we recovered turbidites and hemipelagic clays ranging from upper Pliocene or younger to middle (?) Miocene (radiolarian ages). Core-catcher samples were often barren of radiolarians, hence smear slides were taken from split cores from the lower parts of Holes 694B and 694C to locate intervals with relatively abundant diatoms, and radiolarian slides were prepared from these levels for examination. Even so, the majority of Site 694 cores are barren of radiolarians, or contain only rare, poorly preserved specimens which do not provide useful age information. The oldest datable radiolarians were found in Sample 113-694C-15X-1, 110–112 cm, and are of lower upper to middle Miocene. All samples with stratigraphically useful radiolarians are listed below.

Section 113-694A-1H, CC, contains abundant, moderately preserved radiolarians assignable to the lower Upsilon or upper Tau Zones (lower Pliocene). Species include *Desmospyris spongiosa*, *Clathrocyclas bicornis*, *Antarctissa ewingi*, *Prunopyle titan*, *Antarctissa denticulata*, *Antarctissa strelkovi*, and *Eucyrtidium calvertense*. Rare reworked lower Pliocene and Miocene radiolarians were seen, including *Lychnocanium grande*, *Eucyrtidium cienkowski*, and *Gondwanaria* sp.

Section 113-694B-2H, CC, contains few, moderately preserved upper lower Pliocene radiolarians (lower Upsilon Zone). Species include *Stylatractus universus*, *P. titan*, *D. spongiosa*, *C. bicornis*, *Helotholus vema*, *A. strelkovi*, and *A. denticulata*.

Section 113-694B-13H, CC, Sample 113-694B-14H-1, 30–32 cm, and Section 113-694B-14H, CC, contain rare to few, poorly preserved radiolarians assignable to the lower Tau Zone (basal Pliocene) based on the presence of rare to few *L. grande* and *C. bicornis* and the absence of Miocene forms.

Sections 113-694B-22X, CC, 113-694B-23X, CC, and 113-694C-1W, CC, are uppermost Miocene (upper *Cycladophora spongothorax* Zone), based on the occurrence of *C. spongothorax*, *P. hayesi*, *A. conradae*, *Dendrosphyris haysi*, *E. cienkowski*, *S. universus*, and *Eucyrtidium pseudoinflatum*. Radiolarians are common and poor to moderately preserved in this interval.

Sections 113-694C-5X, CC, 113-694C-9X, CC, and 113-694C-11X, CC, and Samples 113-694C-14X-2, 92–94 cm, and 113-694C-15X-1, 110–112 cm, are lowermost upper Miocene or middle Miocene, based on the occurrence of *P. hayesi*, *Actinomma tanyacantha*, and *Amphistylus angelinus*.

Silicoflagellates

Silicoflagellates were largely absent at this deep-water site, and no zonation is attempted. *Distephanus pseudofibula* is present, however, in Core 694B-14X, just below the thick sequence of sand turbidites of lithostratigraphic Unit II. This occurrence supports the early Pliocene age accorded this unit by diatom stratigraphy. It is interesting to note that at the three sites drilled north of Site 694 (see "Site 695," "Site 696," and "Site 697" chapters, this volume), *Distephanus pseudofibula* is present in several cores immediately above a prominent interval of ice-rafted debris attributed to late Miocene–early Pliocene glaciation.

Palynology

Core-catcher samples from Holes 694A, 694B, and 694C (lower Pliocene to middle Miocene turbidites and hemipelagic clays) contain different amounts of organic matter as observed in smear slides. Some of these samples (694A-1H, CC, 694B-1H, CC, 694B-5X, CC, 694B-15H, CC, 694B-22H, CC, and 694B-23H, CC) were processed with Calgon and gravity solution, but without success due to the large amounts of clay. Processing with hydrofluoric acid (HF) will lead to better results. All palynological assemblages recovered from this interval are believed to be reworked from lower Tertiary or Mesozoic sediments (Truswell, 1986).

An ice-transported coaly particle of 1–2 cm³ was observed in a dark grey (N4/1) clay of Miocene(?) age (694B-5X-2, 40 cm). This particle consists of land-derived organic matter with an approximate thermal alteration index of 3, mainly consisting of cuticles and sporomorphs. Part of the sample was processed with HNO₃ to lighten the palynomorphs. The organic matter is partly well-preserved, with visible cell structures, partly altered, and destroyed by bacteria and/or fungi. The pollen grains show the same preservation patterns. The diversity is low, either because they were derived from a monotonous bog vegetation or because of sorting. The identified genera *Corollina*, *Stereisporites*, *Deltoidospora*, and *Gleichenioidites* indicate an upper Triassic to Cretaceous age for the coal. *Alisporites* is the most common pollen type. The sporomorph spectra of Upper Triassic and Lower Jurassic coal-bearing sandstones and shales from the Beacon and Ferrar Groups of southern Antarctica (Norris, 1965), are similar to that of the ice-rafted coaly particle.

Summary

All biostratigraphic data from Site 694 (Fig. 25), at which we recovered a Quaternary to middle Miocene sediment sequence, are based on siliceous microfossils. Diatoms, silicoflagellates, and radiolarians are rare and poorly to moderately preserved in the upper portion of Site 694 including lithostratigraphic Units I and II. In the lower portion of the section (lithostratigraphic

Units III and IV) diatoms occur more consistently, whereas radiolarians and silicoflagellates are restricted to discrete intervals. Calcareous microfossils and agglutinated benthic foraminifers were not found. Palynomorphs were only found in a single ice-rafted coaly particle containing a Mesozoic sporomorph association.

Lithostratigraphic Unit I (topmost 21.1 m of Site 694) contains a biogenic siliceous interval at its base, which is lower Pliocene (*Nitzschia angulata*/*N. reinholdii* diatom Zone, lower Upper radiolarian Zone, upper portion of Chron C3). Sediments above this interval are dated as Pleistocene and upper Pliocene based upon magnetostratigraphy (see "Paleomagnetism" section, this chapter) and stratigraphic relationships.

Lithostratigraphic Unit II, a sandy interval of about 90 m thickness (21.1–111.5 mbsf), contains reasonably well-preserved diatoms, silicoflagellates, and radiolarians at its base (Core 113-694B-13H and 113-694B-14H), which indicates a level slightly above the Miocene/Pliocene boundary (lowermost Chron C3).

Lithostratigraphic Units III and IV (111.5–391.4 mbsf) can be assigned to the uppermost upper Miocene to middle Miocene. However, because several of the prominent diatom biostratigraphic marker species occur only rarely and inconsistently, the established diatom zonation is only assigned tentatively. The established radiolarian biostratigraphic zonation could not be assigned continuously because radiolarians are too sparse and poorly preserved. The sediment interval from 120 to 200 mbsf is placed in the *Denticulopsis hustedtii* Zone (upper Miocene to lowermost Pliocene). Radiolarians indicate upper Miocene (upper *Cycladophora spongothorax* Zone). The sediments between 200 and 310 mbsf may represent the lower upper to upper middle Miocene *Denticulopsis hustedtii*/*D. lauta* and *Nitzschia denticuloides* Zones. Finally, the lowermost sediment sequence (310–391.2 mbsf) representing most of Lithostratigraphic Unit IV is placed in the middle middle Miocene *Nitzschia grossepunctata* Zone.

The stratigraphic assignment of the Miocene sequence at Site 694 can be resolved more reliably only after more information is collected on stratigraphic ranges of yet undescribed or little-known diatom species. Such data may be provided by detailed study of other sites drilled during Leg 113 and possibly Leg 114.

PALEOMAGNETISM

Introduction

Site 694 is located in the central part of the Weddell Sea abyssal plain. The recovery of 146.6 m of mainly terrigenous sediment from three holes with a depth of 391.3 m presented a difficult task for the determination of a viable magnetostratigraphy. The only partial recovery of fine-grained turbidites and glaciomarine gravelly sands (due to the selectivity of the drilling process and the unknown time span covered by the deposition of the coarse fraction of these sediments) is the key problem for magnetostratigraphic interpretation. We generally sampled for paleomagnetic study only the hemipelagic intervals but also, occasionally, silty muds in the upper parts of turbidites. In addition to the primary aim of deciphering the downhole magnetic polarity of the site we also determined the magnetic susceptibility by whole core measurements.

Magnetostratigraphy

Attempts to define a magnetostratigraphy for Site 694 are based on the measurement of the natural remanent magnetization (NRM) of all 259 samples taken from Holes 694B and 694C. In contrast to the previous sites, we measured all samples in order to gain a better resolution and a more precise definition of

the magnetostratigraphic record. The distribution of inclination values for Holes 694B and 694C (Fig. 26) is clearly bimodal with a bias toward negative inclination values, indicative of normal polarity. However, this still allows us to suggest a tentative magnetostratigraphic interpretation. Figure 27 shows the downhole inclination and intensity plot of the NRM of Hole 694B (Fig. 27A) and Hole 694C (Fig. 27B). Due to the large gaps in recovery, a magnetostratigraphic interpretation of this data set seems impossible to achieve, since it is normally based on a more continuous record and the matching of chron patterns. These patterns cannot be clearly identified if interrupted by numbers of interbedded turbidites of unknown duration and thickness.

Good recovery in the upper three cores of Hole 694B has allowed a preliminary interpretation of this sequence (Fig. 28), as it contains only thin turbidite horizons. A nearly complete Pleistocene and Pliocene magnetostratigraphic record could be identified with an almost constant sedimentation rate of 3 m/m.y. The apparent downhole fluctuation of sedimentation rate in the Pliocene-Pleistocene sequence might actually be less pronounced; this might be demonstrated if the depth-expansion effect of the turbidites could be removed by the use of precise sedimentological data for turbidite position and thickness. A pure hemipelagic sedimentation rate is more likely to lie between 1 and 2 m/m.y.

Below Core 113-694B-3H we found an expanded sequence of coarse-grained turbidite sediments, which permits only an effectively "spot" paleomagnetic sampling of interbedded hemipelagic intervals and some silty parts. The selectivity of the process of drilling and recovering cyclic layers of hemipelagic and coarse-grained sediments is poorly understood. Many reversals were found in the polarity sequence. Several magnetozones are defined by more than one sample and therefore cannot be readily dismissed (these will be subject to shore laboratory demagnetization and cleaning). Thus chronological dating based on magnetostratigraphy alone is impossible at this site below 25 mbsf. Biostratigraphic data imply a middle Miocene age for the bottom of Hole 694C, but the assignment of all magnetozones to the geomagnetic polarity time scale gives a much greater age and obviously is in substantial error. The combined use of biostratigraphic data together with a grouping of magnetozones into larger units does not allow even a tentative assignment to the geomagnetic polarity time scale (GPTS) (Fig. 28), but may provide at least an identification of some prominent polarity intervals. The mainly normal C4A/C5-Chrons, for example, may be correctly identified.

Magnetic Susceptibility

Volume magnetic susceptibility was measured on individual core sections prior to splitting by using the Bartington susceptibility sensor. We measured at 5-cm intervals down each of 70 sections taken from the cores recovered in Holes 694B and 694C. The whole-core susceptibility was clearly related to lithology. Generally the composited downhole susceptibility variation, as illustrated in Figure 29, reflects the major and many minor lithological changes. The occurrence of ice-rafted dropstones is often marked by a sharp high-amplitude peak but this is only noticeable for dropstones of igneous origin. Lithic sedimentary pebbles are not normally resolvable by their susceptibility signature above the general background level of the terrigenous matrix enclosing them. A characteristic feature of the susceptibility variation is the association of the turbidite intervals, particularly those rich in silty-clay laminae, with susceptibility peaks as shown in Figure 30. Susceptibility minima are correlated with some of the lighter-colored, silt-free sand intervals.

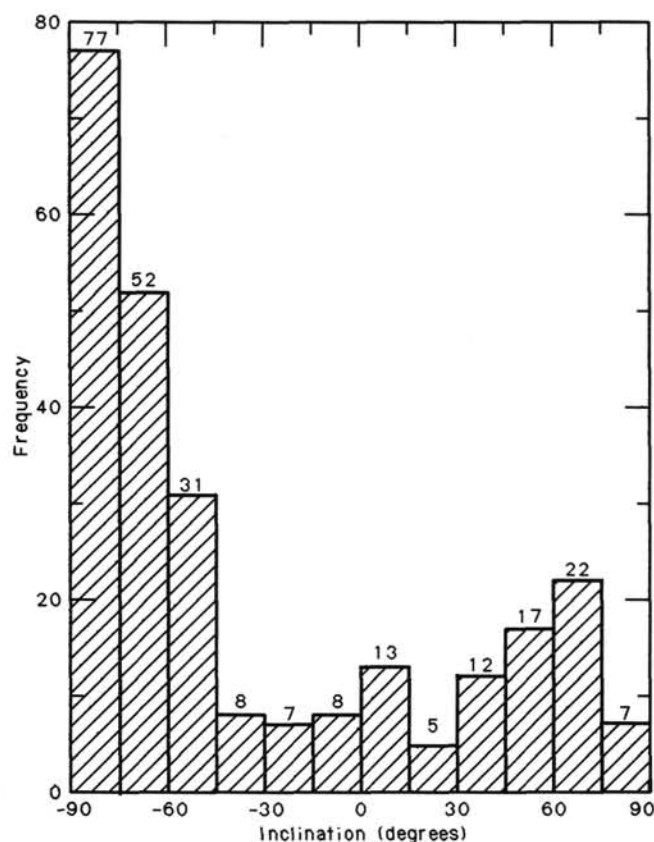


Figure 26. Distribution of NRM inclinations values for Holes 694B and 694C.

SEDIMENTATION RATES

Sedimentation rates for the Quaternary to middle Miocene sequence recovered at Site 694 can only be estimated tentatively and with large uncertainties. The stratigraphic control is poor due to a recovery of less than 30% and the high proportion of turbidites and glaciomarine sediments in the recovered section. The hemipelagic sediments are the only source for magneto- and biostratigraphic age determinations.

A continuous section of Pleistocene through lower Pliocene hemipelagic sediments with interbedded turbidites was encountered in the uppermost three cores of Hole 694B (lithostratigraphic Unit I; 0–21.1 mbsf). The preliminary assignment of the inferred polarity pattern of this interval to the geomagnetic polarity time scale (Fig. 28) provides a mean overall sedimentation rate of 3 m/m.y. (0–14 mbsf) with a range from 1 to 5 m/m.y. due to variable turbidite sedimentation in addition to a hemipelagic sedimentation. The early late Pliocene age assignment of the lowermost portion of Unit I is confirmed biostratigraphically (*Nitzschia angulata*/*N. reinholdii* Diatom Zones, lower Upsilon Radiolarian Zone). In the lowermost 7 m of Unit I the sedimentation rate increases considerably.

Lithostratigraphic Unit II consists of 90.4 m (21.1–111.5 mbsf) of coarse-grained turbidites and was deposited entirely within the lower portion of the Gilbert Chron (C3R-4) representing a time interval of about 0.5 m.y. This provides an overall sedimentation rate of at least 180 m/m.y. for Unit II (Fig. 31). Biostratigraphic data used to construct a sedimentation-rate figure are given in Table 8.

A detailed stratigraphic assignment of lithostratigraphic Unit III (111.5–304.3 mbsf) is not yet feasible based on the siliceous microfossils and the paleomagnetic record (see “Biostratigra-

phy” and “Paleomagnetism” sections, this chapter). For this reason only a rough estimate of the sedimentation rate can be provided from a few biostratigraphic age determinations. The slightly improved recovery within this unit (Fig. 31) has allowed the biostratigraphic tiepoints to be used for a tentative magnetostratigraphic interpretation of the major magnetostratigraphic zonation data as a guideline provided an estimated average sedimentation rate of 20 m/m.y. during deposition of Unit III (Fig. 31).

The lowermost Unit IV of Site 694 (304.3–391.3 mbsf) is tentatively correlated to the middle *Nitzschia grossepunctata* Diatom Zone. Considering the short stratigraphic range of this diatom zone (see “Explanatory Notes” chapter, this volume), a sedimentation rate four to five times faster is estimated for Unit IV in comparison to the upper to middle Miocene sedimentary sequence of Unit III.

The pattern of the sedimentation rate provided for Site 694 shows affinities to the rates estimated for Sites 322, 323, and 325, drilled during DSDP Leg 35 in the Bellingshausen Sea (Hollister, Craddock, et al., 1976). Average sedimentation rates between 10 m/m.y. (Site 325) and 20–30 m/m.y. (Sites 322, 323) were derived for the Quaternary to early Pliocene, thus generally higher than estimated for the same time interval of Site 694. For the uppermost Miocene to lowermost Pliocene a strong increase of the rate, reaching values between 90 and 120 m/m.y., is reported from all three DSDP sites, followed by a decrease of the rate to 10–15 m/m.y. in the upper and middle Miocene. The stratigraphic control of the DSDP sites drilled in the Bellingshausen Sea, however, is inferior even to that of Site 694.

INORGANIC GEOCHEMISTRY

Introduction and Operation

Data on the chemical composition of interstitial water are presented for Holes 694B and 694C. The samples from Hole 694B are from the well-recovered APC-cored interval (0–24.7 mbsf) and the lower well-recovered XCB-cored interval (140.8–179.2 mbsf) (see Fig. 3). Between these intervals average recovery was less than 20% and did not allow closer sampling. Hole 694C was washed down to 179.2 mbsf and XCB-cored down to 391.3 mbsf. Due to poor recovery the upper 118 m of this hole is represented by one sample at 210.4 mbsf only. Three samples were obtained from the lower 86.9 mbsf. Eight (four from each hole, two of 10-cm and six of 5-cm thickness) whole-round sediment samples were squeezed and analyzed.

In each hole, drilling mud of the same composition as used at Site 693 was used during XCB-coring.

The chemical data are summarized in Table 9. For details on sampling and analytical procedures see “Explanatory Notes” chapter, this volume.

Evaluation of Data

For overall evaluation of the data, a charge balance was carried out. As for the previous sites, this was conducted assuming the sodium-to-chloride ratio of the interstitial water equals that of present-day seawater. The calculations reveal that to maintain electroneutrality at all depths, the sodium-to-chloride ratio would have to decrease systematically from seawater value (0.858) near the surface to about 0.840 at 374.65 mbsf (Section 113-694C-22X-2). This involves a 2% decrease in sodium concentration. This is only a rough estimate since it is subjected to the cumulative uncertainty of all the methods. Similar variations of comparable magnitude were observed at the three previous sites.

Special studies at Site 693 demonstrated that contamination of the samples by drilling-mud filtrate is detected as low chlo-

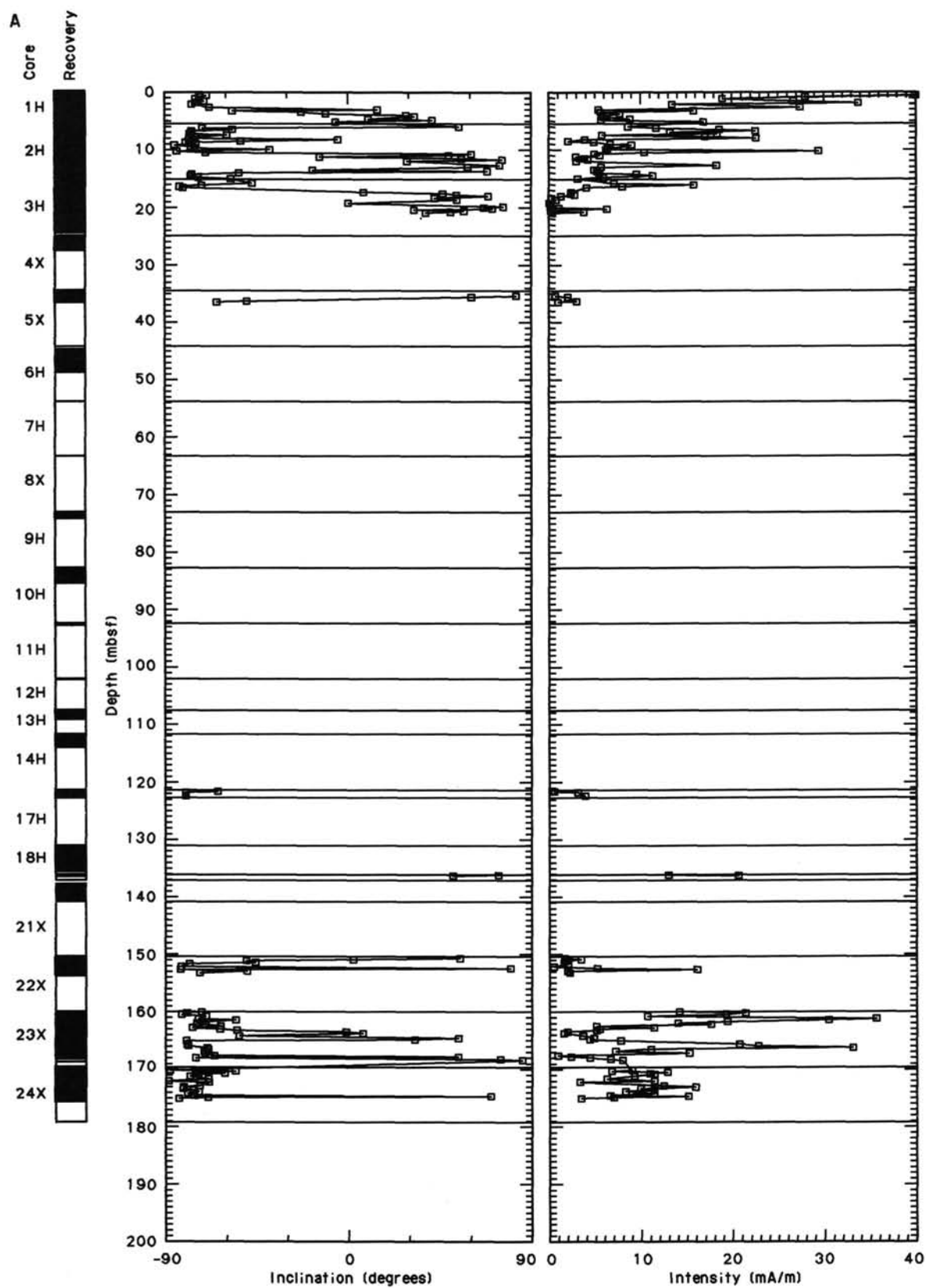


Figure 27. Downhole variation of NRM inclination and intensity. A. Hole 694B. B. Hole 694C. Patterned areas in the column on the left indicate recovery.

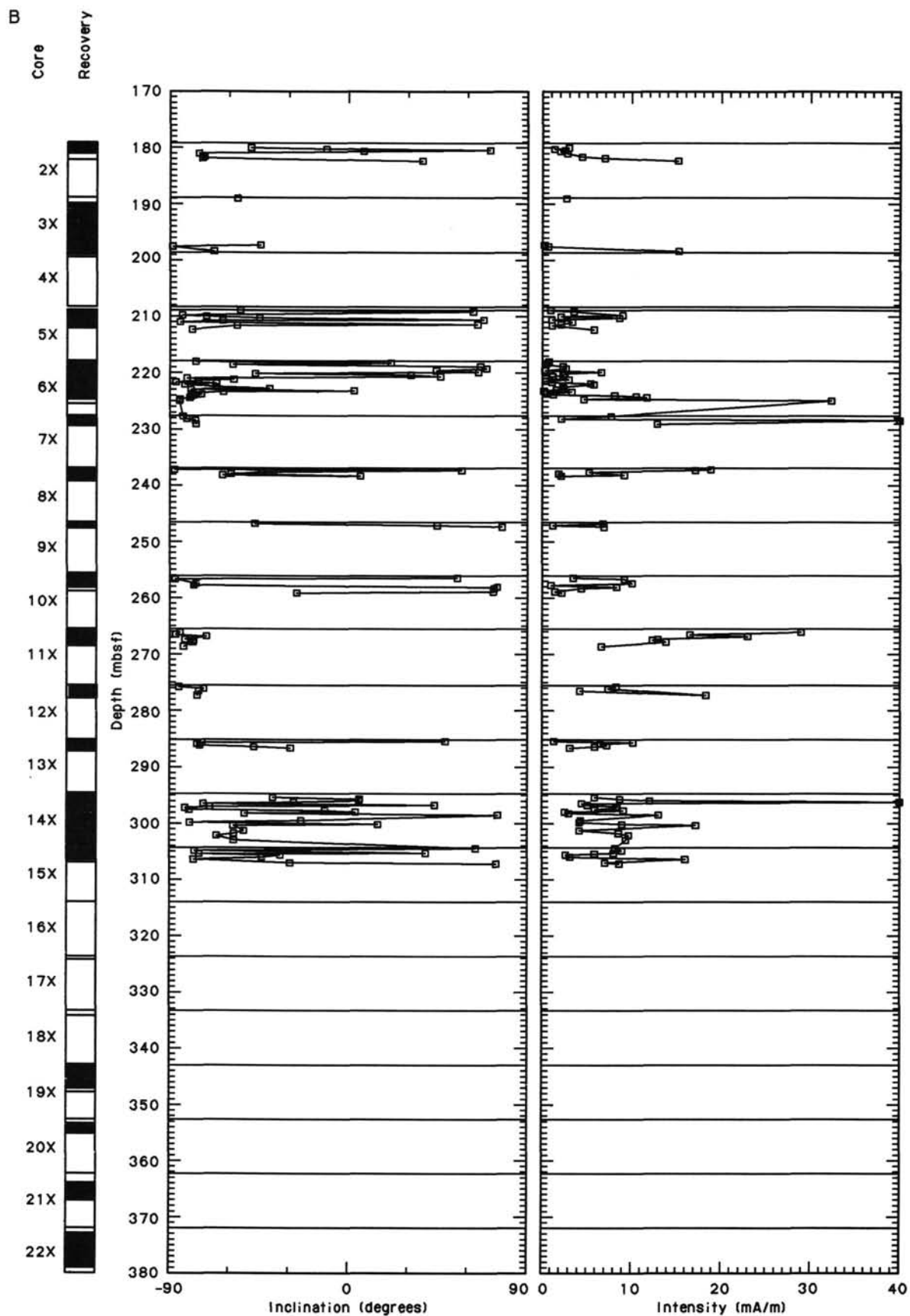


Figure 27 (continued).

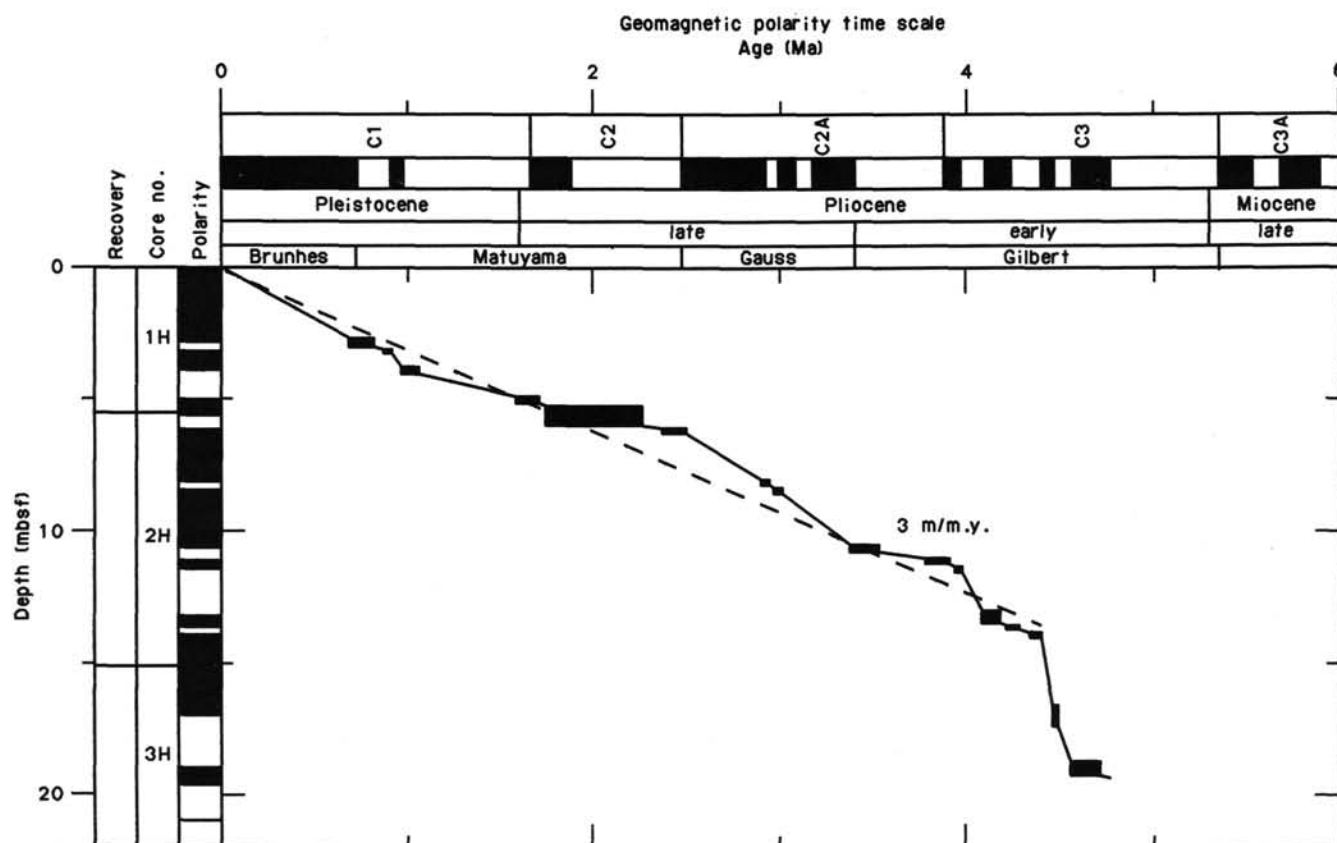


Figure 28. Preliminary assignment of inferred polarity pattern from Cores 113-694B-1H to 113-694B-3H, to the geomagnetic polarity time scale. An average sedimentation rate from middle early Pliocene through Pleistocene can be estimated as 3 m/m.y. (dashed line). See Table 8 for biostratigraphic data assigned for each datum.

ride concentrations. There are no indications that contamination by drilling-mud filtrate has taken place at Site 694.

Due to the low recovery, the samples occur scattered throughout the drilled sequence. However, the smooth concentration profiles (linear for several elements) allow the concentration of major constituents to be obtained by interpolation at any depth.

Chlorinity and Salinity

Chloride data are presented in Figure 32A and Table 9. Except for the two lower readings in the shallower samples (Table 9), the concentration of chloride does not vary systematically. Assuming the same chloride/salinity relation as in seawater ($S‰ = 1.80655 \text{ Cl‰}$; Stumm and Morgan, 1981) the average chloride concentration below 150 mbsf (569.2 mmol/L) corresponds to a salinity of 35.2‰. The concentration of chloride in the shallower samples corresponds to a salinity of 34.2 and 34.5‰, respectively, both of which are comparable to the salinity of present-day seawater (34.6‰) as given by Sverdrup et al. (1942).

Salinities measured using the optical refractometer differ from those calculated from the chloride observations by about 1‰-unit.

pH

The pH (Fig. 32B and Table 9) varies between 7.79 and 8.44. The only significant shift in pH occurs between 151.85 (Section 113-694B-22X-1) and 210.35 mbsf (Section 113-694C-5X-1) where an increase from 7.91 to 8.44 is observed. A shift of similar magnitude is observed at Site 693 (pH increase from 7.76 at

46.8 mbsf to 8.15 at 104.6 mbsf). The average pH (8.1) is similar (within experimental errors) to the average pH measured at Site 693 (8.0) and higher than the average pH measured at Site 689 and 690 (pH = 7.7).

Alkalinity, Sulfate

The alkalinity data are presented in Figure 32C. The alkalinity varies between 2.75 and 3.55 meq./L with an average of 3.3 meq./L. As at Site 693, the alkalinity does not exhibit vertical concentration gradients. The low level (only about 30% enrichment relative to seawater) indicates low bacterial activity.

The sulfate profile is presented in Figure 32D. The concentration of sulfate decreases linearly from close to sea level (28.1 mmol/L) in the upper section (Section 113-694B-1H-2) to 15.4 mmol/L at 374.6 mbsf (Section 113-694C-22X-2). This profile is very similar to that at Site 693. Based on the stable alkalinity level, the profile of sulfate most probably represents a diffusion-controlled gradient to a reaction zone below, although the existence of sulfate reduction throughout can not be excluded. Evidently, diffusion of sulfate keeps up with bacterial reduction, thus the latter is slow.

Phosphate and Ammonia

The concentration profile for phosphate is presented in Figure 32E and Table 9. The concentrations of phosphate are everywhere close to the detection limit. This low level is consistent with the low rate of oxidation of organic matter as inferred from the alkalinity and sulfate data.

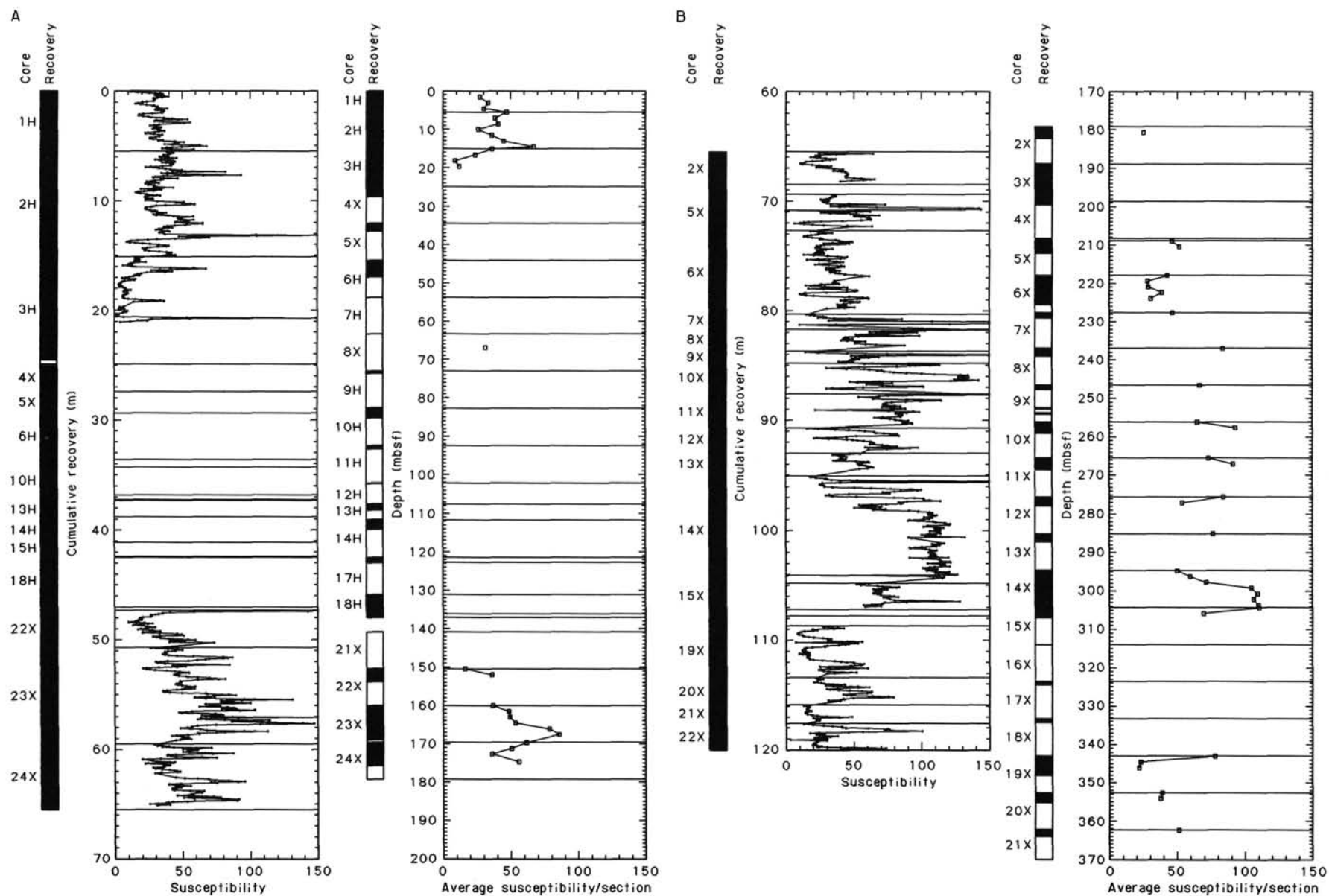


Figure 29. Downhole variation of whole core magnetic susceptibility and average susceptibility per section. A. Hole 694B. B. Hole 694C. Susceptibility values are in c.g.s. units ($\times 10^{-6}$ G/Oe). The depth axis represents cumulative thickness excluding the nonrecovered turbiditic sequences.

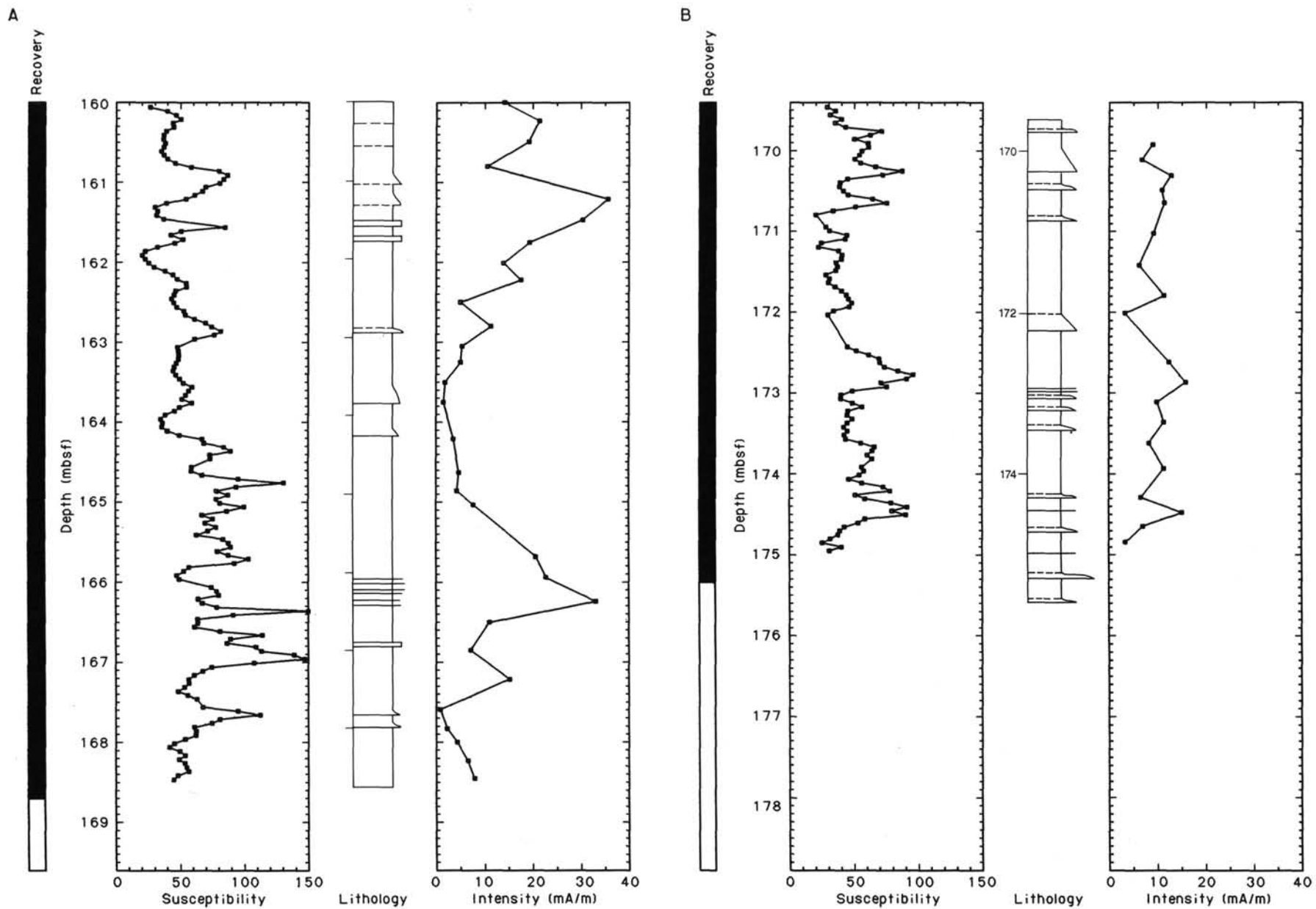


Figure 30. Comparison of whole-core magnetic susceptibility with NRM intensity and lithology. A. Core 113-694B-23X. B. Core 113-694B-24X.

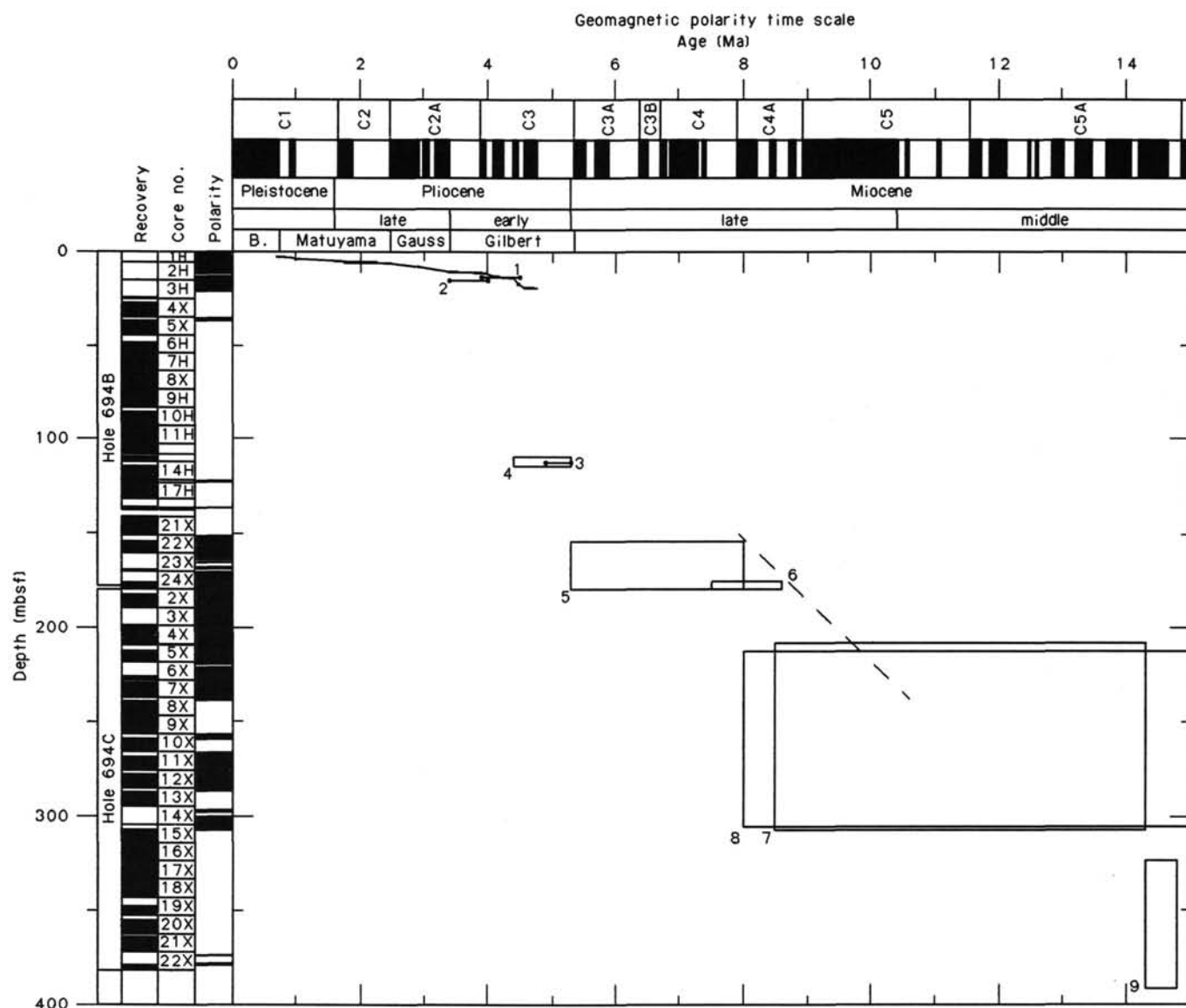


Figure 31. Sedimentation-rate curve for Holes 694B and 694C. Depth presentation of sedimentation-rate curve used for estimation of sedimentation rates. Assignment of magnetic reversal boundaries explained in text. See Table 8 for biostratigraphic data assigned to each datum. (For further explanation see "Sedimentation Rates" section, "Site 689" chapter, this volume.)

Figure 32F shows the ammonia profile. The concentration varies from close to the detection limit (0.01 mmol/L) in the shallower sections to 0.6 mmol/L at 345.9 mbsf (Section 113-694C-22X-2). The high detection limit is caused by high blanks. The spurious peak in the lower sample (Section 113-694C-22X-2, Table 9) is caused by contamination and is not included in the figure.

The linear ammonia profile supports the proposed explanation for sulfate concentrations, that there is a reaction zone below in which reduction of sulfate takes place. Possibly, the Cretaceous organic-rich claystones observed at Sites 692 and 693, if eroded from the margin and redeposited here, provide the material for these processes. However, a mechanism for removal of the produced alkalinity must be postulated for this hypothesis to work (see potassium discussion below).

Calcium and Magnesium

Calcium and magnesium data are presented in Figures 32G and 32H, respectively. The concentration of calcium varies between close to seawater value (10.25 mmol/L) in the shallower

section (Section 113-694B-1H-2) and 25.49 mmol/L at 374.6 mbsf (Section 113-694C-22X-2). Below 150 mbsf the calcium profile exhibits a nearly perfect ($r = 0.997$, $n = 6$) linear concentration/depth relationship. The slope of the gradient (3.3 mmol/L/100 m) is very close to the slope of the calcium gradient observed at Site 689 (3.6 mmol/L/100 m).

The concentration of magnesium varies between 35.08 mmol/L at 374.6 mbsf (Section 113-694C-22X-2) to close to seawater concentration (52.52 mmol/L) in the upper section (Section 113-694B-1H-2). As with calcium, the linearity of the magnesium profile is striking and suggests that magnesium is diffusing to a reaction zone below. The downhole Mg/Ca ratio is shown in Fig. 32I.

Potassium

The concentration of potassium (Fig. 32J and Table 9) decreases from 10.4 mmol/L in the upper section (Section 113-694B-1H-2) to 3.8 mmol/L at 374.6 mbsf (Section 113-694C-22X-2). The depletion of potassium relative to seawater is more extensive than observed at the previous Leg 113 sites. The view

Table 8. Biostratigraphic data used to construct sedimentation-rate figure (Fig. 28).

Datum number	Depth range (mbsf)	Age (Ma)	Datum or zone
1	13.4	3.9–4.5	<i>N. angulata</i> / <i>N. reinholdii</i> Zone - D
2	15.2	3.2–4.0	lower Upsilon Zone - R
3	112.0	4.9–5.3	Co-occurrence of <i>T. torokina</i> and <i>C. insignis</i> / <i>F. triangularis</i> - D
4	109.1–114.0	4.4–5.5	lower Tau Zone - R
5	153.8–179.2	5.3–8.0	upper <i>C. spongothorax</i> Zone - R
6	174.9–179.2	7.5–8.6	<i>D. dimorpha</i> acme - D
7	208.9–306.9	8.0–14.2	<i>D. hustedtii</i> / <i>D. lauta</i> / <i>N. denticuloides</i> Zones - D
8	212.2–305.4	8.0–15.0	Occurrence of <i>A. tanyacantha</i> - R
9	323.6–391.3	14.3–14.8	<i>N. grossepunctata</i> Zone - D

Note: D = diatoms; R = radiolarians.

is generally held (MacKenzie and Garrels, 1966; Manheim and Sayles, 1974; Gieskes and Lawrence, 1976) that potassium is removed from interstitial water by authigenic formation or alteration of clay minerals. The inferred decrease in sodium concentration (see evaluation of data discussion above) is of similar magnitude. The protons released during the reversed weathering involving this amount of cations would account for the "missing" alkalinity by conversion of bicarbonate to carbon dioxide.

Dissolved Silica

The concentration of dissolved silica (Fig. 32K) varies between 165 $\mu\text{mol/L}$ at 2.95 mbsf (Section 113-694B-1H-2) and 1190 $\mu\text{mol/L}$ at 374.6 mbsf (Section 113-694C-22X-2). In all samples, the levels fall between quartz saturation and amorphous silica saturation (based on thermodynamic data provided by Stumm and Morgan, 1981). Most of the variations in dissolved silica takes place in the upper 150 mbsf where sample coverage is poor. Below 150 mbsf the content of diatoms varies between 0% and 35%. Generally, preservation of diatoms is poor. The reversed weathering mechanism constitutes an interesting link between interstitial water chemistry and preservation of diatoms.

Reversed weathering involves uptake of cations from the pore water. To maintain charge balance, protons are released at the same rate. The reactions deplete pore water of silica. The solubility of silica in the pore water is so low that dissolution of less than 0.01% (volume) diatoms is enough to saturate the pore water, thus there is no direct link between instantaneous concentration of dissolved silica and observed degree of preservation of diatoms. Instead, if silica is involved in reversed weathering reactions, the concentration of the much more soluble cations (for a quantitative estimate integrated fluxes will have to be considered) will give an estimate of the degree of dissolution. For otherwise similar physicochemical conditions, one would expect

preservation of diatoms to be poorest when deposited with minerals or weathering products serving as precursors for authigenic clays. Even poorer preservation would be observed with simultaneous deposition of carbonates since these would act as a sink for the released protons, driving the reaction even further toward dissolution. It is generally observed that there is a decrease in diatom preservation with increasing carbonate. This relationship was also observed at Sites 689 and 690.

ORGANIC GEOCHEMISTRY

Light Hydrocarbons

Concentrations of methane were extremely low at Site 694, reaching a maximum of 29 μL of methane per liter of sediment in the deepest sample, 374.6 mbsf. Data are presented in Table 10. Methane and other light hydrocarbons exhibit moderately well-developed exponential increases in concentration with depth (Fig. 33). No such gradients have been observed in other Leg 113 holes, though they have been reported at several earlier DSDP and ODP sites, where overall concentrations were higher. Figure 34 shows well-developed increasing concentration gradients at Site 652 on the lower Sardinian margin (Shipboard Scientific Party, 1987), and similar phenomena are reported by Whelan et al. (1984) for Site 397, Canary Islands. The generation of such gradients is discussed below.

Methane/ethane ratios are low in all samples, not exceeding 10.3 (122.7 mbsf). Despite low ratios, once again no drilling hazard is represented because gas concentrations are minimal. As in other Leg 113 Cenozoic sections, bacterial generation of methane is not evident. Information on the progressive increase of methane with depth was conveyed to the Operations Superintendent during the course of drilling.

The apparent gradients shown in Figure 33 are enhanced by the successive appearances of butanes and pentanes at 122.70 mbsf, and of *n*-hexane at 333.9 m (Table 10). The cause of the gradients cannot be determined, but two general cases of gradient formation are reviewed for comparison. First, in the case of sediments at temperatures exceeding 50°C, exponential increases in light hydrocarbon concentrations due to progressive catagenesis are to be expected (Hunt, 1979). In the present instance, the attainment of 50°C at 375 mbsf would require an unrealistically high gradient, 134°C/km. The thermal gradient at Site 694 is unknown, but is probably substantially less than this. However, it is conceivable that the observed light hydrocarbon concentration gradients represent the earliest stages of catagenesis.

A second possible analogy involves diffusion-generated gradients above and below stratigraphic units exhibiting high concentrations of light hydrocarbons. For example, at Site 652, Leg 107 (Shipboard Scientific Party, 1987), the gradients occur as shown in Figure 34. Here the apparent source is a thin suite of

Table 9. Summary of shipboard interstitial water data, Site 694.

Core, section, interval (cm)	Depth (mbsf)	Volume (mL)	pH	Alk. (meq/L)	Sal. (g/kg)	Mg (mmol/L)	Ca (mmol/L)	Cl (mmol/L)	SO ₄ (mmol/L)	PO ₄ ($\mu\text{mol/L}$)	K (mmol/L)	NH ₄ (mmol/L)	SiO ₂ ($\mu\text{mol/L}$)	Mg/Ca ($\mu\text{mol/L}$)
113-694B-														
1H-2, 145–150	2.95	45	7.91	3.10	34.5	52.52	10.25	553.6	28.1	1.0	10.4	0.01	165	5.12
3H-2, 120–125	17.80	60	7.79	2.75	35.5	52.14	11.13	559.0	28.3	1.8	9.0	0.01	360	4.68
22X-1, 145–150	151.85	30	7.91	3.07	37.0	44.54	18.19	570.8	23.0	2.0	5.7	0.27	880	2.45
24X-2, 120–125	172.30	25	7.99	3.40	35.0	43.30	18.47	565.4	21.7	1.5	4.7	0.20	910	2.34
113-694C														
5X-1, 145–150	210.35	15	8.38	3.15	36.5	43.47	20.17	570.8	20.6	2.0	5.2	0.40	720	2.16
14X-4, 115–125	300.35	25	8.44	3.00	35.5	39.82	22.47	572.3	18.3	0.7	3.8	0.55	860	1.77
19X-2, 145–150	345.95	15	8.20	3.55	35.0	36.03	24.40	567.8	16.2	1.2	3.3	0.61	1010	1.48
22X-2, 115–125	374.65	45	8.20	3.01	36.0	35.08	25.49	568.3	15.4	1.5	3.8	1.42	1190	1.38

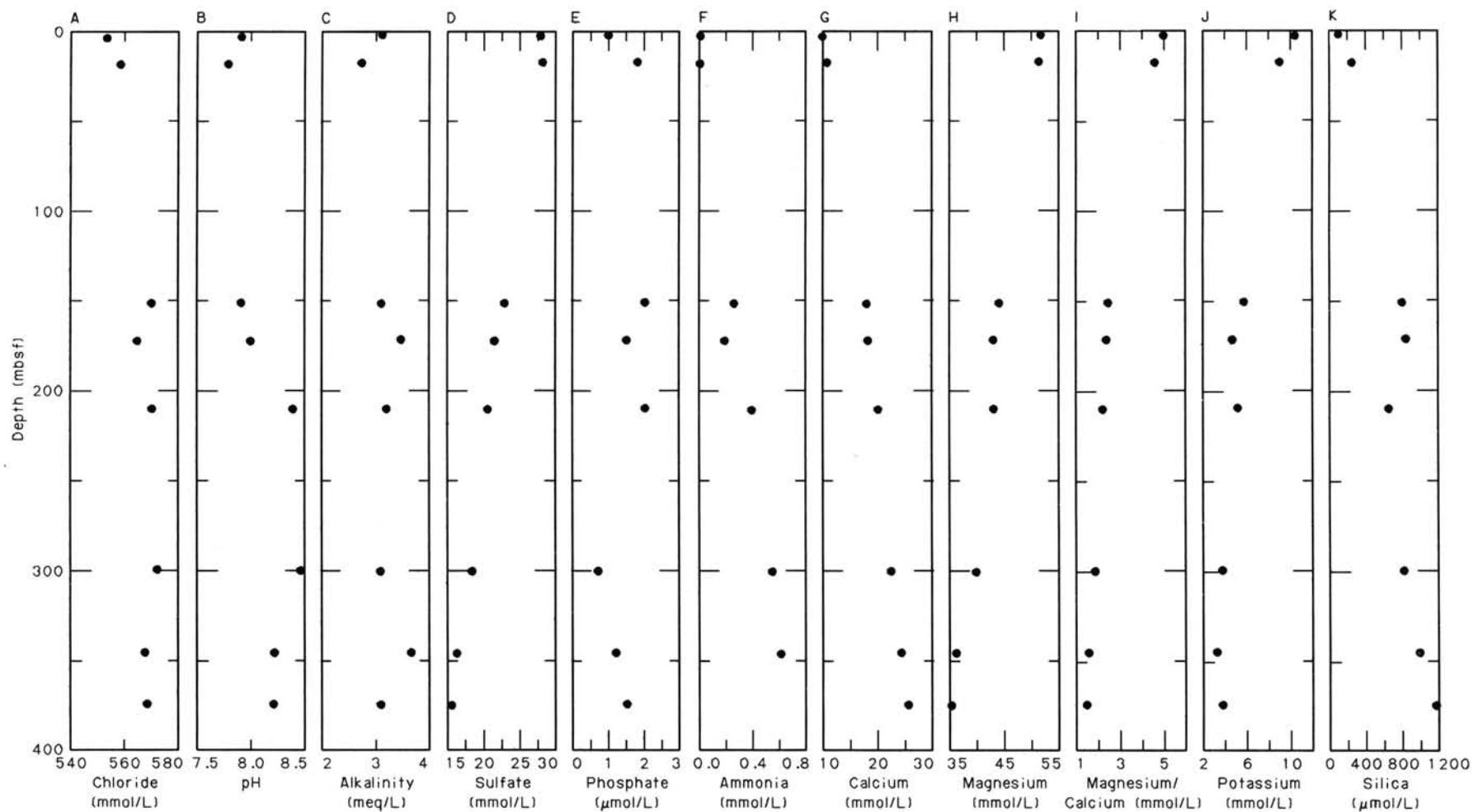


Figure 32. Concentrations vs. depth for Holes 694B and 694C. A. Chloride. B. pH. C. Alkalinity. D. Sulfate. E. Phosphate. F. Ammonia. G. Calcium. H. Magnesium. I. Magnesium/calcium ratio. J. Potassium. K. Silica.

Table 10. Comparison of light hydrocarbon composition ratios, Holes 694B and 694C.

Core, section interval (cm)	Depth (mbsf)	Methane	Ethane	Propane	<i>i</i> -C ₄	<i>n</i> -C ₄	<i>i</i> -C ₅	<i>n</i> -C ₅	<i>i</i> -C ₆	<i>n</i> -C ₆
		Microliters (gas)/liter (sediment)								
113-694B-										
1H-2, 145-150	0.15	0.2	1.5	0.4	0.2	—	—	—	—	—
2H-3, 147-150	9.97	2.1	0.4	0.2	—	—	—	—	—	—
3H-3, 145-150	19.55	2.1	0.4	0.6	—	—	—	—	—	—
10H-1, 147-150	83.97	3.6	0.6	0.3	—	—	—	—	—	—
15H-CC, —	122.70	11.3	1.1	0.4	0.1	0.2	0.1	0.1	—	—
22X-1, 145-150	151.85	1.8	1.1	0.6	1.6	0.4	—	—	—	—
24X-2, 117-120	172.27	2.0	0.2	—	—	—	—	—	—	—
113-694C										
5X-1, 145-150	210.35	13.1	1.3	3.6	0.6	1.4	0.1	0.1	—	—
8X-1, 145-150	238.35	11.0	1.9	1.5	0.3	0.5	—	—	—	—
11X-1, 146-150	266.96	2.1	3.4	1.3	1.9	0.5	—	—	—	—
18X-1, 62-64	333.92	2.7	5.6	2.9	0.5	1.9	tr	tr	2.2	—
19X-2, 145-150	345.95	10.8	6.8	2.9	5.8	1.0	0.1	0.3	—	0.8
22X-2, 115-120	374.65	29.0	3.1	1.4	1.5	0.3	0.04	0.04	—	0.2

Miocene oil shales at 605 mbsf, containing 8.5%–11% organic carbon. In this instance, methane and ethane are above background level over more than 250 m of section, and propane over slightly more than 100 m. Whelan et al. (1984) describe a similar example from Site 397, Leg 47, off the Canary Islands where methane is elevated over an interval of 250 m, ethane over 200 m, and propane over 100 m.

Rock-Eval Data

Table 11 presents Rock-Eval measurements. Two kerogen types are evident, as shown in Figure 35. One group of four

samples has hydrogen index values between 200 and 320 mg hydrocarbons/g carbon. Their T_{max} values vary from 426°C to 537°C, suggesting maturities ranging from optimum, equivalent to a vitrinite reflectance of approximately 0.8%, to extremely mature. Evidently such characteristics must partially reflect previous sedimentary cycles. It is suggested that these sediments contain a mixture of first-cycle planktonic kerogen, similar to that in the Aptian at Site 692, as well as of recycled, highly mature kerogens. The second group of kerogens is seen in the lower left corner of Figure 35. Both indices are low, suggesting high maturity and reworking, as in the cases of the kerogens of all of

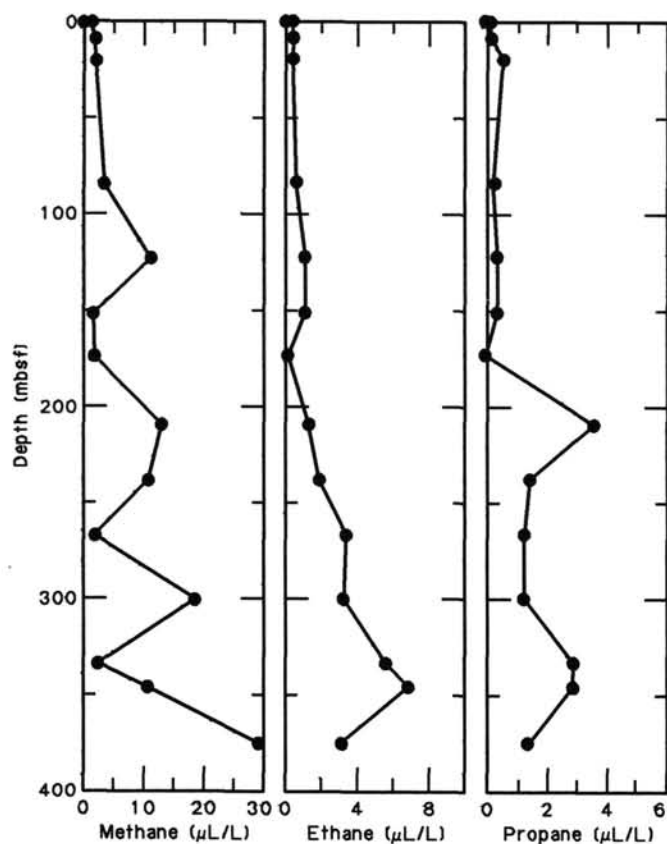


Figure 33. Methane, ethane, and propane concentrations vs. depth, Site 694.

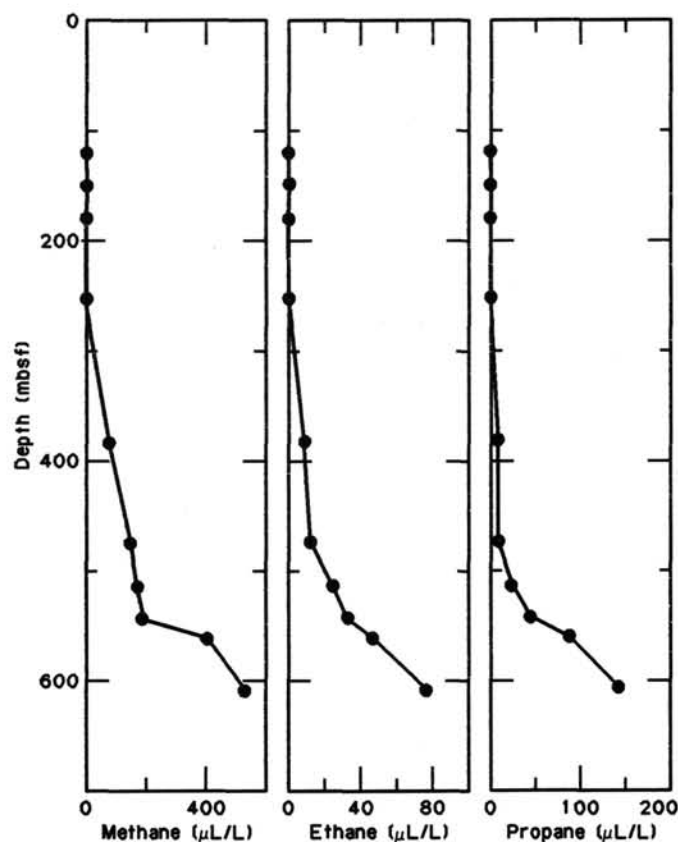


Figure 34. Methane, ethane, and propane concentrations vs. depth from Site 652 in the lower Sardinian margin. (Leg 107) showing concentration gradients above a Miocene oil shale at 605 mbsf.

Table 11. Rock-Eval data, Holes 694B and 694C.

Core, section, interval (cm)	Depth (mbsf)	S ₁	S ₂	S ₃	TOC (%)	HI	OI	T _{max} (°C)
		mg(HC)/g(rock)		mg(CO ₂)/ g(rock)		mg/g(C)	mg/g(C)	
113-694B-								
1H-2, 145-150	0.15	0.00	0.67	0.09	0.76	88	11	551
2H-3, 147-150	9.97	0.01	0.60	0.00	0.25	240	0	518
3H-3, 145-150	19.55	0.00	0.55	0.00	0.26	211	0	537
10H-1, 147-150	83.97	0.00	0.01	0.00	0.01	100	0	427
15H-CC, —	122.70	0.00	0.00	0.00	0.07	0	0	(310)
22X-1, 145-150	151.85	0.01	0.23	0.05	0.75	30	6	490
24X-1, 117-120	172.27	0.01	0.20	0.00	0.10	200	0	426
113-694C-								
5X-1, 145-150	210.35	0.00	0.02	0.00	0.14	14	0	419
8X-1, 145-150	238.35	0.01	0.16	0.00	0.29	55	0	516
11X-1, 146-150	266.96	0.02	0.36	0.09	0.59	61	15	489
14X-4, 115-120	300.35	0.03	0.30	0.05	0.60	50	8	482
18X-1, 62-64	333.92	0.05	0.48	0.00	0.15	320	0	445
19X-2, 145-150	345.95	0.03	0.37	0.07	0.50	74	14	444
Standard (observed)		0.04	8.55	1.05	2.86	298	36	409
Standard (known values)		0.10	8.62	1.00	2.86	340	33	419

the Cenozoic sections previously seen (Sites 689, 690, and 693). Most of the second group possess expectably high values of T_{max} (500°C or greater). In the few which do not, organic carbon contents are close to, or below, 0.1%, at which level instrument function becomes erratic (Deroo et al., 1984).

SUMMARY AND CONCLUSIONS

Site 694 is located on the northern part of the abyssal plain of the Weddell Basin (66°50.8'S, 33°26.79'W) in 4653 m of water. The site is located about 900 km north of East Antarctica and about 900 km east of the Antarctic Peninsula. Site 694 is the deepest of seven sites that form a depth transect in the Weddell Sea region for studies of vertical water-mass evolution and related sediment history around Antarctica during the Cenozoic and Late Mesozoic.

The site was selected to obtain a continuously cored, largely terrigenous sequence of hemipelagic clays and turbidites to provide a record of continental erosion during the glacial and preglacial climatic regimes of Antarctica, and data related to the history of bottom-water production in the Weddell Sea. Seismic reflection profiles near the site exhibit a relatively thick (~1 s two-way traveltime) sequence of parallel-layered and moderately reflective sediments interpreted as interbedded hemipelagic sediments and fine-grained turbidites.

Site 694 includes three holes: Hole 694A is a single APC core from 0 to 9.8 mbsf; Hole 694B consists of 15 APC, 7 XCB, and 2 washed cores from 0 to 179.2 mbsf providing 37.4% recovery; Hole 694C consists of 1 washed core from 0 to 179.2 mbsf and 22 XCB cores from 179.2 to 391.3 mbsf with 33.8% recovery. Drilling at Site 694 had to be postponed on two occasions because of closely approaching icebergs, but at no time did this require abandonment of a hole. The quality of the cores is only good in the uppermost part of the sequence; otherwise core quality is moderate to highly disturbed. The site was abandoned at 391.3 mbsf, still well above target depth, when the XCB became stuck at the bottom of the drill string, requiring a drill-pipe trip, and we decided to spend no further time at this location.

The sedimentary sequence is predominantly terrigenous in origin with a generally minor biosiliceous component and fluctuating abundances of ice-rafted material throughout. Calcareous material is not present. Almost all of the sediments are interpreted to be hemipelagic silts and clays and turbidites. Changes

in magnetic susceptibility, *P*-wave velocity data, and sediment lithology are closely correlated. The sequence ranges in age from the middle middle Miocene to the Quaternary.

A paleomagnetic polarity stratigraphy could only be established in the topmost 20 m of Hole 694B, which extends from the Brunhes Chron to the early Gilbert Chron. Below this level, poor core recovery and the presence of numerous sand layers

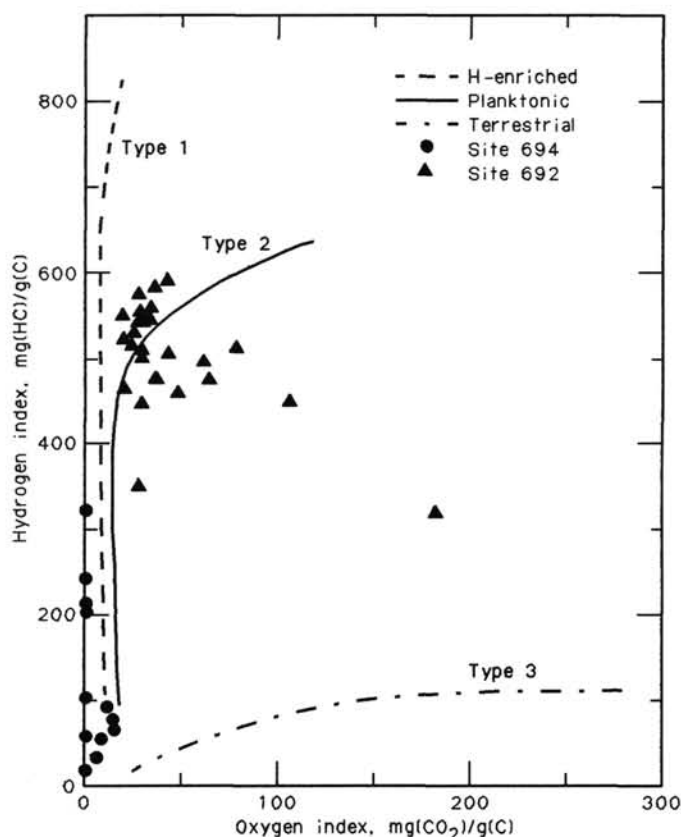


Figure 35. Rock-Eval data Site 694 compared with Lower Cretaceous kerogens at Site 692.

have made magnetostratigraphic age assignment difficult. The biostratigraphic age assignments for Site 694 are derived from diatoms, radiolarians, and silicoflagellates. No calcareous microfossils, palynomorphs, and agglutinated benthic foraminifers were observed. Diatom and radiolarian assemblages provide only a broadly-defined zonation, especially for the Miocene. Numerous intervals are either completely barren of microfossils or contain only rare, poorly-preserved forms of little value for age determinations. The oldest datable radiolarian assemblage is at 305 mbsf and is middle to lower upper Miocene. Assemblages of displaced neritic diatoms occur in Miocene sediments. Determination of the stratigraphic ranges of rare or poorly-known species of diatoms in sequences at other Weddell Sea sites may assist in the dating of Site 694.

The sequence at Site 694 has been divided into four lithostratigraphic units (see Fig. 3) based upon differences in grain size, diatom content, lithification, and inferred sedimentation processes.

Unit I, lower Pliocene to Quaternary, extends from the seafloor to 21.1 mbsf and is a highly condensed sequence. The sediment is composed primarily of clay and clayey mud with minor silt, sand, and diatom-bearing clayey mud. These are interpreted as cyclic fine-grained turbidites and hemipelagic sediments.

Unit II, lowermost Pliocene, extends from 21.1 to 111.5 mbsf. Recovery was very poor in this unit because of its unconsolidated nature. The sediment is dominated by well- to moderately-sorted lithic quartz sands, and is interpreted as a sandy turbidite sequence.

Unit III, middle Miocene to lowermost Pliocene, extends from 111.5 to 304.3 mbsf. This unit consists of a variety of sediments of hemipelagic and turbiditic origin, including graded silt sequences, with or without diatoms; diatom-bearing silty and clayey muds with interbedded silts and sandy muds; and at the base, a homogeneous gravel-bearing sandy and silty mud considered to be of glaciomarine origin. Unit III has been divided into five subunits based on compositional differences and inferred processes of sedimentation.

Unit IV, middle middle Miocene, extends from 304.3 to 391.3 mbsf. The major sediment types are diatom-bearing and diatom claystones, with silts near the base. This unit becomes increasingly lithified downward. Sand, excluding ice-rafted detritus, is almost absent. Sponge spicules are important components (8%–10%) in a few intervals near the base. The graded silts represent fine-grained turbidites; the mudstones are of either hemipelagic or turbiditic origin. The base of Unit IV is marked by a hard layer of silicified claystone displaying subconchoidal fracture and resembling chert.

The lithic material in the coarse turbidite layers in several intervals has provided preliminary information about the sediment source regions, although additional work is required. The lithic grains are dominated by sedimentary rocks with a few volcanic and plutonic rocks. The most likely source areas are considered to have been the southern Antarctic Peninsula and the catchment area of the Ronne ice shelf.

Ice-rafted debris of a wide size range was found in varying amounts in the hemipelagic sediments throughout the sequence, suggesting changes in the intensity of Antarctic glaciation from the middle Miocene to the present day. Core recovery was sufficient only to suggest very general patterns. Ice-rafted material was not observed in lowest Pliocene Unit II, is sparse in upper and upper middle Miocene Subunits IIIC and IIID, abundant in Subunit IIIE (upper middle Miocene), and occurs in only a few thin intervals in Unit IV (middle Miocene). The glacial dropstones are mainly sedimentary rocks. This suggests a dominant West Antarctic source for the dropstones at Site 694, in contrast with the primarily igneous and metamorphic dropstones found at Site 693 that are probably derived from East Antarctica.

It seems therefore that the main source of the turbidites and the glacial material at Site 694 is the Antarctic Peninsula and the region south of the Weddell Sea, rather than East Antarctica. Since turbidites and glacial-marine depositional processes are in part climatically controlled, Site 694 has provided valuable information about the development of glaciation on West Antarctica. The presence of subrounded and subangular sand grains in Subunit IIID suggests that some subaqueous transport and rounding occurred prior to deposition in deep water during the late middle to early late Miocene. Larger quartz grains are rounded and polished. Ice-rafting appears to have been unimportant during this interval, although several very weathered dropstones occur. An abundance of iron-rich chlorite in the middle Miocene and younger sediments indicates supply from an area undergoing chemical weathering. Displaced benthic and neritic planktonic diatoms occur throughout much of the Miocene, but are particularly conspicuous in the middle Miocene, indicating an absence or near absence of ice cover over the shallow part of the West Antarctic continental shelf during the period of deposition. These observations suggest that the middle to lower upper Miocene sediments were deposited prior to the development of major West Antarctic glaciation and ice-sheet formation. Such an interpretation is in accord with previous interpretations of Ciesielski et al. (1982) for the development of the West Antarctic ice-sheet no earlier than the late Miocene. If this is correct, then most of the ice-rafted debris in the middle Miocene at Site 694 was probably derived from the south-eastern Weddell Sea, including East Antarctica. This interpretation is supported by changes in the clay mineral associations in the sequence. An abundance of magnesium-rich chlorite in one sample of middle Miocene age at the base of the sequence may have resulted from the physical erosion of a metamorphic terrain, which most likely lay in East, rather than West Antarctica. Additional analyses are required.

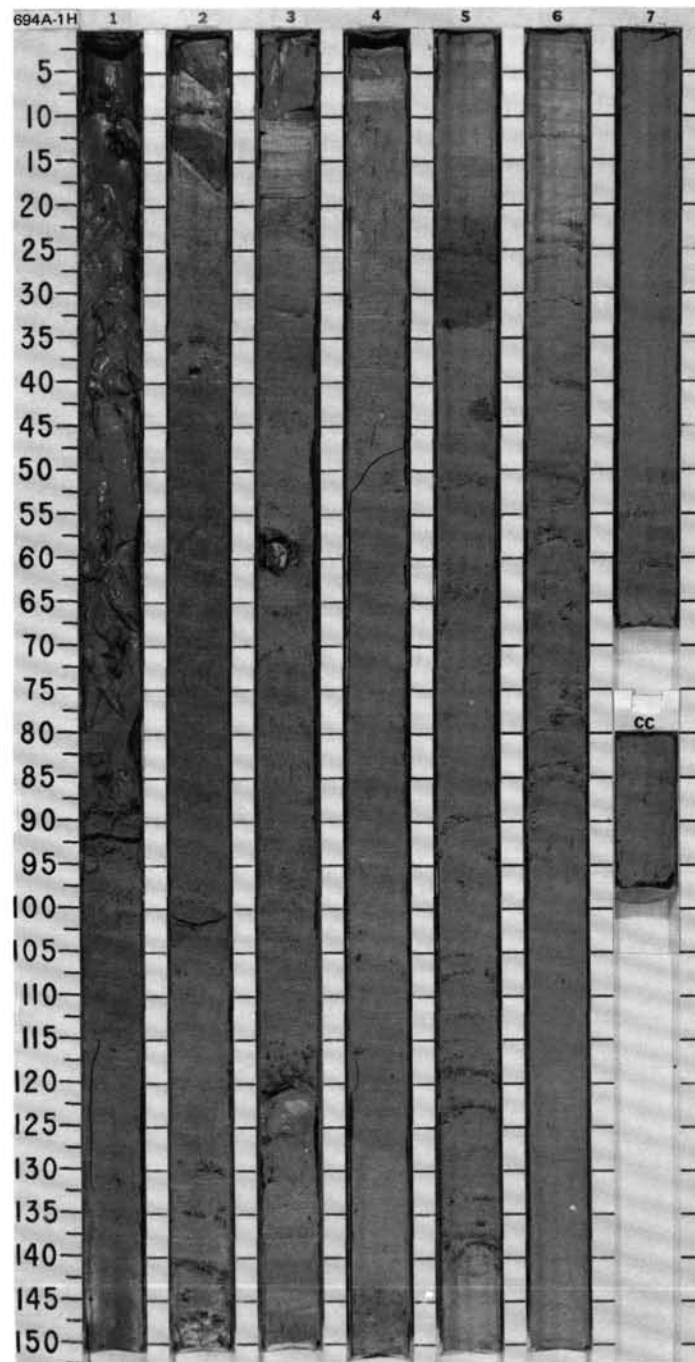
Deposition of the thick (90 m) sandy turbidite sequence represented by Unit II was extremely rapid (~180 m/m.y. or more), and occurred within an interval of only 0.5 m.y. or less during the early Gilbert Chron (C3R4) before 4.8 Ma, in the earliest Pliocene. This rapid turbiditic deposition occurred during an interval marked elsewhere by major climatic cooling, increased and highly variable $\delta^{18}\text{O}$ values, and low sea level (Hodell et al., 1986). High rates of turbidite sedimentation in this interval probably resulted from an expanding, yet unstable, West Antarctic ice-sheet. From 4.8 Ma to the present day, turbidite deposition has been much reduced at Site 694, indicating that West Antarctica ceased to be a major source of sediment supply to this part of the Weddell abyssal plain. From this it could be concluded that the West Antarctic ice-sheet has been a relatively permanent and stable feature since earliest Pliocene times. Until now suitable stratigraphic sequences were not available to determine whether this ice-sheet had been unstable during the late Neogene. Ciesielski and Weaver (1974) and Ciesielski et al. (1982) speculated that early Pliocene warming would have caused at least a partial deglaciation (ungrounding) of the West Antarctic ice-sheet and most grounded ice along the periphery of the continent. The Site 694 sequence would suggest that early Pliocene warming did not destabilize the West Antarctic ice-sheet. The significance of the turbidite record at Site 694 underlines the importance of more detailed study of provenance of the lithic grains which is still in progress.

Site 323, to the west of the Antarctic Peninsula and located in the eastern part of the Bellingshausen Basin at a water depth of 4993 m (Hollister, Craddock, et al., 1976) provides additional information on the glacial state of West Antarctica. Site 323 was spot-cored at long intervals, has poor core recovery, and is poorly dated, but does provide a general stratigraphic record for comparison with Site 694. The section at Site 323 is marked

by several layers of silicified claystone at about 400 mbsf. The middle Miocene silicified claystone at the base of Site 694, which probably caused the loss of the hole, appears to be correlative with the uppermost silicified claystone at Site 323. Both sites contain conspicuous numbers of displaced neritic diatoms and intervals of abundant sponge spicules above, or in close association with, the silicified claystone layers. Of considerable climatic significance is the presence of fresh-water diatoms in sediments associated with the silicified claystone layer in Site 323 (Schrader, 1976). These forms are characteristic of lakes in temperate climatic regions (Hollister, Craddock et al., 1976) and further support our interpretation of Site 694 evidence of an absence of major West Antarctic glaciation during the middle Miocene. No Neogene spores or pollen, potentially derived from West Antarctica, were found in Site 694 sediments. The similar sediment sequences of apparently the same thickness at both sites suggests that the post-middle Miocene sedimentary regime at Site 694 was almost completely dominated by the West Antarctic source, as was certainly the case at Site 323. The greatly reduced thickness of Paleogene and older terrigenous sediments at Site 323 is explained by the much more northerly original position of Site 323 and the intervention of a mid-ocean ridge crest between that site and the Antarctic Peninsula (Barker, 1982; Cande et al., 1982).

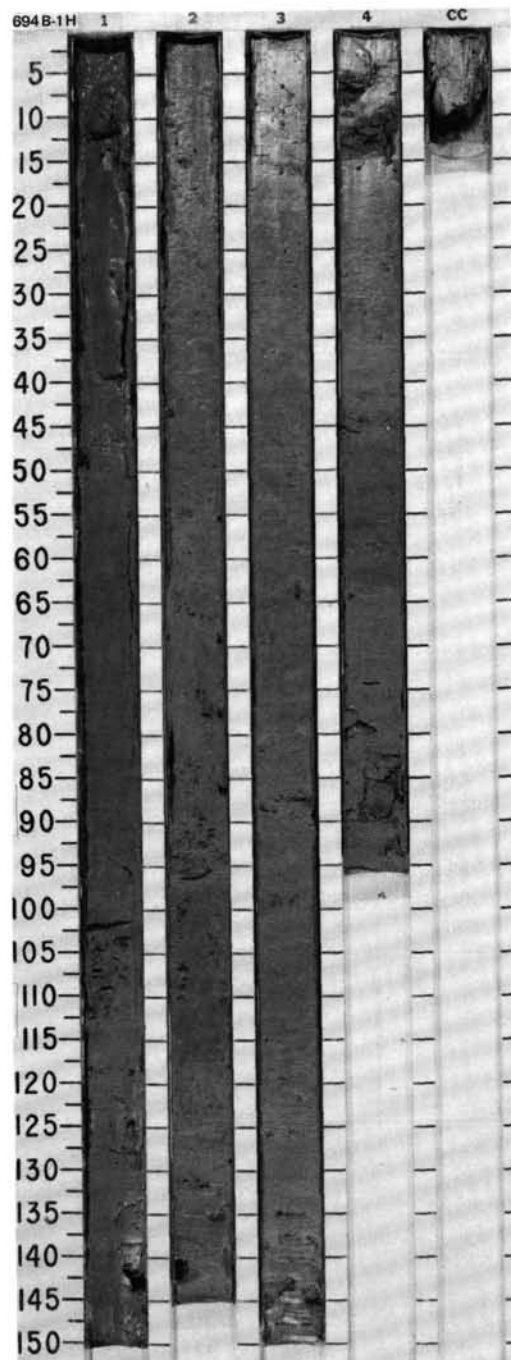
REFERENCES

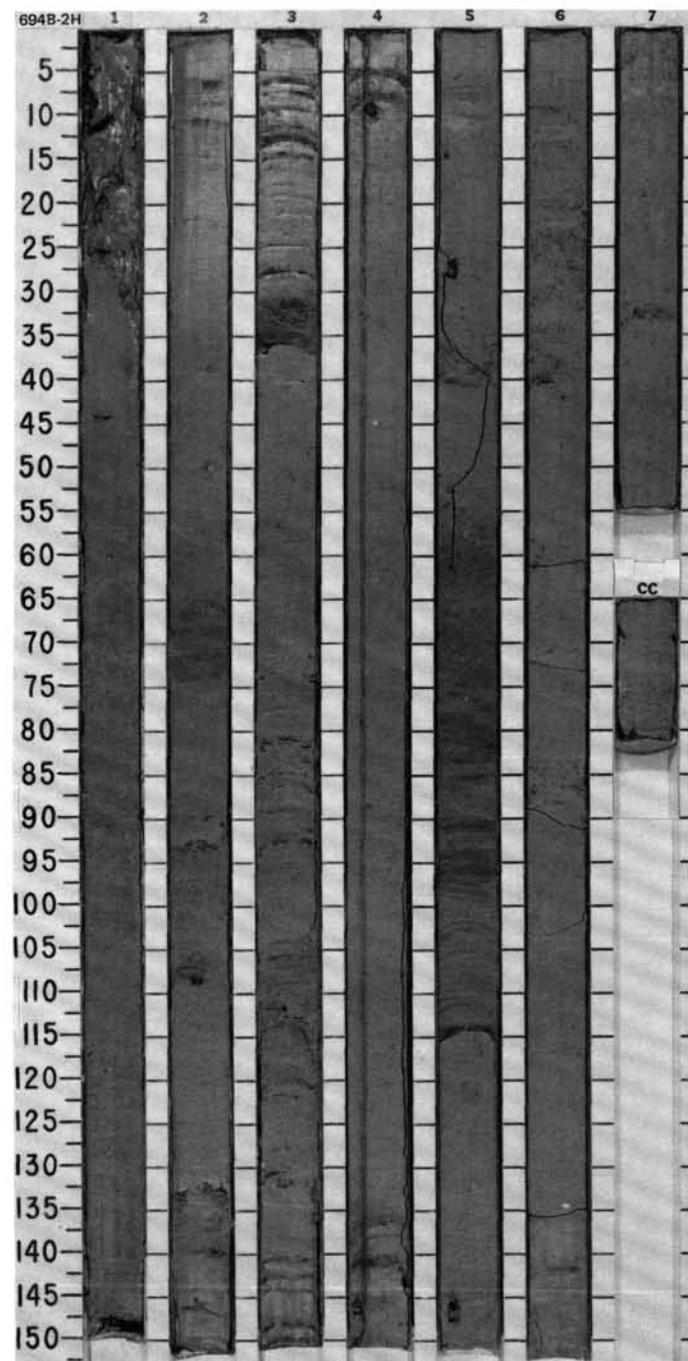
- Barker, P. F., 1982. The Cenozoic subduction history of the Pacific margin of the Antarctic Peninsula: Ridge crest-trench interactions. *J. Geol. Soc. London*, 139:787-801.
- Barron, J. A., and Keller, G., 1982. Widespread Miocene deep-sea hiatuses: coincidence with periods of global cooling. *Geology*, 10:577-581.
- Boyce, R. E., 1976. Definitions and laboratory techniques of compressional sound velocity parameters and water content, wet-bulk density, and porosity parameters by gravimetric and gamma ray attenuation techniques. In Schlanger, S. O., Jackson, E. D., et al., *Init. Repts. DSDP*, 33: Washington (U.S. Govt. Printing Office), 931-935.
- Brady, H. T., 1977. *Thalassiosira torokina* n. sp. (diatom) and its significance in late Cenozoic biostratigraphy. *Antarct. J.*, 12:122-123.
- Brindley, G. W., and Brown, G. (Eds.), 1984. *Crystal Structures of Clay Minerals and their X-ray Identification*: London (London Mineralogical Society).
- Cande, S. C., Herron, E. M., and Hall, B. R., 1982. The early Cenozoic tectonic history of the southeast Pacific. *Earth Planet. Sci. Lett.*, 57:63-74.
- Carlson, R. L., Gangi, A. F., and Snow, K. R., 1986. Empirical reflection travel time versus depth and velocity versus depth functions for the deep-sea sediment column. *J. Geophys. Res.*, 91:8249-8266.
- Ciesielski, P. F., 1983. The Neogene and Quaternary diatom biostratigraphy of subantarctic sediments, Deep Sea Drilling Project Leg 71. In Ludwig, W. J., Krashenninnikov, V. A., et al., *Init. Repts. DSDP*, 71: Washington (U.S. Govt. Printing Office), 635-665.
- Ciesielski, P. F., and Weaver, F. M., 1974. Early Pliocene temperature changes in the Antarctic Seas. *Geology*, 12:511-515.
- Ciesielski, P. F., Ledbetter, M. T., and Ellwood, B. B., 1982. The development of Antarctic glaciation and the Neogene paleo-environment of the Maurice Ewing Bank. *Mar. Geol.*, 46:1-51.
- Davies, T. A., Weser, O. E., Luyendyk, B. P., and Kidd, R. B., 1975. Unconformities in the sediments of the Indian Ocean. *Nature*, 253: 15.
- Deroo, G., Herbin, J. P., and Huc, A. Y., 1984. Organic geochemistry of Cretaceous black shales from Deep Sea Drilling Site 530, Leg 75, eastern south Atlantic. In Ludwig, W. J., Krashenninnikov, V. A., et al., *Init. Repts. DSDP*, 75: Washington (U.S. Govt. Printing Office), 983-999.
- Dunoyer de Segonzac, G., 1969. Les Minéraux Argileux dans la Diagenèse: Passage au Métamorphisme. *Sci. Géol. Strasbourg Mém.* 29.
- Gieskes, J. M., and Lawrence, J. R., 1976. Interstitial water studies, Leg 35. In Hollister, C. D., Craddock, C., et al., *Init. Repts. DSDP*, 35: Washington (U.S. Govt. Printing Office), 407-424.
- Haq, B. U., 1976. Coccoliths in cores from the Bellingshausen Abyssal Plain and Antarctic Continental Rise (DSDP Leg 35). In Hollister, C. D., and Craddock, C., et al., *Init. Repts. DSDP*, 35: Washington (U.S. Govt. Printing Office), 557-567.
- Hodell, D. A., Elmsstrom, K. M., and Kennett, J. P., 1986. Latest Miocene benthic $S^{18}O$ changes, global ice volume, sea level and the "Mesinian salinity crisis." *Nature*, 320:411-414.
- Hollister, C. D., Craddock, C., et al., 1976. *Init. Repts. DSDP*, 35: Washington (U.S. Govt. Printing Office).
- Hunt, J. M., 1979. *Petroleum Geochemistry and Geology*: San Francisco (W. H. Freeman).
- Kennett, J. P., Burns, R. E., Andrews, J. E., Churkin, M., Davies, T. A., Dumitricu, P., Edwards, A. P., Galehouse, J. S., Packham, G. H., and Van der Lingen, G. J., 1972. Australian-Antarctic continental drift, paleocirculation changes and Oligocene deep-sea erosion. *Nature Phys. Sci.*, 239:51.
- Kennett, J. P., and Von der Borch, C. C., 1985. Southwest Pacific Cenozoic paleoceanography. In Kennett, J. P., Von der Borch, C. C., et al., *Init. Repts. DSDP*, 90: Washington (U.S. Govt. Printing Office), 1493-1517.
- MacKenzie, F. T., and Garrels, R. M., 1966. Chemical mass balance between rivers and oceans. *Amer. J. Sci.*, 264:507-525.
- Manheim, F. T., and Sayles, F. L., 1974. Composition and origin of interstitial waters of marine sediments. In Goldberg, E. D. (Ed.), *The Sea* (Vol. 5): New York (Wiley), 527-568.
- Millot, G., 1964. *Géologie des Argiles*: Paris (Masson).
- Norris, G., 1965. Triassic and Jurassic miospores and acritarchs from the Beacon and Ferrar Groups, Victoria Land, Antarctica. *N. Z. J. Geol. Geophys.*, 8:236-77.
- Roegl, F., 1976. Late Cretaceous to Pleistocene Foraminifera from the southeast Pacific Basin, DSDP Leg 35. In Hollister, C. D., Craddock, C., et al., *Initial Reports DSDP*, 35: Washington (U.S. Govt. Printing Office), 539-555.
- Rona, P. A., 1973. Worldwide unconformities in marine sediments related to eustatic changes of sea level. *Nature Phys. Sci.*, 244:25.
- Schrader, H. J., 1976. Cenozoic planktonic diatom biostratigraphy of the Southern Pacific ocean. In Hollister, C. D., Craddock, C., et al., *Init. Repts. DSDP*, 35: Washington (U.S. Govt. Printing Office), 605-671.
- Shipboard Scientific Party, 1987. Site 652. In Kastens, K. A., Mascle, J., et al., *Proc. ODP, Init. Repts.*, 107: College Station, TX (Ocean Drilling Program), 403-597.
- Stumm, W., and Morgan, J. J. (Eds.), 1981. *Aquatic Chemistry* (2nd Ed.): New York (Wiley).
- Suess, E., von Huene, R., et al., 1988. *Proc. ODP, Init. Repts.*, 112: College Station, TX (Ocean Drilling Program).
- Sverdrup, H. U., Johnson, M. W., and Fleming, R. (Eds.), 1942. *The Oceans: Their Physics, Chemistry and General Biology*: Englewood Cliffs, N.J. (Prentice-Hall).
- Truswell, E. M., 1986. Palynology. In Barrett, P. J., Antarctic Cenozoic history from the MSSTS-1 drillhole, McMurdo Sound. *DSIR Bull.*, 237:131-134.
- Ugolini, F. C., and Jackson, M. L., 1982. Weathering and mineral synthesis in Antarctic soils. In Craddock, C. (Ed.), *Antarct. Geosci.*, I.U.G.S. Ser. B, 4:1101-1108.
- Von Herzen, R. P., and Maxwell, A. E., 1959. The measurement of thermal conductivity of deep-sea sediments by a needle probe method. *J. Geophys. Res.*, 65:1535-1541.
- Weaver, F. M., and Gombos, A. M., 1981. Southern high-latitude diatom biostratigraphy. Soc. Econ. Paleontol. Mineral. Spec. Publ., 32: 445-470.
- Whelan, J. J., Hunt, J. M., Jasper, J., and Huc, A., 1984. Migration of C_1 - C_8 Hydrocarbons in Marine Sediments. Woods Hole Oceanogr. Contrib. 5634.



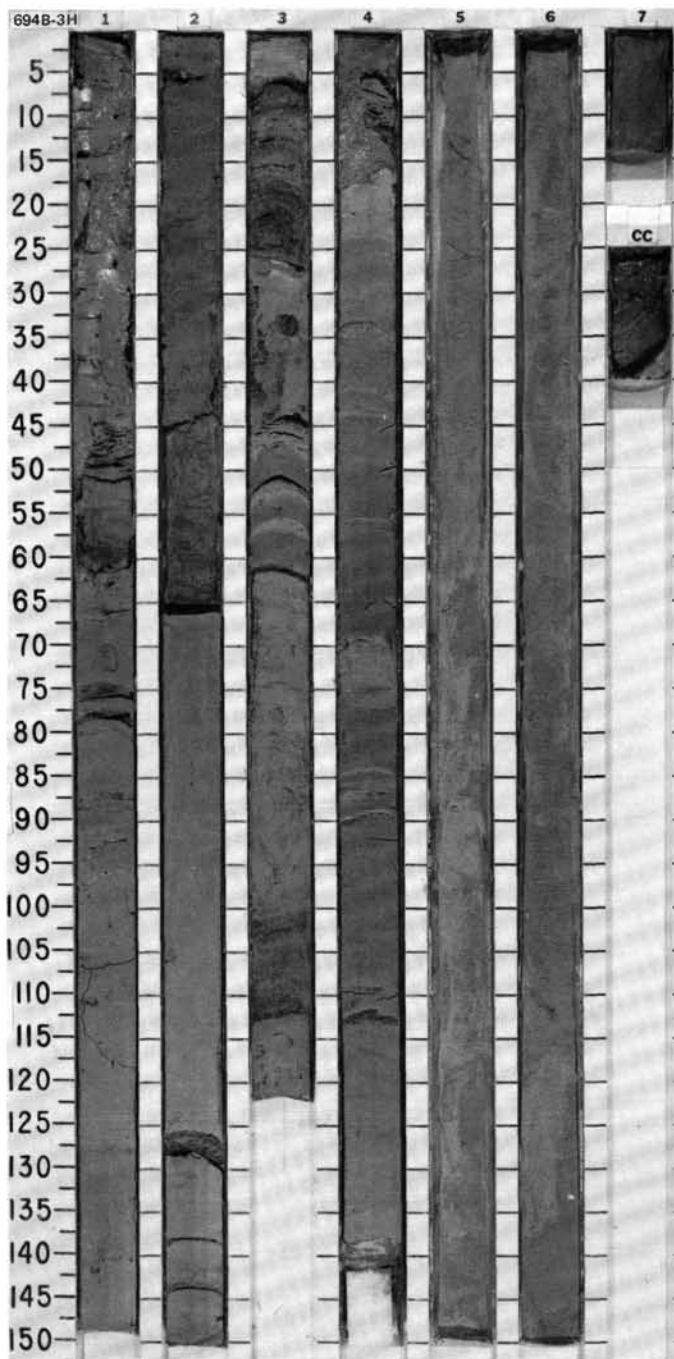
SITE 694 HOLE B CORE 1H CORED INTERVAL 4653.4-4658.9 mbsl; 0-5.5 mbsf

TIME-ROCK UNIT	BIOSTRAT. ZONE/ FOSSIL CHARACTER	PHYS. PROPERTIES	CHEMISTRY	SECTION	METERS	GRAPHIC LITHOLOGY	DRILLING DISTURB.	SED. STRUCTURES	SAMPLES	LITHOLOGIC DESCRIPTION
PLEISTOCENE	FORAMINIFERS NANNOFOSSILS RADIOLARIANS DIATOMS PALYMONOPHS PALEOMAGNETICS	PHYS. PROPERTIES	CHEMISTRY	SECTION	METERS	GRAPHIC LITHOLOGY	DRILLING DISTURB.	SED. STRUCTURES	SAMPLES	LITHOLOGIC DESCRIPTION
B										CLAYEY MUD
B										Major lithology: Clayey mud, mainly dark grayish brown (2.5Y 4/2) and grayish brown (2.5Y 5/2); mottled with dark grayish brown (10YR 4/2) or olive gray (5Y 5/2). Moderate to strong bioturbation; color tends to be more gray or olive outside burrows and more brown inside. Few small dropstones in Sections 2 and 3; one in Section 2, 142 cm, is manganese-coated.
B										Minor lithologies: Silt, grayish brown (2.5Y 5/2, 5/3), occurs as sharp-based graded laminae or very thin beds in Sections 2 and 3. Similar beds in Section 1 are very disturbed and occur as clasts. Silt, light olive brown (2.5Y 5/4), occurs in two very thin sharp-based graded beds at the top of Section 4, and as a thin bed at the base of Section 4, both disturbed by drilling. Graded bed of sandy mud to silt, light olive brown (2.5Y 5/4), in Section 4, 44-63 cm. Parallel lamination occurs near the base.
B										SMEAR SLIDE SUMMARY (%):
B										1, 50 D 2, 50 D 3, 50 D 4, 47 M 4, 61 M
B										TEXTURE:
B										Sand 2 1 1 15 70
B										Silt 23 35 25 85 30
B										Clay 75 64 74 — —
B										COMPOSITION:
B										Quartz 15 25 15 72 75
B										Feldspar 3 3 3 7 7
B										Mica 3 3 5 5 5
B										Clay 77 64 74 — —
B										Accessory minerals:
B										Heavy minerals 1 2 2 3 1
B										Opaque minerals 1 3 1 10 5
B										Amphibole — — Tr 3 7



SITE 694

TIME - ROCK UNIT	BIOSTRAT. ZONE/ FOSSIL CHARACTER						PHYS. PROPERTIES	CHEMISTRY	SECTION	METERS	GRAPHIC LITHOLOGY	DRILLING DISTURB.	SED. STRUCTURES	SAMPLES	LITHOLOGIC DESCRIPTION
	FORAMINIFERS	NANNOFOSILS	RADIOLARIANS	DIAZONES	PALYMONOPHUS	PALEOMAGNETICS									
LOWER PLIOCENE	B	B	B	B	B	Gilbert	V-1460 $\phi=89^\circ \gamma=1.76$ $\phi=68$ V-1490		1	0.5 1.0			*		CLAY, CLAYEY MUD, and SILT Major lithologies: Clay and clayey mud, olive gray (5Y 5/2) and gray (5Y 5/1), with absent to moderate mottling and bioturbation. Silt, with multiple colors including pale yellow (5Y 7/3), olive brown (5Y 4/4), light yellowish brown (2.5Y 6/4), and light olive brown (2.5Y 5/3). The silt is commonly laminated and graded. Minor lithology: Sandy mud, pale olive (5Y 6/3), totally disturbed by coring. Grading is sometimes continuous from a thin, 1-2-grain-thick sand layer to clay layer. Bases are sharp and commonly scoured; tops are both sharp and gradational. Thicknesses of the silty intervals range from about 1 mm to 66 cm. In Section 2, 147 cm, a ball and pillow structure is present in a thin, 1-mm-thick, silty lamina. No coarsening or thickening upward is observed.
									2				*		SMEAR SLIDE SUMMARY (%): TEXTURE: Sand Tr 2 — 62 — Silt 97 48 10 38 96 12 — 18 Clay 3 50 90 — 4 88 82 COMPOSITION: Quartz 80 28 6 — 81 5 4 Feldspar 2 1 — — Tr — — Mica — Tr — 2 2 2 2 Clay 3 2 90 — 4 88 82 Volcanic glass 4 — — Tr 8 1 — Accessory minerals — 8 — 6 — — 2 Opaque minerals 5 4 4 6 — — 4 10 Amphibole 4 4 — 4 1 — — Glauconite 2 1 — 2 Tr Tr — Radiolarians — Tr — — — — —
									3				*		
									4				*		
									5						
									6						
									7						

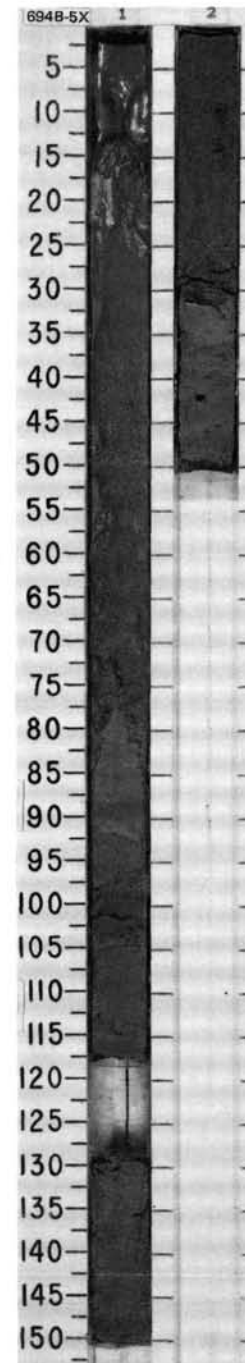
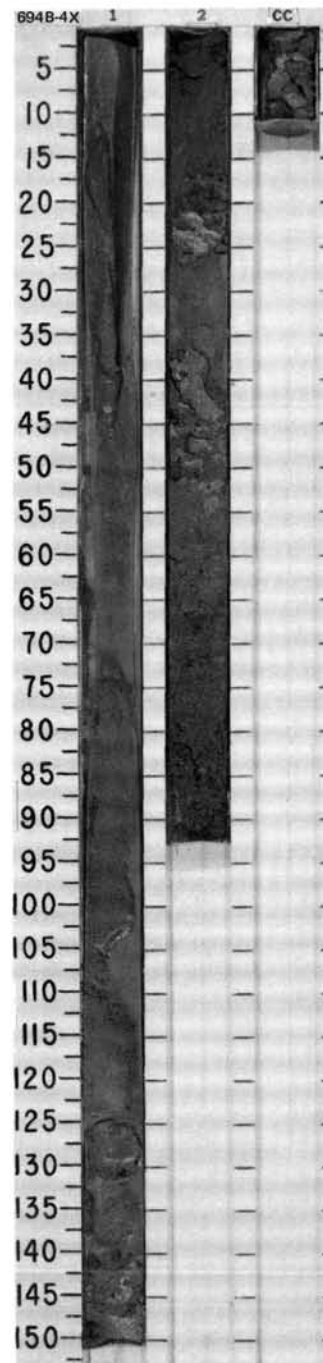


SITE 694 HOLE B CORE 4X CORED INTERVAL 4678.1-4687.7 mbsl; 24.7-34.3 mbsf

TIME-ROCK UNIT	BIOSTRAT. ZONE/ FOSSIL CHARACTER					SECTION	METERS	GRAPHIC LITHOLOGY	DRILLING DISTURB.	SED. STRUCTURES	SAMPLES	LITHOLOGIC DESCRIPTION
	FORAMINIFERS	NANNOFOSSILS	RADIOLARIANS	DIATOMS	PALYNOMORPHS							
LOWER PLIOCENE	B	B	B	B	B							<p>SANDY MUD and SAND</p> <p>Major lithologies: Sandy mud and sand, totally disturbed by coring, with clay clasts that are gray (5Y 5/1) and light gray (2.5Y 7/2). Sand is graded from fine at top to coarse at base.</p> <p>SMEAR SLIDE SUMMARY (%):</p> <p>2.40 M</p> <p>TEXTURE:</p> <p>Silt 8 Clay 92</p> <p>COMPOSITION:</p> <p>Mica Tr Clay 92 Accessory minerals 4 Opaque minerals 4</p>
						1	0.5					
						2	1.0					

SITE 694 HOLE B CORE 5X CORED INTERVAL 4687.7-4697.4 mbsl; 34.3-44.0 mbsf

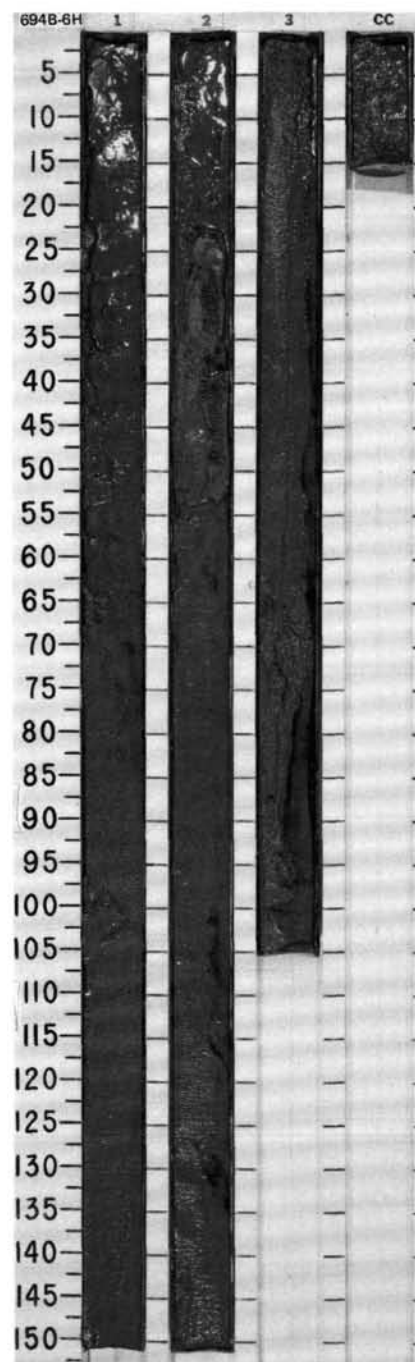
TIME-ROCK UNIT	BIOSTRAT. ZONE/ FOSSIL CHARACTER					SECTION	METERS	GRAPHIC LITHOLOGY	DRILLING DISTURB.	SED. STRUCTURES	SAMPLES	LITHOLOGIC DESCRIPTION
	FORAMINIFERS	NANNOFOSSILS	RADIOLARIANS	DIATOMS	PALYNOMORPHS							
LOWER PLIOCENE	B	B	B	R.P	Coaly dropstone palynomorphs of Mesozoic age							<p>SAND AND CLAY</p> <p>Major lithologies: Sand, gray (5Y 5/1), fine to coarse-grained. Clay, gray (N 4/1), as distinct color bands.</p> <p>Minor lithology: Silt; a graded layer, Section 1, 95-101 cm, may be partially caused by drilling disturbance.</p> <p>Dropstone, coal, 0.5 cm in diameter, in Section 2, 40 cm.</p> <p>SMEAR SLIDE SUMMARY (%):</p> <p>1.87 D</p> <p>TEXTURE:</p> <p>Silt 9 Clay 91</p> <p>COMPOSITION:</p> <p>Quartz 1 Feldspar Tr Clay 91 Accessory minerals 2 Opaque minerals 6</p>
						1	0.5					
						2	1.0					



SITE 694 HOLE B CORE 6H CORED INTERVAL 4697.4-4707.0 mbsl; 44.0-53.6 mbsf

TIME-ROCK UNIT	BIOSTRAT. ZONE/ FOSSIL CHARACTER					SECTION	METERS	GRAPHIC LITHOLOGY	DRILLING DISTURB.	SED. STRUCTURES	SAMPLES	LITHOLOGIC DESCRIPTION
	FORAMINIFERS	NANNOFOSSILS	RADIOLARIANS	DIATOMS	PALYNOMORPHS							
LOWER PLIOCENE	B											<p>SAND</p> <p>Major lithology: Sand, gray (2.5Y 5/1), reworked coarse-grained turbidite. Soupy because of drilling.</p> <p>Minor lithology: Silty mud in Section 2, 21-52 cm, gray (2.5Y 5/1), very disturbed.</p> <p>SMEAR SLIDE SUMMARY (%):</p> <p>2, 73 M</p> <p>TEXTURE:</p> <p>Sand Tr Silt 60 Clay 40</p> <p>COMPOSITION:</p> <p>Quartz 44 Feldspar 2 Clay 40 Volcanic glass 4 Accessory minerals: Opaque minerals 6 Amphiboles 4</p>
	B					1	0.5					
	B					2	1.0					
	B					3						
						CC						

CORES 113-694B-7H TO 8H NO RECOVERY

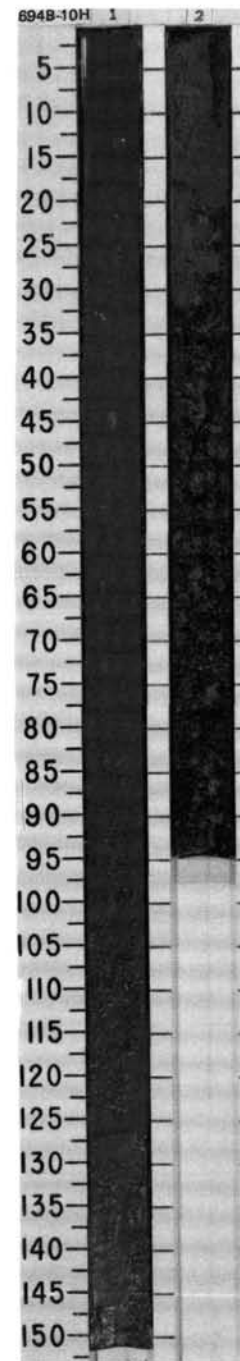
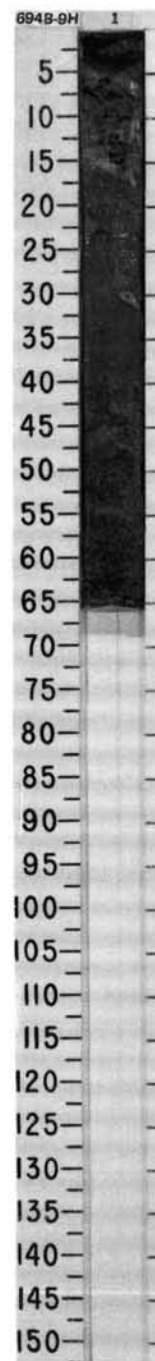


SITE 694 HOLE B CORE 9H CORED INTERVAL 4726.2-4735.9 mbsl; 72.8-82.5 mbsf

TIME-ROCK UNIT	BIOSTRAT. ZONE/ FOSSIL CHARACTER					SECTION	METERS	GRAPHIC LITHOLOGY	DRILLING DISTURB.	SED. STRUCTURES	SAMPLES	LITHOLOGIC DESCRIPTION
	FORAMINIFERS	NANNOFOSSILS	RADIOLARIANS	DIATOMS	PALYNOMORPHS							
LOWER PLIOCENE	B	B	B	B	B	1	0.5				*	<p>SAND</p> <p>Major lithology: Sand, olive gray (5Y 5/2), graded from very coarse to fine sand/coarse silt. Base is grayish brown (2.5Y 5/2), top is olive gray. Sand grains are subangular to subrounded clear gray quartz, black opaques, fine-grained metasediments, and less common garnet, biotite, and pyrite.</p> <p>Minor lithology: Clayey mud in Section 1, 5-15 cm, grayish brown (2.5Y 5/2), mixed with smaller dark gray patches (N 4/0). Mid-section, 45-50 cm, clasts of grayish brown clay (2.5Y 4/2).</p> <p>SMEAR SLIDE SUMMARY (%):</p> <p>1, 14 M</p> <p>TEXTURE:</p> <p>Sand 1 Silt 42 Clay 57</p> <p>COMPOSITION:</p> <p>Quartz 27 Feldspar 3 Mica 4 Clay 57 Volcanic glass 2 Accessory minerals: Opaque minerals 4 Glauconite 1 Amphibole 2</p>

SITE 694 HOLE B CORE 10H CORED INTERVAL 4735.9-4745.6 mbsl; 82.5-92.2 mbsf

TIME-ROCK UNIT	BIOSTRAT. ZONE/ FOSSIL CHARACTER					SECTION	METERS	GRAPHIC LITHOLOGY	DRILLING DISTURB.	SED. STRUCTURES	SAMPLES	LITHOLOGIC DESCRIPTION
	FORAMINIFERS	NANNOFOSSILS	RADIOLARIANS	DIATOMS	PALYNOMORPHS							
LOWER PLIOCENE	B	B	B	R.P.	B	1	0.5				*	<p>SAND</p> <p>Major lithology: Sand, (dark) gray (5Y 4.5/1), graded unit in Section 1, 0-125 cm, coarse and poorly sorted to fine and well-sorted; and fine, well-sorted sand from Section 1, 125 cm, to Section 2, 30 cm. Coarse and poorly sorted in Section 2, 30-95 cm. The lower two beds are not graded.</p> <p>Minor lithology: Clasts of clay, 1-2 cm across, mainly light olive brown (2.5Y 5/4), in Section 1, and olive (5Y 4/3) in Section 2. Clasts of greenish gray (5G 5/1) clay in Section 2, 43 and 92 cm; clasts of fine sand, gray (5Y 5/1), in Section 2, 41 and 92 cm.</p> <p>SMEAR SLIDE SUMMARY (%):</p> <p>1, 13 1, 30 2, 21 2, 42 M D D M</p> <p>TEXTURE:</p> <p>Sand — 79 79 7 Silt 11 15 20 48 Clay 89 6 1 45</p> <p>COMPOSITION:</p> <p>Quartz 6 84 84 40 Feldspar 1 5 3 5 Mica 2 Tr 2 3 Clay 89 6 1 47 Volcanic glass 1 — — — Accessory minerals: Heavy minerals — — 3 Tr Opaque minerals 1 4 5 3 Glauconite — 1 — 1 Amphibole — — 3 1</p>
						2	1.0				*	

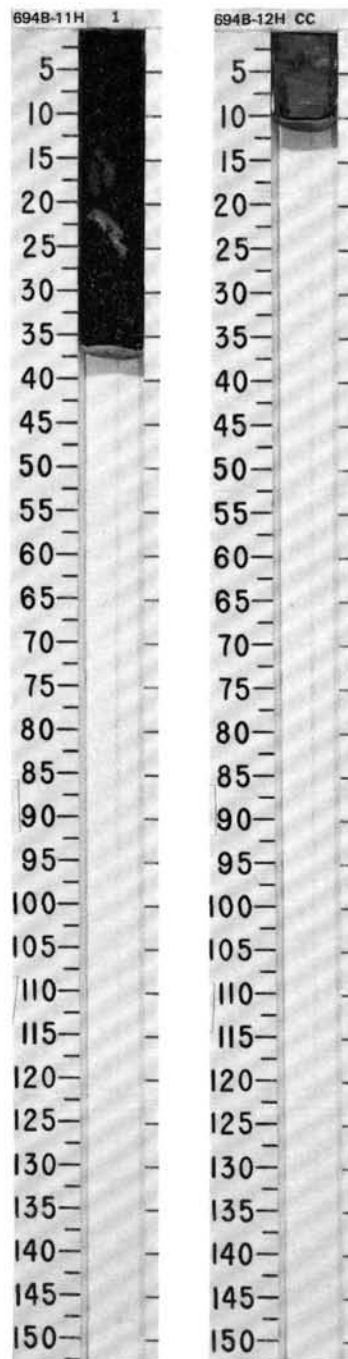


SITE 694 HOLE B CORE 11H CORED INTERVAL 4745.6-4755.3 mbsl; 92.2-101.9 mbsf

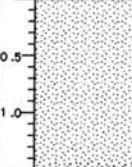
TIME-ROCK UNIT	BIOSTRAT. ZONE/ FOSSIL CHARACTER				PALEOMAGNETICS	PHYS. PROPERTIES	CHEMISTRY	SECTION	METERS	GRAPHIC LITHOLOGY	DRILLING DISTURB.	SED. STRUCTURES	SAMPLES	LITHOLOGIC DESCRIPTION									
	FORAMINIFERS	NANNOFOSSILS	RADIOLARIANS	DIATOMS																			
LOWER PLIOCENE	B	B	B	B	B			1						SAND									
														Major lithology: Sand, dark gray (dominantly N 4/0), very coarse, well-sorted, subangular to subrounded grains. Mainly lithic fragments (green and gray fine-grained metasediments) with about 15% quartz, some feldspar, and rare garnet. Minor lithologies: Clayey mud, very dark gray (5Y 3/1) and clay, dark greenish gray (5GY 4/1); both occur as clasts up to 6 cm long.									
SMEAR SLIDE SUMMARY (%):																							
<table><tr><td></td><td>1, 16</td><td>1, 22</td></tr><tr><td></td><td>M</td><td>M</td></tr></table>																1, 16	1, 22		M	M			
	1, 16	1, 22																					
	M	M																					
TEXTURE:																							
<table><tr><td>Sand</td><td>1</td><td>1</td></tr><tr><td>Silt</td><td>24</td><td>19</td></tr><tr><td>Clay</td><td>75</td><td>80</td></tr></table>															Sand	1	1	Silt	24	19	Clay	75	80
Sand	1	1																					
Silt	24	19																					
Clay	75	80																					
COMPOSITION:																							
<table><tr><td>Quartz</td><td>20</td><td>15</td></tr><tr><td>Feldspar</td><td>3</td><td>2</td></tr><tr><td>Clay</td><td>75</td><td>80</td></tr></table>															Quartz	20	15	Feldspar	3	2	Clay	75	80
Quartz	20	15																					
Feldspar	3	2																					
Clay	75	80																					
Accessory minerals:																							
<table><tr><td>Heavy minerals</td><td>1</td><td>2</td></tr><tr><td>Opaque minerals</td><td>2</td><td>1</td></tr></table>															Heavy minerals	1	2	Opaque minerals	2	1			
Heavy minerals	1	2																					
Opaque minerals	2	1																					

SITE 694 HOLE B CORE 12H CORED INTERVAL 4755.3-4760.8 mbsl; 101.9-107.4 mbsf

TIME-ROCK UNIT	BIOSTRAT. ZONE/ FOSSIL CHARACTER				PALEOMAGNETICS	PHYS. PROPERTIES	CHEMISTRY	SECTION	METERS	GRAPHIC LITHOLOGY	DRILLING DISTURB. SED. STRUCTURES	SAMPLES	LITHOLOGIC DESCRIPTION
	FORAMINIFERS	NANNOFOSSILS	RADIOLARIANS	DIATOMS									
LOWER PLIOCENE	B	B	B	R.P.	B			CC					SILTY MUD and CLAYEY MUD
Major lithologies: Silty mud, dark greenish gray (5GY 4/1); slightly sandy from CC, 3-6 cm. Clayey mud, dark greenish gray (5GY 4/1), from 6 cm to base of CC at 11 cm.													
SMEAR SLIDE SUMMARY (%):													
CC, 4 D CC, 7 D													
TEXTURE:													
Sand 2 —													
Silt 68 30													
Clay 30 70													
COMPOSITION:													
Quartz 61 22													
Feldspar 10 5													
Mica 1 —													
Clay 20 70													
Accessory minerals:													
Heavy minerals 1 1													
Opaque minerals 4 2													
Hornblende 3 —													



SITE 694 HOLE B CORE 13H CORED INTERVAL 4760.8-4764.9 mbsl; 107.4-111.5 mbsf

TIME-ROCK UNIT	BIOSTRAT. ZONE/ FOSSIL CHARACTER				SECTION	METERS	GRAPHIC LITHOLOGY	DRILLING DISTURB.	SED. STRUCTURES	SAMPLES	LITHOLOGIC DESCRIPTION																																				
	FORAMINIFERS	NANNOFOSSILS	RADIOLARIANS	DIATOMS																																											
												PALYNOFORMPHS																																			
													PALEOMAGNETICS																																		
PHYS. PROPERTIES				CHEMISTRY																																											
LOWER PLIOCENE	B	B	R.P	R.P		0.5			◇	*	<p>SAND</p> <p>Major lithology: Sand, very coarse, dark gray (N 4/0), subangular to subrounded, few very angular grains. Mainly lithic fragments with about 10% quartz.</p> <p>Minor lithology: Clay and clayey mud clasts, dark gray (N 4/0) and dark greenish gray (5GY 4/1), occur in middle and basal section. Middle of Section 1 has a watery clay matrix.</p>																																				
	B				1			◇	*	<p>SMEAR SLIDE SUMMARY (%):</p> <table><tr><td></td><td>1, 28</td><td>1, 146</td></tr><tr><td></td><td>M</td><td>M</td></tr></table> <p>TEXTURE:</p> <table><tr><td>Sand</td><td>Tr</td><td>Tr</td></tr><tr><td>Silt</td><td>10</td><td>25</td></tr><tr><td>Clay</td><td>90</td><td>75</td></tr></table> <p>COMPOSITION:</p> <table><tr><td>Quartz</td><td>7</td><td>9</td></tr><tr><td>Feldspar</td><td>—</td><td>2</td></tr><tr><td>Mica</td><td>3</td><td>7</td></tr><tr><td>Clay</td><td>88</td><td>75</td></tr></table> <p>Accessory minerals:</p> <table><tr><td>Amphibole</td><td>Tr</td><td>—</td></tr><tr><td>Opaque minerals</td><td>2</td><td>3</td></tr><tr><td>Heavy minerals</td><td>Tr</td><td>4</td></tr></table>			1, 28	1, 146		M	M	Sand	Tr	Tr	Silt	10	25	Clay	90	75	Quartz	7	9	Feldspar	—	2	Mica	3	7	Clay	88	75	Amphibole	Tr	—	Opaque minerals	2	3	Heavy minerals	Tr	4
		1, 28	1, 146																																												
		M	M																																												
	Sand	Tr	Tr																																												
Silt	10	25																																													
Clay	90	75																																													
Quartz	7	9																																													
Feldspar	—	2																																													
Mica	3	7																																													
Clay	88	75																																													
Amphibole	Tr	—																																													
Opaque minerals	2	3																																													
Heavy minerals	Tr	4																																													
					1.0		◇	*																																							
							◇	*																																							
							◇	*																																							

SITE 694 HOLE B CORE 14H CORED INTERVAL 4764.9-4774.6 mbsl; 111.5-121.2 mbsf

TIME- ROCK UNIT	BIOSTRAT. ZONE/ FOSSIL CHARACTER				SECTION	METERS	GRAPHIC LITHOLOGY	DRILLING DISTURB.	SED. STRUCTURES	SAMPLES	LITHOLOGIC DESCRIPTION																																																																																																																
	FORAMINIFERS	NANNOFOSSILS	RADIOLARIANS	DIATOMS																																																																																																																							
LOWER PLIOCENE	B		LOWER TAU								<p>SAND and SANDY MUD</p> <p>Major lithologies: Sand, dark greenish gray (5GY 4/1), coarse tail-graded from fine, poorly sorted sand at the base of Section 2, through fine, moderately sorted sand at the base of Section 1, to sandy mud (47% silt) at the top of the bed, Section 1, 75 cm. Sand, dark gray (5Y 4/1), fine, moderately sorted, in Section 1, 0-24 cm; scoured base, but not graded.</p> <p>Minor lithologies: Clay and clayey mud in Section 1, 22-77 and 99-106 cm, dark greenish gray (5GY 4/1) to very dark gray (5Y 3/1). Diatom-bearing clayey mud in Section 1, 24-34 cm, dark greenish gray (5GY 4/1), and a few scattered sand grains in Section 1, 65-69 cm. Silt, dark gray (5Y 4/1); two graded beds in Section 1, 34-40 and 56-60 cm.</p> <p>SMEAR SLIDE SUMMARY (%):</p> <table><tr><td></td><td>1, 30</td><td>1, 31</td><td>1, 70</td><td>1, 85</td><td>1, 103</td><td>2, 60</td></tr><tr><td></td><td>M</td><td>M</td><td>M</td><td>D</td><td>M</td><td>D</td></tr></table> <p>TEXTURE:</p> <table><tr><td>Sand</td><td>5</td><td>—</td><td>1</td><td>50</td><td>1</td><td>70</td></tr><tr><td>Silt</td><td>85</td><td>30</td><td>31</td><td>47</td><td>32</td><td>25</td></tr><tr><td>Clay</td><td>10</td><td>70</td><td>68</td><td>3</td><td>67</td><td>5</td></tr></table> <p>COMPOSITION:</p> <table><tr><td>Quartz</td><td>63</td><td>9</td><td>14</td><td>81</td><td>20</td><td>80</td></tr><tr><td>Feldspar</td><td>3</td><td>1</td><td>2</td><td>3</td><td>2</td><td>5</td></tr><tr><td>Mica</td><td>2</td><td>—</td><td>5</td><td>2</td><td>3</td><td>3</td></tr><tr><td>Clay</td><td>10</td><td>70</td><td>68</td><td>3</td><td>67</td><td>5</td></tr></table> <p>Accessory minerals:</p> <table><tr><td>Amphibole</td><td>3</td><td>—</td><td>—</td><td>5</td><td>2</td><td>1</td></tr><tr><td>Glaucinite</td><td>2</td><td>—</td><td>1</td><td>1</td><td>1</td><td>Tr</td></tr><tr><td>Rutile</td><td>—</td><td>—</td><td>—</td><td>—</td><td>Tr</td><td>—</td></tr><tr><td>Opaque minerals</td><td>7</td><td>—</td><td>2</td><td>3</td><td>2</td><td>5</td></tr><tr><td>Heavy minerals</td><td>3</td><td>—</td><td>3</td><td>1</td><td>—</td><td>1</td></tr><tr><td>Diatoms</td><td>7</td><td>20</td><td>5</td><td>Tr</td><td>3</td><td>Tr</td></tr><tr><td>Sponge spicules</td><td>Tr</td><td>—</td><td>—</td><td>1</td><td>—</td><td>—</td></tr></table>		1, 30	1, 31	1, 70	1, 85	1, 103	2, 60		M	M	M	D	M	D	Sand	5	—	1	50	1	70	Silt	85	30	31	47	32	25	Clay	10	70	68	3	67	5	Quartz	63	9	14	81	20	80	Feldspar	3	1	2	3	2	5	Mica	2	—	5	2	3	3	Clay	10	70	68	3	67	5	Amphibole	3	—	—	5	2	1	Glaucinite	2	—	1	1	1	Tr	Rutile	—	—	—	—	Tr	—	Opaque minerals	7	—	2	3	2	5	Heavy minerals	3	—	3	1	—	1	Diatoms	7	20	5	Tr	3	Tr	Sponge spicules	Tr	—	—	1	—	—
		1, 30	1, 31	1, 70	1, 85	1, 103	2, 60																																																																																																																				
		M	M	M	D	M	D																																																																																																																				
	Sand	5	—	1	50	1	70																																																																																																																				
	Silt	85	30	31	47	32	25																																																																																																																				
Clay	10	70	68	3	67	5																																																																																																																					
Quartz	63	9	14	81	20	80																																																																																																																					
Feldspar	3	1	2	3	2	5																																																																																																																					
Mica	2	—	5	2	3	3																																																																																																																					
Clay	10	70	68	3	67	5																																																																																																																					
Amphibole	3	—	—	5	2	1																																																																																																																					
Glaucinite	2	—	1	1	1	Tr																																																																																																																					
Rutile	—	—	—	—	Tr	—																																																																																																																					
Opaque minerals	7	—	2	3	2	5																																																																																																																					
Heavy minerals	3	—	3	1	—	1																																																																																																																					
Diatoms	7	20	5	Tr	3	Tr																																																																																																																					
Sponge spicules	Tr	—	—	1	—	—																																																																																																																					

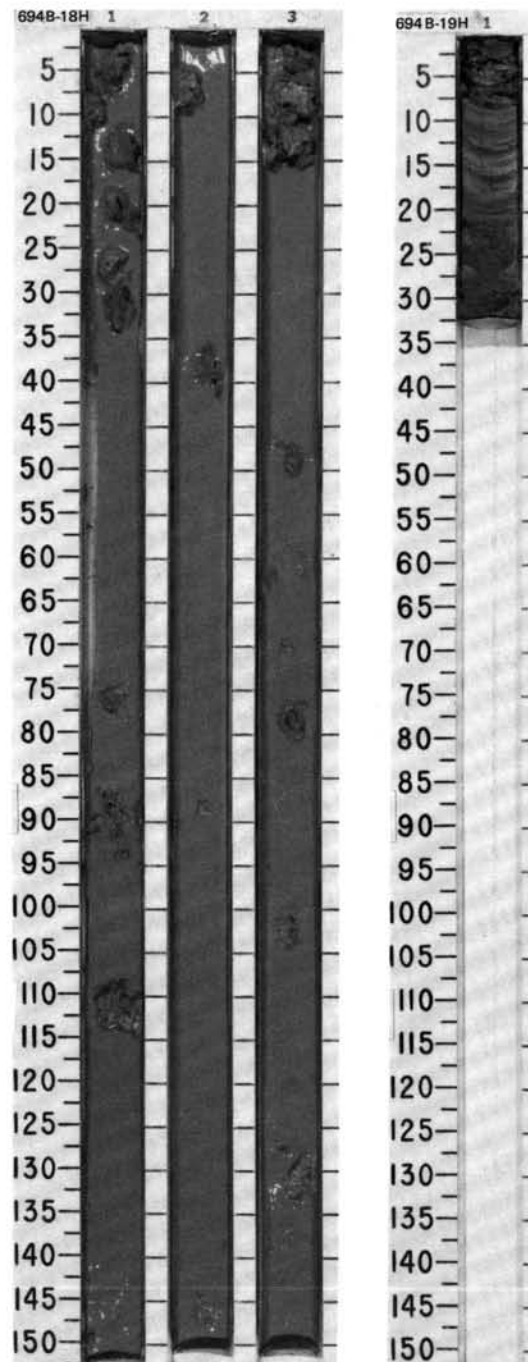


SITE 694 HOLE B CORE 18H CORED INTERVAL 4784.3-4789.3 mbsl; 130.9-135.9 mbsf

TIME-ROCK UNIT	BIOSTRAT. ZONE/ FOSSIL CHARACTER					PHYS. PROPERTIES	CHEMISTRY	SECTION	METERS	GRAPHIC LITHOLOGY	DRILLING DISTURB.	SED. STRUCTURES	SAMPLES	LITHOLOGIC DESCRIPTION																																																				
	FORAMINIFERS	NANNOFOSSILS	RADIOLARIANS	DIATOMS	PALYNOMORPHS																																																													
?	B																																																																	
	B								0.5				* *	DRILLING MUD, CLAY, and CLAYEY MUD Major lithologies: Drilling mud with clasts of sand, dark gray (5Y 4/1); clay, grayish brown (5Y 5/2), and clayey mud, dark gray (N 4/0). Actual sediment forms about 2% of this alleged 4.5 m core. SMEAR SLIDE SUMMARY (%): <table><tr><td></td><td>1, 13 D</td><td>1, 30 D</td><td>2, 7 D</td></tr></table> TEXTURE: <table><tr><td>Sand</td><td>—</td><td>88</td><td>3</td></tr><tr><td>Silt</td><td>18</td><td>10</td><td>20</td></tr><tr><td>Clay</td><td>82</td><td>2</td><td>77</td></tr></table> COMPOSITION: <table><tr><td>Quartz</td><td>10</td><td>83</td><td>15</td></tr><tr><td>Feldspar</td><td>Tr</td><td>5</td><td>2</td></tr><tr><td>Mica</td><td>5</td><td>3</td><td>3</td></tr><tr><td>Clay</td><td>82</td><td>2</td><td>77</td></tr><tr><td>Volcanic glass</td><td>—</td><td>Tr</td><td>—</td></tr><tr><td>Accessory minerals</td><td>—</td><td>1</td><td>—</td></tr><tr><td>Opaque minerals</td><td>3</td><td>2</td><td>3</td></tr><tr><td>Amphiboles</td><td>Tr</td><td>2</td><td>Tr</td></tr><tr><td>Heavy minerals</td><td>Tr</td><td>2</td><td>Tr</td></tr></table>		1, 13 D	1, 30 D	2, 7 D	Sand	—	88	3	Silt	18	10	20	Clay	82	2	77	Quartz	10	83	15	Feldspar	Tr	5	2	Mica	5	3	3	Clay	82	2	77	Volcanic glass	—	Tr	—	Accessory minerals	—	1	—	Opaque minerals	3	2	3	Amphiboles	Tr	2	Tr	Heavy minerals	Tr	2	Tr
		1, 13 D	1, 30 D	2, 7 D																																																														
	Sand	—	88	3																																																														
	Silt	18	10	20																																																														
	Clay	82	2	77																																																														
	Quartz	10	83	15																																																														
	Feldspar	Tr	5	2																																																														
	Mica	5	3	3																																																														
	Clay	82	2	77																																																														
Volcanic glass	—	Tr	—																																																															
Accessory minerals	—	1	—																																																															
Opaque minerals	3	2	3																																																															
Amphiboles	Tr	2	Tr																																																															
Heavy minerals	Tr	2	Tr																																																															
B								1.0				* *																																																						
B																																																																		
B																																																																		
B																																																																		
B																																																																		

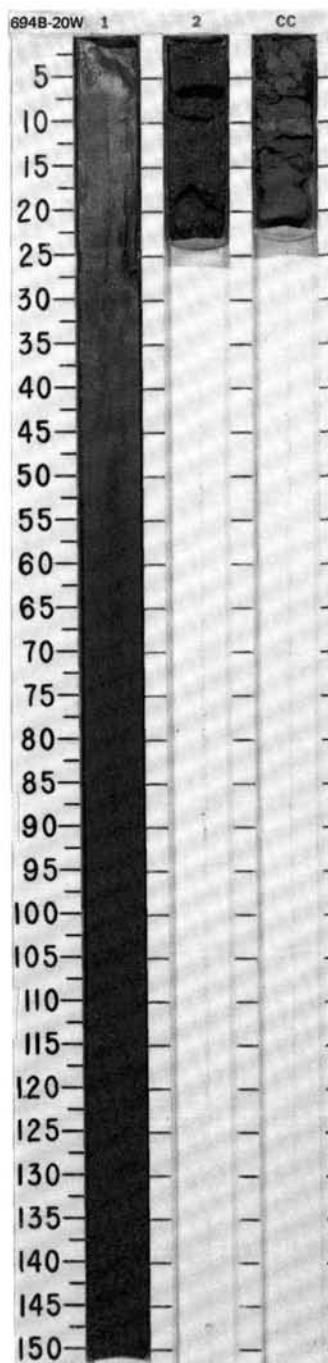
SITE 694 HOLE B CORE 19H CORED INTERVAL 4789.3-4790.3 mbsl; 135.9-136.9 mbsf

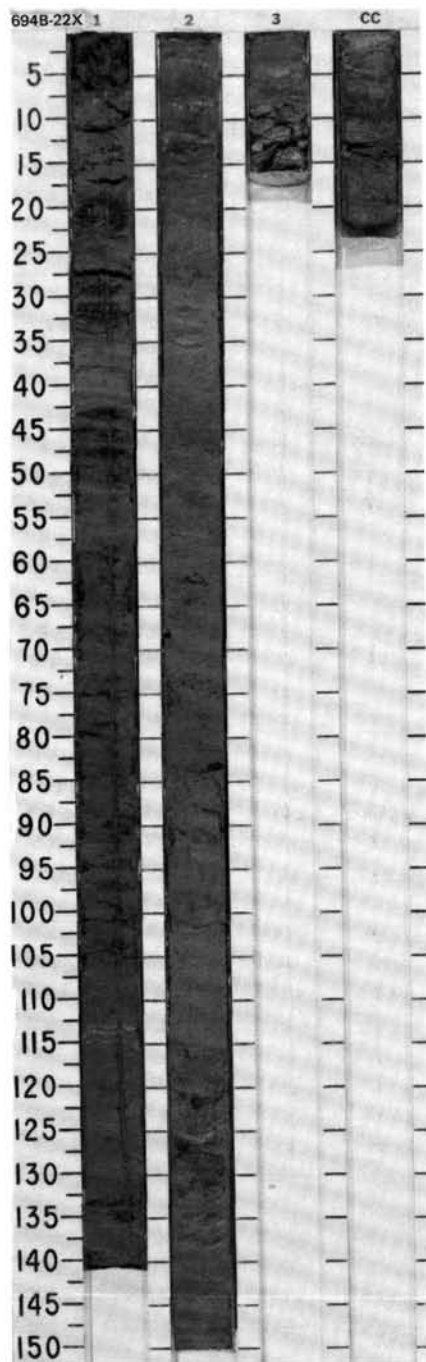
TIME-ROCK UNIT	BIOSTRAT. ZONE/ FOSSIL CHARACTER					PHYS. PROPERTIES	CHEMISTRY	SECTION	METERS	GRAPHIC LITHOLOGY	DRILLING DISTURB. SED. STRUCTURES	SAMPLES	LITHOLOGIC DESCRIPTION
	FORAMINIFERS	NANNOFOSSILS	RADIOLARIANS	DIATOMS	PALYNOMORPHS								
?	B	B	B	B	B	19H 00-30		1				*	CLAY, CLAYEY MUD, and SAND Major lithologies: Clay, dark bluish gray (5B 4/1). Clayey mud, Section 1, 22-30 cm, with sand, dark greenish gray (5G 4/1); probably caused by drilling disturbance, for example by the destruction of a sand or silt bed. SMEAR SLIDE SUMMARY (%): 1, 17 D TEXTURE: Sand 7 Silt 73 Clay 20 COMPOSITION: Quartz 66 Feldspar 10 Rock fragments 1 Clay 20 Volcanic glass Tr Accessory minerals 2 Opaque minerals 1
	B												
	B												

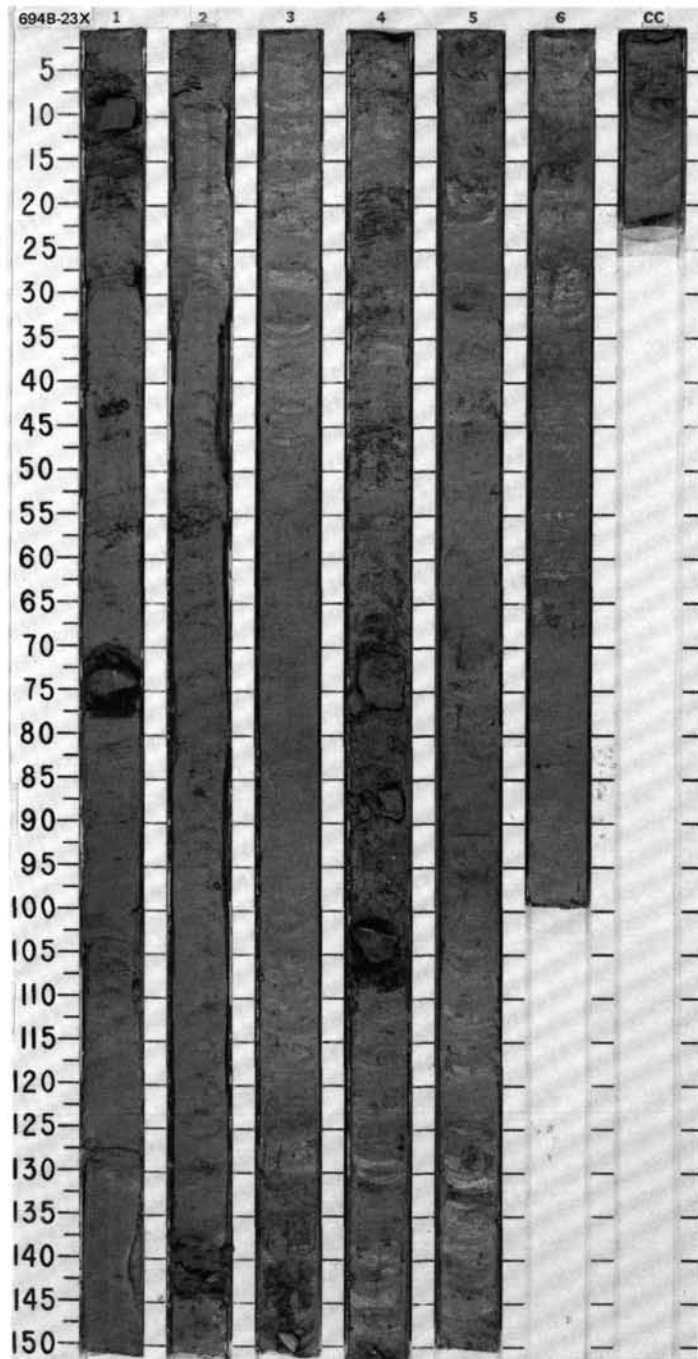


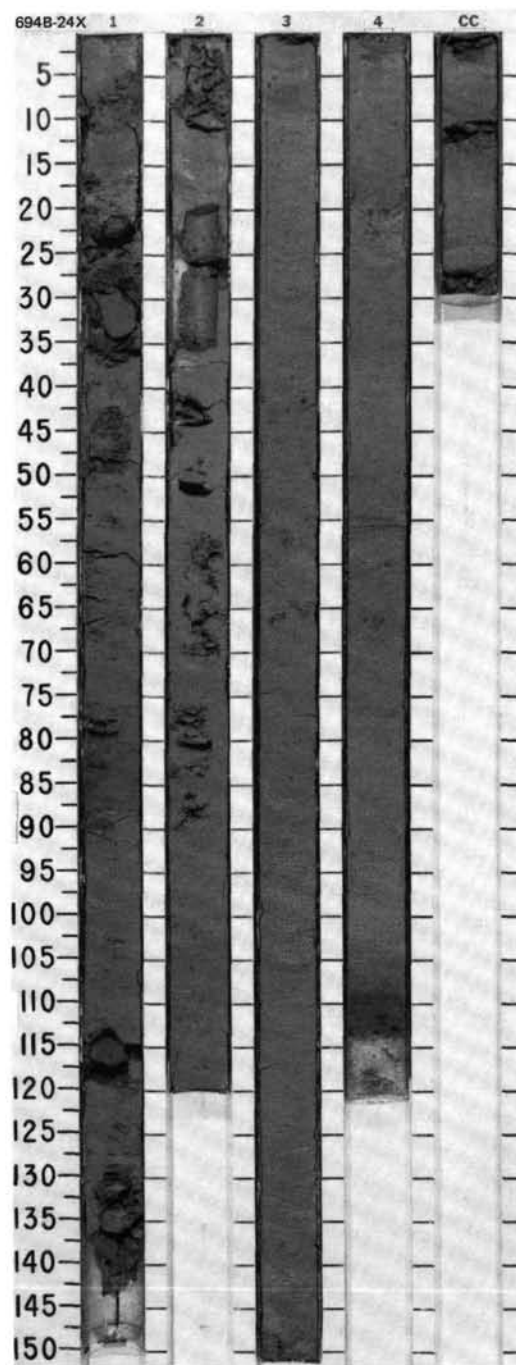
[illegible]

SITE		694		HOLE		B		CORE		21X		CORED INTERVAL		4794.2-4803.8 mbsl; 140.8-150.4 mbsf	
TIME-ROCK UNIT	BIOSTRAT. ZONE/ FOSSIL CHARACTER				PHYS. PROPERTIES	CHEMISTRY	SECTION	METERS	GRAPHIC LITHOLOGY	DRILLING DISTURB.	SED. STRUCTURES	SAMPLES	LITHOLOGIC DESCRIPTION		
	FORAMINIFERS	NANNOFOSSILS	RADIOLARIANS	DIAZONES											
?	B	B	B	R.P.	B								CLAY Major lithology: Clay, dark greenish gray (5BG 4/1), with some admixed sand. Dropstone present but may be downhole contamination. SMEAR SLIDE SUMMARY (%): TEXTURE: Silt Clay COMPOSITION: Quartz Mica Clay Accessory minerals: Opaque minerals Nannofossils CC D 15 85 8 2 85 — Tr *contaminated		



SITE 694

[illegible]

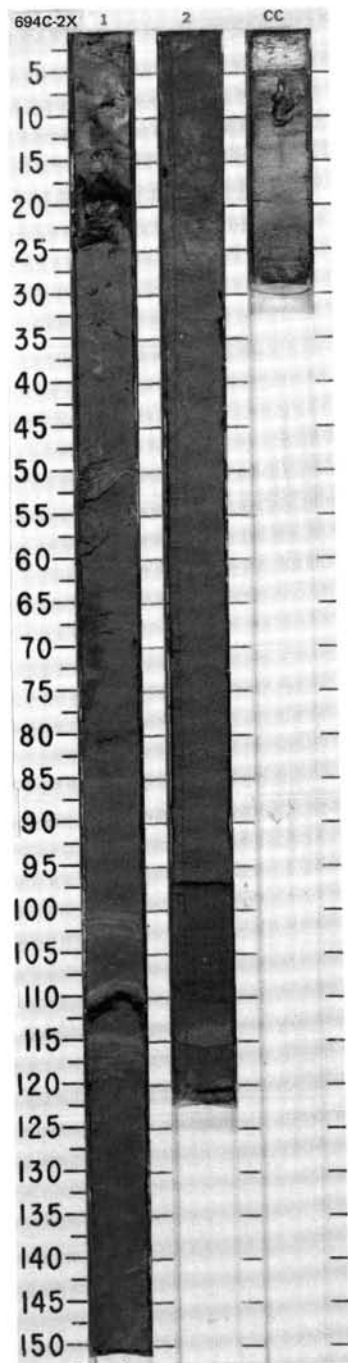
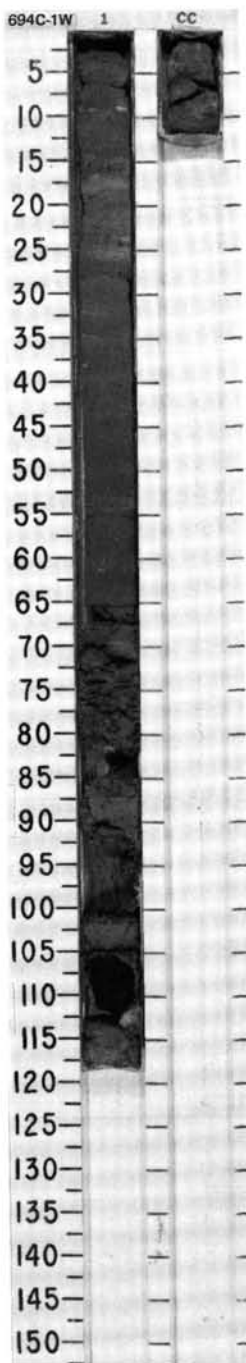
[illegible]

SITE 694 HOLE C CORE 1W CORED INTERVAL 0.0-4832.6 mbsl; 0.0-179.2 mbsf

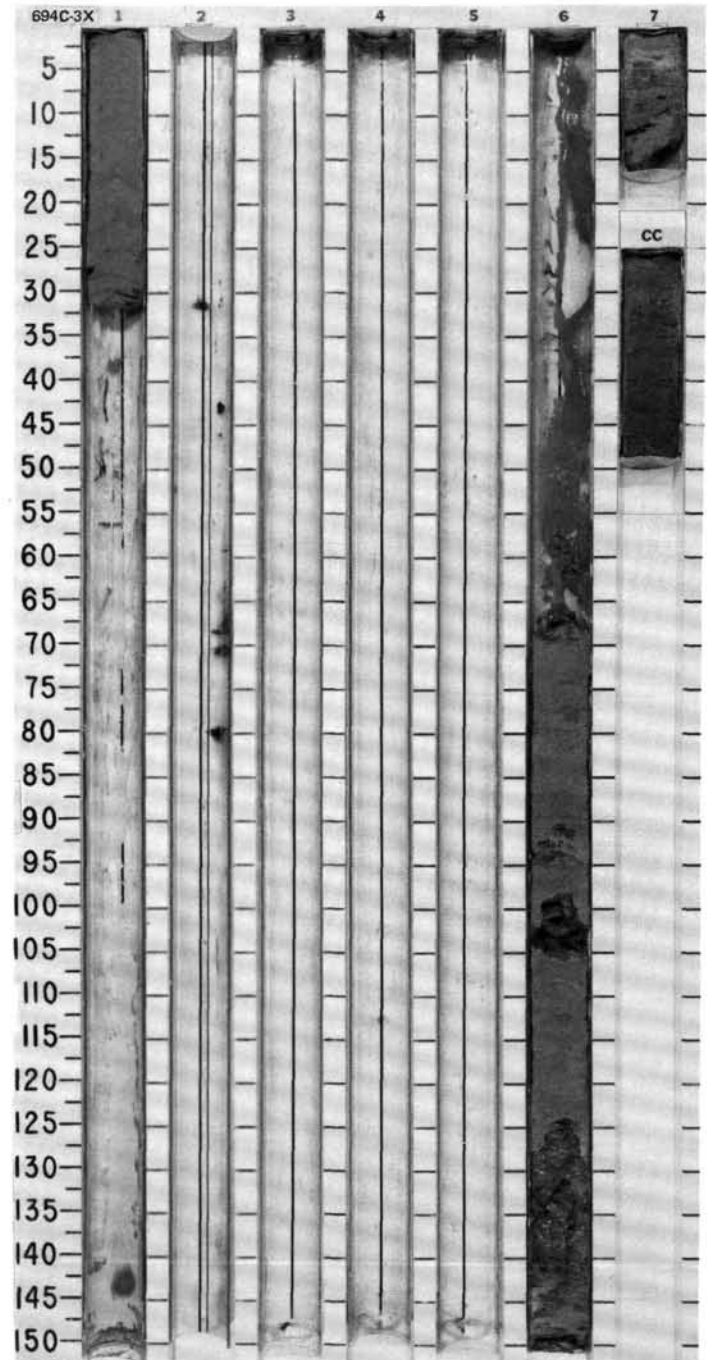
TIME-ROCK UNIT	BIOSTRAT. ZONE/ FOSSIL CHARACTER				PALEOMAGNETICS	PHYS. PROPERTIES CHEMISTRY	SECTION	METERS	GRAPHIC LITHOLOGY	DRILLING DISTURB.	SED. STRUCTURES	SAMPLES	LITHOLOGIC DESCRIPTION
	FORAMINIFERS	NANNOFOSSILS	RADIOLARIANS	DIATOMS									
							1	0.5					WASH CORE
							1.0						Clayey mud and silty mud.
							CC						

SITE 694 HOLE C CORE 2X CORED INTERVAL 4832.6-4842.3 mbsl; 179.2-188.9 mbsf

TIME-ROCK UNIT	BIOSTRAT. ZONE/ FOSSIL CHARACTER						PHYS. PROPERTIES CHEMISTRY	SECTION	METERS	GRAPHIC LITHOLOGY	DRILLING DISTURB.	SED. STRUCTURES	SAMPLES	LITHOLOGIC DESCRIPTION
	FORAMINIFERS	NANNOFOSSILS	RADIOLARIANS	DIAZONES	PALYNOGEOGRAPHY	PALEOMAGNETICS								
UPPER MIOCENE	B	B	R.P	B		V-181 ● V-198 ● V-200 ● V-211		1	0.5 1.0					CLAY, CLAYEY MUD, and SILT
								2				*		Major lithologies: Clay, dark greenish gray (5BG 4/1), minor to moderate bioturbation. Clayey mud, dark gray (N 4/0), moderate bioturbation, scattered sand grains; Section 1, 120 cm, to Section 2, 15 cm. May represent background (non-turbidite) sedimentation. Silt, gray (5Y 5/1), occurs as graded beds, 1-4 cm thick, i.e., bases of turbidites which are dominantly clay. Silt, dark gray (N 4/0), graded bed (coarse to fine silt) in Section 1, 62-80 cm.
								CC				*		Minor lithologies: Sandy mud, grading to silt, dark greenish gray (5GY 4/1), in Section 2, 31-110 cm. Silty mud, gray (N 5/0), graded bed (coarse to fine silt) in CC, 5-22 cm. Base is scoured.
														SMEAR SLIDE SUMMARY (%):
														1, 40 D 1, 50 M 1, 63 M 2, 60 D CC, 18 D
														TEXTURE:
														Sand — — 3 10 40
														Silt 16 95 92 85 50
														Clay 84 5 5 5 10
														COMPOSITION:
														Quartz 5 75 90 82 71
														Feldspar — 5 2 2 3
														Mica 7 5 — 3 1
														Clay 84 5 5 5 10
														Accessory minerals:
														Amphibole — 2 1 2 2
														Glaucanite — Tr Tr — —
														Garnet — — — 3
														Opaque minerals 3 5 2 3 5
														Heavy minerals 1 2 — 3 5
														Diatoms — — 1 —
														Sponge spicules — 1 Tr Tr Tr

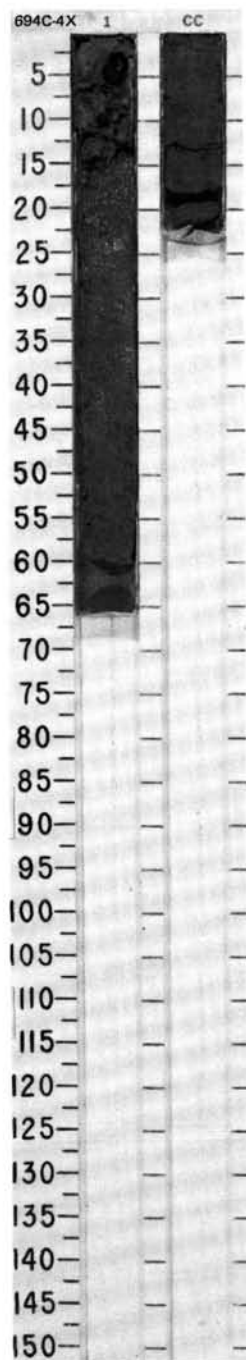


TIME-ROCK UNIT	BIOSTRAT. ZONE/ FOSSIL CHARACTER					PHYS. PROPERTIES	CHEMISTRY	SECTION	METERS	GRAPHIC LITHOLOGY	DRILLING DISTURB.	SED. STRUCTURES	SAMPLES	LITHOLOGIC DESCRIPTION		
	FORAMINIFERS	NANNOFOSSILS	RADIOLARIANS	DIAZONIS	PALYOMORPHS											
UPPER MIOCENE	B					V-1640 7-2.00 0-41 •		1	0.5	VOID			*	SILTY MUD, CLAYEY MUD, and SILT Major lithologies: Silty mud in Section 1, 0-30 cm, greenish gray (5G 5/1), relatively homogeneous with minor bioturbation. Clayey mud, greenish gray (5GY 5/1), in Section 6, 70-100, 107-124, and 140 cm, and in Section 7, 5 and 10-16 cm; moderate bioturbation. Silt, greenish gray (5BG 5/1), in CC and in thin layers in Section 6. Section 6, 76-80 cm, appears slightly coarser and sand clasts are present in Section 6, 140-150 cm. SMEAR SLIDE SUMMARY (%): TEXTURE: COMPOSITION:		
	B						2	1.0	1, 15 D						6, 80 D	7, 8 D
	B						3		Sand 10 Tr 20 Silt 60 45 80 Clay 30 55 —						Quartz 53 37 65 Feldspar — — 2 Rock fragments Tr — 15 Mica — 2 — Clay 30 55 — Volcanic glass 4 5 — Accessory minerals 10 — 8 Amphibole 2 Tr 4 Glauconite Tr — 6 Opaque minerals 1 1 — Diatoms Tr Tr — Sponge spicules — Tr —	
	B						4									
	F.P						5									
							6									
							7									
					CC								*			



SITE 694 HOLE C CORE 4X CORED INTERVAL 4852.0-4861.7 mbsl; 198.6-208.3 mbsf

TIME - ROCK UNIT	BIOSTRAT. ZONE/ FOSSIL CHARACTER				CHEMISTRY	SECTION	METERS	GRAPHIC LITHOLOGY	DRILLING DISTURB.	SED - STRUCTURES	SAMPLES	LITHOLOGIC DESCRIPTION
	FORAMINIFERS	NANNOFOSSILS	RADIOLARIANS	DIATOMS								
UPPER MIOCENE												
	B	B	B	B		1					*	SAND and SANDY MUD
						0.5					*	Major lithologies: Sand, dark greenish gray (5GY 4/1). Sandy mud, gray (2.5Y 5/1), may be part of "drilling turbidite," gets coarser downsection, including CC.
						CC						Minor lithology: Clayey mud in Section 1, 0-13, greenish gray (5B 4/1) and gray (5G 5/1).
												Dropstone in Section 1, 2-5 cm (3 cm long), black manganese-iron coating on igneous plutonic rock, subrounded.
												SMEAR SLIDE SUMMARY (%):
												1, 4
												D
												TEXTURE:
												Sand
												40
												Silt
												60
												Clay
												60
												10
												COMPOSITION:
												Quartz
												19
												Feldspar
												4
												Rock fragments
												—
												15
												Mica
												60
												Clay
												2
												10
												Volcanic glass
												—
												6
												Accessory minerals
												5
												Opaque minerals
												10
												3
												Amphiboles
												—
												1
												Sponge spicules
												Tr
												—



SITE 694 HOLE C CORE 5X CORED INTERVAL 4861.7-4871.3 mbsl; 208.3-217.9 mbsf

TIME-ROCK UNIT	BIOSTRAT. ZONE/ FOSSIL CHARACTER				SECTION METERS	GRAPHIC LITHOLOGY	DRILLING DISTURB. SED. STRUCTURES SAMPLES	LITHOLOGIC DESCRIPTION			
	FORAMINIFERS	NANNOFOSSILS	RADIOLARIANS	DIATOMS							
									PALYNOMORPHS	PHYS. PROPERTIES	CHEMISTRY
UPPER MIOCENE	R.P. A. <i>tanyacantha</i> - mid C. <i>spongothorax</i> Zones F.M-P F.P F.M F.M				1	0.5 1.0					
	B <i>D. hustedtii</i> - ? <i>D. hustedtii/D. lauta</i>				2						
	1.99 2.22 1.92 1.564 0-51 0-50 0-56				CC						
	</										

CLAYEY MUD and SANDY MUD

Major lithologies: Clayey mud, predominantly greenish gray (5G 5/1) in Section 1; dark gray (N 4/1) to dark greenish gray (5G 4/1) in Section 2, 4-20 cm; greenish gray (5G 5/1) in Section 2, 95-145 cm; and dark greenish gray (5G 4/1) to greenish gray (5G 5/1) in CC. Color laminations are present in the CC. There are two 1-cm-thick laminations in Section 2: coarse silt at 11-12 cm, and fine sand at 23-24 cm. Sandy mud, greenish gray (5G 4/1) to dark greenish gray (5GY 4/1) in Section 1, 118 cm, and Section 2, 0-4 cm; and dark greenish gray (5G 4/1) to dark gray (N 4/1) in Section 2, 20-95 cm. The upper interval is graded and the lower interval shows some lamination. Each lamina is approximately 2-mm thick and they are 3-4-cm apart.

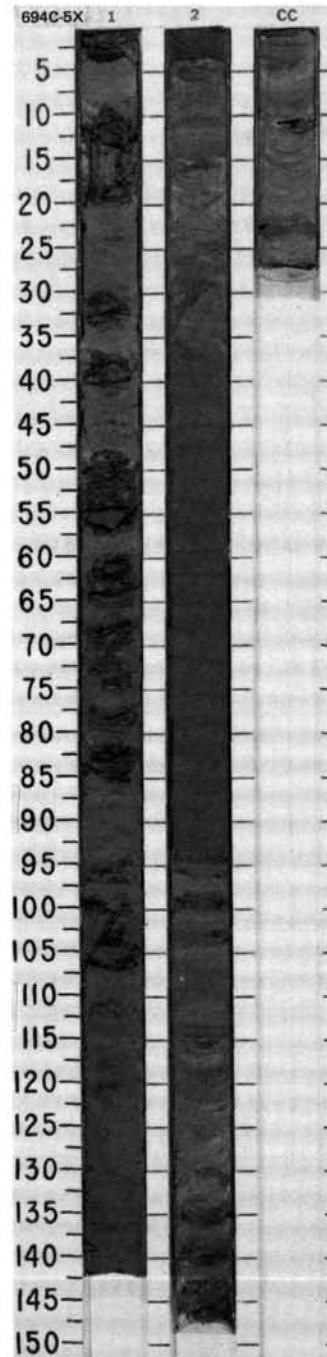
Minor lithologies: Coarse silt and fine sand in CC, 11-12 and 23-24 cm, as very thin beds.

SMEAR SLIDE SUMMARY (%):

	1, 45 D	1, 129 M	2, 63 D	2, 129 D
TEXTURE:				
Sand	—	60	40	Tr
Silt	25	42	30	40
Clay	75	8	30	60

COMPOSITION:

Quartz	10	46	30	20
Feldspar	2	14	2	—
Rock fragments	—	5	20	—
Mica	2	—	2	—
Clay	75	8	30	60
Volcanic glass	—	5	1	—
Accessory minerals	5	4	11	11
Opaque minerals	1	4	3	3
Amphiboles	—	Tr	—	—
Glaucinite	—	5	—	—
Diatoms	5	7	Tr	6
Radiolarians	Tr	Tr	—	Tr
Sponge spicules	—	2	1	Tr



SITE

694

HOLE

C

CORE

6X

CORED INTERVAL

4871.3-4881.0 mbsi

217.9-227.6 mbsi

TIME - ROCK UNIT

FORAMINIFERS

NANNOFOSSILS

RADIOLARIANS

DIAZONES

PALYNOMORPHS

PALEOMAGNETICS

PHYS. PROPERTIES

CHEMISTRY

SECTION

METERS

GRAPHIC LITHOLOGY

DRILLING DISTURB.

SED. STRUCTURES

SAMPLES

BIOSTRAT. ZONE/ FOSSIL CHARACTER

F.P

C.MP

F.M

A.M

F.MP

C.P

B

B

B

V-1738

V-1738

V-1738

V-1738

V-1738

V-1738

V-1738

V-1738

V-1738

V-1738

V-1738

V-1738

V-1738

V-1738

V-1738

V-1738

V-1738

V-1738

V-1738

V-1738

V-1738

V-1738

V-1738

V-1738

V-1738

V-1738

V-1738

V-1738

V-1738

V-1738

V-1738

V-1738

V-1738

V-1738

V-1738

V-1738

V-1738

V-1738

V-1738

V-1738

V-1738

V-1738

V-1738

V-1738

V-1738

V-1738

V-1738

V-1738

V-1738

V-1738

V-1738

V-1738

V-1738

V-1738

V-1738

V-1738

V-1738

V-1738

V-1738

V-1738

V-1738

V-1738

V-1738

V-1738

V-1738

V-1738

V-1738

V-1738

V-1738

V-1738

V-1738

V-1738

V-1738

V-1738

V-1738

V-1738

V-1738

V-1738

V-1738

V-1738

V-1738

V-1738

V-1738

V-1738

V-1738

V-1738

V-1738

V-1738

V-1738

V-1738

V-1738

V-1738

V-1738

V-1738

V-1738

V-1738

V-1738

V-1738

V-1738

V-1738

V-1738

V-1738

V-1738

V-1738

V-1738

V-1738

V-1738

V-1738

V-1738

V-1738

V-1738

V-1738

V-1738

V-1738

V-1738

V-1738

V-1738

V-1738

V-1738

V-1738

V-1738

V-1738

V-1738

V-1738

V-1738

V-1738

V-1738

V-1738

V-1738

V-1738

V-1738

V-1738

V-1738

V-1738

V-1738

V-1738

V-1738

V-1738

V-1738

V-1738

V-1738

V-1738

V-1738

V-1738

V-1738

V-1738

V-1738

V-1738

V-1738

V-1738

V-1738

V-1738

V-1738

V-1738

V-1738

V-1738

V-1738

V-1738

V-1738

V-1738

V-1738

V-1738

V-1738

V-1738

V-1738

V-1738

V-1738

V-1738

V-1738

V-1738

V-1738

V-1738

V-1738

V-1738

V-1738

V-1738

V-1738

V-1738

V-1738

V-1738

V-1738

V-1738

V-1738

V-1738

V-1738

V-1738

V-1738

V-1738

V-1738

V-1738

V-1738

V-1738

V-1738

V-1738

V-1738

V-1738

V-1738

V-1738

V-1738

V-1738

V-1738

V-1738

V-1738

V-1738

V-1738

V-1738

V-1738

V-1738

V-1738

V-1738

V-1738

V-1738

V-1738

V-1738

V-1738

V-1738

V-1738

V-1738

V-1738

V-1738

V-1738

V-1738

V-1738

V-1738

V-1738

V-1738

V-1738

V-1738

V-1738

V-1738

V-1738

V-1738

V-1738

V-1738

V-1738

V-1738

V-1738

V-1738

V-1738

V-1738

V-1738

V-1738

V-1738

V-1738

V-1738

V-1738

V-1738

V-1738

V-1738

V-1738

V-1738

V-1738

V-1738

V-1738

V-1738

V-1738

V-1738

V-1738

V-1738

V-1738

V-1738

V-1738

V-1738

V-1738

V-1738

V-1738

V-1738

V-1738

V-1738

V-1738

V-1738

V-1738

V-1738

V-1738

V-1738

V-1738

V-1738

V-1738

V-1738

V-1738

V-1738

V-1738

V-1738

V-1738

V-1738

V-1738

V-1738

V-1738

V-1738

V-1738

V-1738

V-1738

V-1738

V-1738

V-1738

V-1738

V-1738

V-1738

V-1738

V-1738

V-1738

V-1738

V-1738

V-1738

V-1738

V-1738

V-1738

V-1738

V-1738

V-1738

V-1738

V-1738

V-1738

V-1738

V-1738

V-1738

V-1738

V-1738

V-1738

V-1738

V-1738

V-1738

V-1738

V-1738

V-1738

V-1738

V-1738

V-1738

V-1738

V-1738

V-1738

V-1738

V-1738

V-1738

V-1738

V-1738

V-1738

V-1738

V-1738

V-1738

V-1738

V-1738

V-1738

V-1738

V-1738

V-1738

V-1738

V-1738

V-1738

V-1738

V-1738

V-1738

V-1738

V-1738

V-1738

V-1738

V-1738

V-1738

V-1738

V-1738

V-1738

V-1738

V-1738

V-1738

V-1738

V-1738

V-1738

V-1738

V-1738

V-1738

V-1738

V-1738

V-1738

V-1738

V-1738

V-1738

V-1738

V-1738

V-1738

V-1738

V-1738

V-1738

V-1738

V-1738

V-1738

V-1738

V-1738

V-1738

V-1738

V-1738

V-1738

V-1738

V-1738

V-1738

V-1738

V-1738

V-1738

V-1738

V-1738

V-1738

V-1738

V-1738

V-1738

V-1738

V-1738

V-1738

V-1738

V-1738

V-1738

V-1738

V-1738

V-1738

V-1738

V-1738

V-1738

V-1738

V-1738

V-1738

V-1738

V-1738

V-1738

V-1738

V-1738

V-1738

V-1738

V-1738

V-1738

V-1738

V-1738

V-1738

V-1738

V-1738

V-1738

V-1738

V-1738

V-1738

V-1738

V-1738

V-1738

V-1738

V-1738

V-1738

V-1738

V-1738

V-1738

V-1738

V-1738

V-1738

V-1738

V-1738

V-1738

V-1738

V-1738

V-1738

V-1738

V-1738

V-1738

V-1738

V-1738

V-1738

V-1738

V-1738

V-1738

V-1738

V-1738

V-1738

V-1738

V-1738

V-1738

V-1738

V-1738

V-1738

V-1738

V-1738

V-1738

V-1738

V-1738

V-1738

V-1738

V-1738

V-1738

V-1738

V-1738

V-1738

V-1738

V-1738

V-1738

V-1738

V-1738

V-1738

V-1738

V-1738

V-1738

V-1738

V-1738

V-1738

V-1738

V-1738

V-1738

V-1738

V-1738

V-1738

V-1738

V-1738

V-1738

V-1738

V-1738

V-1738

V-1738

V-1738

V-1738

V-1738

V-1738

V-1738

V-1738

V-1738

V-1738

V-1738

V-1738

V-1738

V-1738

V-1738

V-1738

V-1738

V-1738

V-1738

V-1738

V-1738

V-1738

V-1738

V-1738

V-1738

V-1738

V-1738

V-1738

V-1738

V-1738

V-1738

V-1738

V-1738

V-1738

V-1738

V-1738

V-1738

V-1738

V-1738

V-1738

V-1738

V-1738

V-1738

V-1738

V-1738

V-1738

V-1738

V-1738

V-1738

V-1738

V-1738

V-1738

V-1738

V-1738

V-1738

V-1738

V-1738

V-1738

V-1738

V-1738

V-1738

V-1738

V-1738

V-1738

V-1738

V-1738

V-1738

V-1738

V-1738

V-1738

V-1738

V-1738

V-1738

V-1738

V-1738

V-1738

V-1738

V-1738

V-1738

V-1738

V-1738

V-1738

V-1738

V-1738

V-1738

V-1738

V-1738

V-1738

V-1738

V-1738

V-1738

V-1738

V-1738

V-1738

V-1738

V-1738

V-1738

V-1738

V-1738

V-1738

V-1738

V-1738

V-1738

V-1738

V-1738

V-1738

V-1738

V-1738

V-1738

V-1738

V-1738

V-1738

V-1738

V-1738

V-1738

V-1738

V-1738

V-1738

V-1738

V-1738

V-1738

V-1738

V-1738

V-1738

V-1738

V-1738

V-1738

V-1738

V-1738

V-1738

V-1738

V-1738

V-1738

V-1738

V-1738

V-1738

V-1738

V-1738

V-1738

V-1738

V-1738

V-1738

V-1738

V-1738

V-1738

V-1738

V-1738

V-1738

V-1738

V-1738

V-1738

V-1738

V-1738

V-1738

V-1738

V-1738

V-1738

V-1738

V-1738

V-1738

V-1738

V-1738

V-1738

V-1738

V-1738

V-1738

V-1738

V-1738

V-1738

V-1738

V-1738

V-1738

V-1738

V-1738

V-1738

V-1738

V-1738

V-1738

V-1738

V-1738

V-1738

V-1738

V-1738

V-1738

V-1738

V-1738

V-1738

V-1738

V-1738

V-1738

V-1738

V-1738

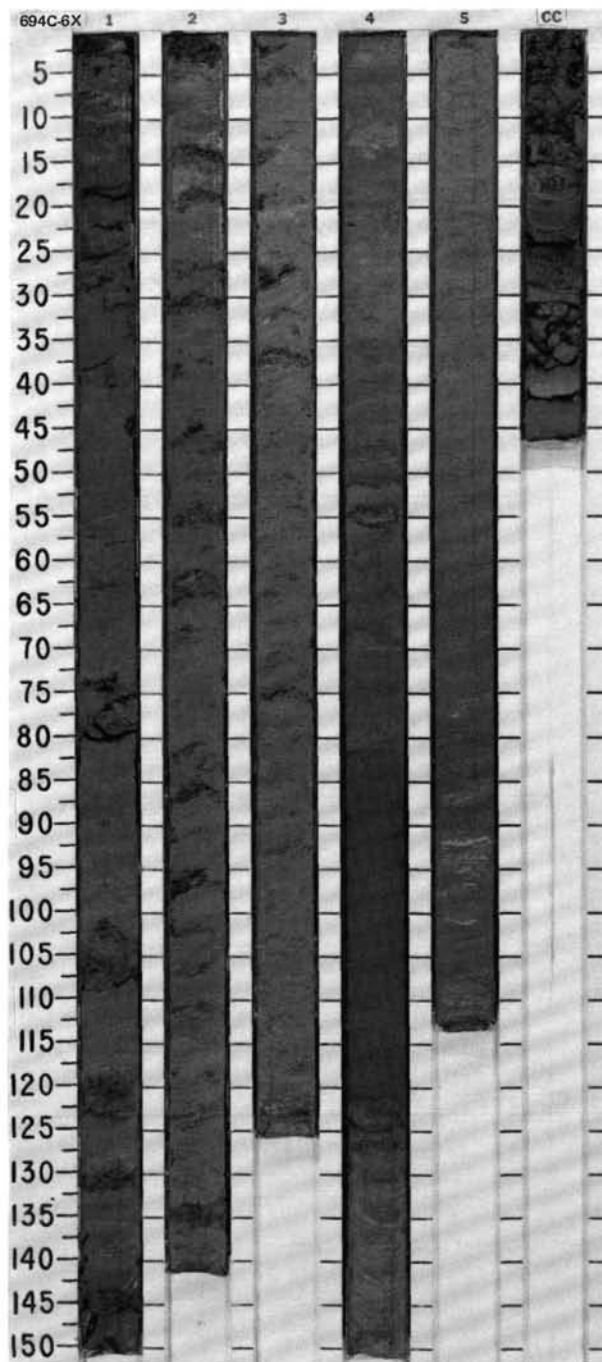
V-1738

V-1738

V-1738

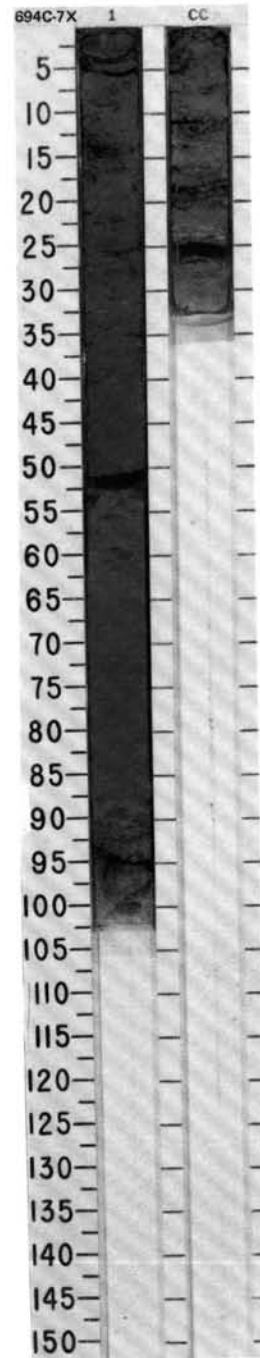
V-1738

V



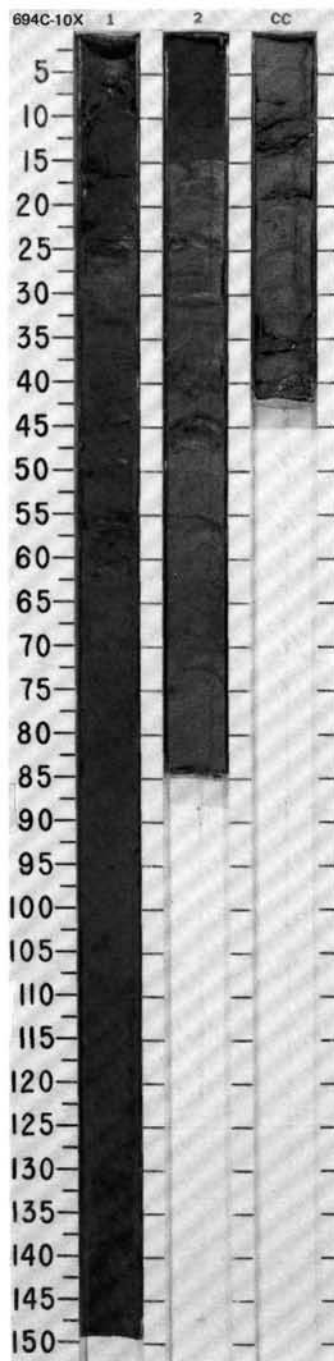
SITE 694 HOLE C CORE 7X CORED INTERVAL 4881.0-4890.3 mbsl; 227.6-236.9 mbsf

TIME-ROCK UNIT	BIOSTRAT. ZONE/ FOSSIL CHARACTER				SECTION	METERS	GRAPHIC LITHOLOGY	DRILLING DISTURB. SED. STRUCTURES	SAMPLES	LITHOLOGIC DESCRIPTION
	FORAMINIFERS	NANNOFOSSILS	RADIOLARIANS	DIATOMS						
UPPER MIOCENE										

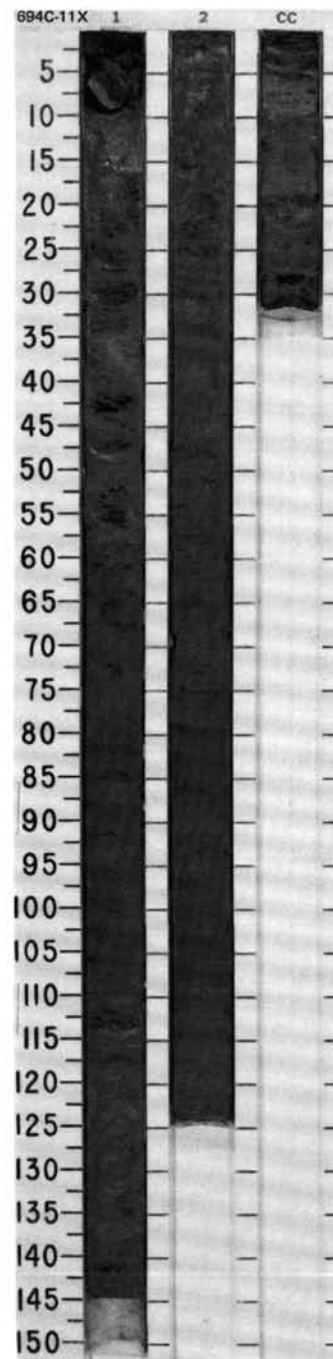


TIME-ROCK UNIT	BIOSTRAT. ZONE/ FOSSIL CHARACTER								SECTION	METERS	GRAPHIC LITHOLOGY	DRILLING DISTURB.	SED. STRUCTURES	SAMPLES	LITHOLOGIC DESCRIPTION																																																					
	FORAMINIFERS	NANNOFOSSILS	RADOLARIANS	DIATOMS	PALYNOMORPHS	PALEOMAGNETICS	PHYS. PROPERTIES	CHEMISTRY																																																												
UPPER MIOCENE	<div><div>E.P.I.B</div><div><i>A. tanyacantha</i> - mid <i>C. spongothorax</i> Zones <i>D. hustedtii</i> / <i>D. lauta</i> - <i>N. denticuloides</i> F.M.P</div><div>B</div></div>								1 0.5 0				* *	<p>CLAY (CLAYSTONE)</p> <p>Major lithology: Clay (claystone), dark gray (N 4/0) and dark greenish gray (5GY 4/1, 5BG 4/1), biscuited; transition from clay to claystone. Minor bioturbation is visible near silty laminae in Section 1, 77-81 cm, and at the top of CC. Claystone in CC is (just) diatom-bearing.</p> <p>Minor lithology: Diatom clayey mud in Section 1, 0-10 cm, dark greenish gray (5GY 4/1) and greenish gray (5G 5/1), occurs in two layers 1-3 cm thick. There are silty laminae in Section 1, 77-81 cm, and at the top of the CC.</p> <p>Three 2-cm dropstones, subrounded, weathered, and Mn-coated, in Section 1, 26-32 cm; one is a fine-grained igneous rock.</p> <p>SMEAR SLIDE SUMMARY (%):</p> <table><tr><td></td><td>1, 6 M</td><td>1, 60 D</td></tr><tr><td colspan="3">TEXTURE:</td></tr><tr><td>Sand</td><td>2</td><td>—</td></tr><tr><td>Silt</td><td>53</td><td>20</td></tr><tr><td>Clay</td><td>45</td><td>80</td></tr><tr><td colspan="3">COMPOSITION:</td></tr><tr><td>Quartz</td><td>13</td><td>8</td></tr><tr><td>Feldspar</td><td>3</td><td>Tr</td></tr><tr><td>Mica</td><td>—</td><td>1</td></tr><tr><td>Clay</td><td>45</td><td>80</td></tr><tr><td>Volcanic glass</td><td>4</td><td>1</td></tr><tr><td colspan="3">Accessory minerals:</td></tr><tr><td>Opaque minerals</td><td>—</td><td>1</td></tr><tr><td>Glaucinite</td><td>1</td><td>1</td></tr><tr><td>Amphibole</td><td>1</td><td>2</td></tr><tr><td>Heavy minerals</td><td>—</td><td>1</td></tr><tr><td>Diatoms</td><td>33</td><td>5</td></tr><tr><td>Sponge spicules</td><td>Tr</td><td>—</td></tr></table>		1, 6 M	1, 60 D	TEXTURE:			Sand	2	—	Silt	53	20	Clay	45	80	COMPOSITION:			Quartz	13	8	Feldspar	3	Tr	Mica	—	1	Clay	45	80	Volcanic glass	4	1	Accessory minerals:			Opaque minerals	—	1	Glaucinite	1	1	Amphibole	1	2	Heavy minerals	—	1	Diatoms	33	5	Sponge spicules	Tr	—
	1, 6 M	1, 60 D																																																																		
TEXTURE:																																																																				
Sand	2	—																																																																		
Silt	53	20																																																																		
Clay	45	80																																																																		
COMPOSITION:																																																																				
Quartz	13	8																																																																		
Feldspar	3	Tr																																																																		
Mica	—	1																																																																		
Clay	45	80																																																																		
Volcanic glass	4	1																																																																		
Accessory minerals:																																																																				
Opaque minerals	—	1																																																																		
Glaucinite	1	1																																																																		
Amphibole	1	2																																																																		
Heavy minerals	—	1																																																																		
Diatoms	33	5																																																																		
Sponge spicules	Tr	—																																																																		



[illegible]

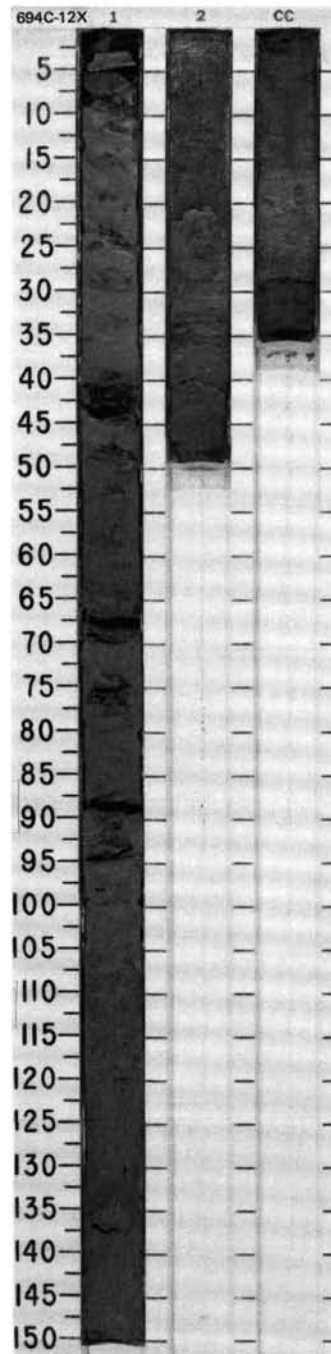
TIME-ROCK UNIT	BIOSTRAT. ZONE/ FOSSIL CHARACTER					PHYS. PROPERTIES	CHEMISTRY	SECTION	METERS	GRAPHIC LITHOLOGY	DRILLING DISTURB.	SED. STRUCTURES	SAMPLES	LITHOLOGIC DESCRIPTION
	FORAMINIFERS	NANNOFOSSILS	RADIOLARIANS	DIATOMS	PALYNOBORPHS									
LOWER UPPER - MIDDLE MIOCENE	B					Y-1.75 0-60		1	0.5 1.0			* * * * *	DIATOM-BEARING SILTY MUD, DIATOM SILTY MUD, and DIATOM-BEARING SANDY MUD Major lithologies: Diatom-bearing silty mud and diatom silty mud, dark gray (N 4/0 to N3 5/0), disturbed by drilling; drilling biscuits throughout, containing streaks and patches of silt and sand; no primary structures preserved. Diatom-bearing sandy mud, dark gray (N 4/0), forms graded bed in Section 2, 74-123 cm. Base is sharp and rests on 2 cm of silt; top is a slurried mass of sand and mud extending up to Section 2, 45 cm (drilling disturbance?); also in Section 1, 9-24 cm, but may not be in place. Minor lithologies: Diatom clayey mud in CC, 0-10 cm, dark gray (N 4/0). Diatom sandy mud in CC, 10-31 cm, dark gray (SY 4/1), graded. Dropstone at top of core, 5 cm, subangular, sandstone.	
	A.P. A. <i>tanyacantha</i> - mid C. <i>spongothorax</i> Zones													
	C.M. D. <i>hustedtii</i> / D. <i>lauta</i> - <i>Nitzschia denticuloides</i> Zone													
	B													
	B					Y-1.75 0-60		2				* * * * *	DIATOM-BEARING SILTY MUD, DIATOM SILTY MUD, and DIATOM-BEARING SANDY MUD Major lithologies: Diatom-bearing silty mud and diatom silty mud, dark gray (N 4/0 to N3 5/0), disturbed by drilling; drilling biscuits throughout, containing streaks and patches of silt and sand; no primary structures preserved. Diatom-bearing sandy mud, dark gray (N 4/0), forms graded bed in Section 2, 74-123 cm. Base is sharp and rests on 2 cm of silt; top is a slurried mass of sand and mud extending up to Section 2, 45 cm (drilling disturbance?); also in Section 1, 9-24 cm, but may not be in place. Minor lithologies: Diatom clayey mud in CC, 0-10 cm, dark gray (N 4/0). Diatom sandy mud in CC, 10-31 cm, dark gray (SY 4/1), graded. Dropstone at top of core, 5 cm, subangular, sandstone.	
A.P. A. <i>tanyacantha</i> - mid C. <i>spongothorax</i> Zones														
C.M. D. <i>hustedtii</i> / D. <i>lauta</i> - <i>Nitzschia denticuloides</i> Zone														
B														
	B					Y-1.75 0-60		CC				* * * * *	DIATOM-BEARING SILTY MUD, DIATOM SILTY MUD, and DIATOM-BEARING SANDY MUD Major lithologies: Diatom-bearing silty mud and diatom silty mud, dark gray (N 4/0 to N3 5/0), disturbed by drilling; drilling biscuits throughout, containing streaks and patches of silt and sand; no primary structures preserved. Diatom-bearing sandy mud, dark gray (N 4/0), forms graded bed in Section 2, 74-123 cm. Base is sharp and rests on 2 cm of silt; top is a slurried mass of sand and mud extending up to Section 2, 45 cm (drilling disturbance?); also in Section 1, 9-24 cm, but may not be in place. Minor lithologies: Diatom clayey mud in CC, 0-10 cm, dark gray (N 4/0). Diatom sandy mud in CC, 10-31 cm, dark gray (SY 4/1), graded. Dropstone at top of core, 5 cm, subangular, sandstone.	
A.P. A. <i>tanyacantha</i> - mid C. <i>spongothorax</i> Zones														
C.M. D. <i>hustedtii</i> / D. <i>lauta</i> - <i>Nitzschia denticuloides</i> Zone														
B														
	B					Y-1.75 0-60						* * * * *	DIATOM-BEARING SILTY MUD, DIATOM SILTY MUD, and DIATOM-BEARING SANDY MUD Major lithologies: Diatom-bearing silty mud and diatom silty mud, dark gray (N 4/0 to N3 5/0), disturbed by drilling; drilling biscuits throughout, containing streaks and patches of silt and sand; no primary structures preserved. Diatom-bearing sandy mud, dark gray (N 4/0), forms graded bed in Section 2, 74-123 cm. Base is sharp and rests on 2 cm of silt; top is a slurried mass of sand and mud extending up to Section 2, 45 cm (drilling disturbance?); also in Section 1, 9-24 cm, but may not be in place. Minor lithologies: Diatom clayey mud in CC, 0-10 cm, dark gray (N 4/0). Diatom sandy mud in CC, 10-31 cm, dark gray (SY 4/1), graded. Dropstone at top of core, 5 cm, subangular, sandstone.	
A.P. A. <i>tanyacantha</i> - mid C. <i>spongothorax</i> Zones														
C.M. D. <i>hustedtii</i> / D. <i>lauta</i> - <i>Nitzschia denticuloides</i> Zone														
B														

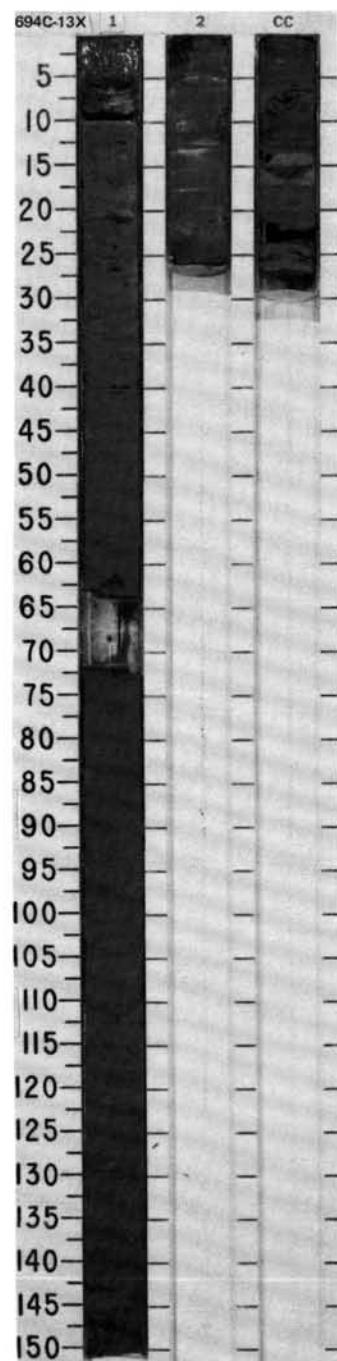


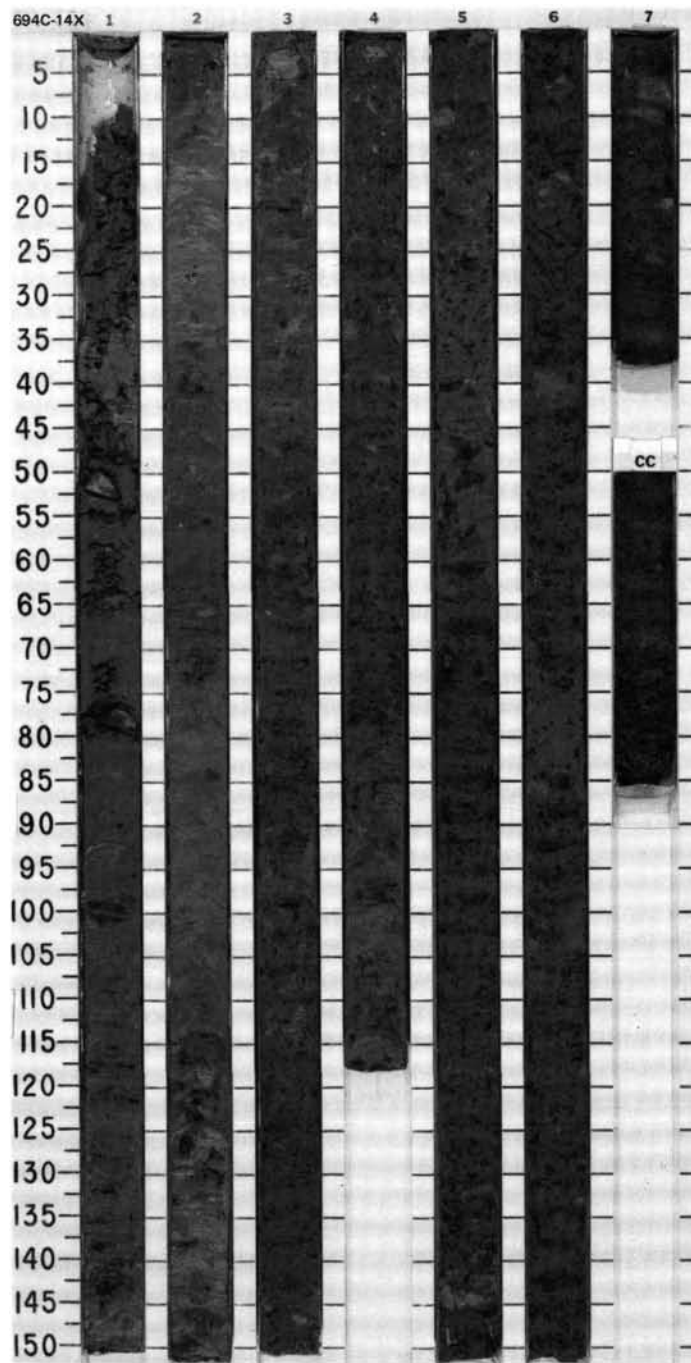
SITE694HOLEC

CORE12XCORED INTERVAL4928.9-4938.5 mbsl; 275.5-285.1 mbsf

TIME - ROCK UNIT	BIOSTRAT. ZONE/ FOSSIL CHARACTER	FORAMINIFERS	NANNOFOSSILS	RADIOLARIANS	DIAZONES	PALYMONOPHOS	PALEOMAGNETICS	PHYS. PROPERTIES	CHEMISTRY	SECTION	METERS	GRAPHIC LITHOLOGY	DRILLING DISTURB.	BED STRUCTURES	SAMPLES	LITHOLOGIC DESCRIPTION	
UPPER LOWER UPPER - MIDDLE MIOCENE		B		R.P		F.M.P	B			1	0.5 1.0		/	*		DIATOM-BEARING SILTY MUD and SANDY MUD Major lithologies: Diatom-bearing silty mud, dark greenish gray (5G 4/1), biscuited, local minor bioturbation. Section 1, around 60 cm, possible water escape structures. Color laminated interval, black (5Y2 5/1), in Section 2, 32-35 cm. Sandy mud, dark greenish gray (5GY 4/1), in graded bed from Section 1, 108 cm, to Section 2, 20 cm. Minor lithologies: Silt, dark greenish gray (5GY 4/1), in graded bed in Section 1, 60-70 cm. Silt clasts and streaks above may result from water escape or bioturbation. Silty mud, greenish gray (5GY 5/1), in graded bed at base of Section 2, 38-49 cm. Silty mud and sandy mud, dark gray (N 4/0), very dark gray (N 3/0) and dark greenish gray (5GY 4/1); interbedded in CC. Thought to represent an interval of sand much thicker than 35 cm, but this is all that was recovered. Dropstone at top of core, 6 cm, angular, laminated siltstone.	
						<i>D. hustedtii / D. lauta - N. denticulooides</i>	B			2				*			
										CC					*		
																	SMEAR SLIDE SUMMARY (%):
																1, 35 1, 120 CC, 32 D D M TEXTURE: Sand 3 70 25 Silt 59 20 50 Clay 38 10 25 COMPOSITION: Quartz 45 72 65 Feldspar — — 2 Mica 1 1 — Clay 38 10 25 Accessory minerals: Amphibole 2 2 1 Glauconite Tr — — Garnet — 3 2 Opaque minerals 2 2 3 Heavy minerals 1 2 2 Diatoms 10 7 — Radiolarians Tr Tr — Sponge spicules 1 1 —	



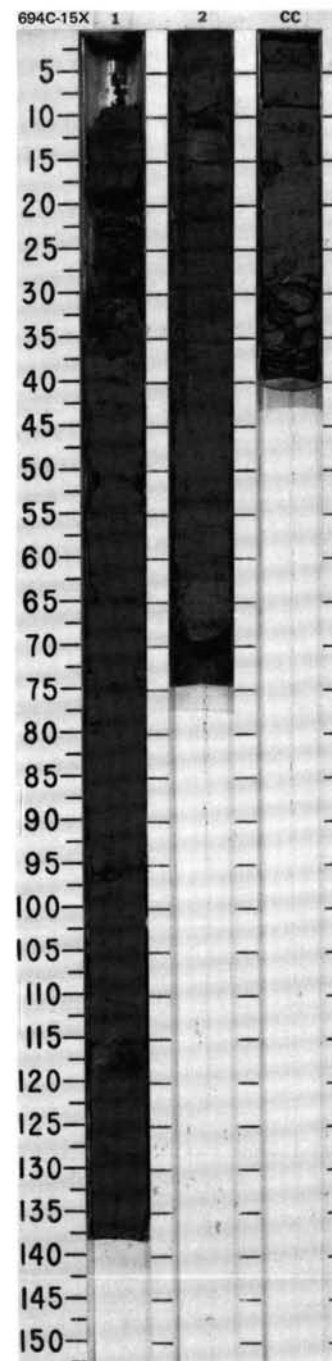
SITE 694

[illegible]

SITE 694 HOLE C CORE 15X CORED INTERVAL 4957.7-4967.4 mbsl; 304.3-314.0 mbsf

TIME-ROCK UNIT	BIOSTRAT. ZONE/ FOSSIL CHARACTER				PHYS. PROPERTIES	CHEMISTRY	SECTION	METERS	GRAPHIC LITHOLOGY	DRILLING DISTURB.	SED. STRUCTURES	SAMPLES	LITHOLOGIC DESCRIPTION																																																																																																						
	FORAMINIFERS	NAUPOSSIDS	RADIOLARIANS	DIAZONES																																																																																																															
UPPER MIDDLE MIOCENE	B. A. <i>tanyacantha</i> range				V-1712 V-192 V-50		1	0.5 1.0					DIATOM SILTY MUD and SILTY MUD Major lithologies: Diatom silty mud, dark greenish gray (5G 4/1), homogeneous sediment moderately to slightly disturbed by drilling. Silty mud in Section 2, different grays (5Y 5/1, 6/1) alternating on a scale of 5-15 cm, slightly disturbed by drilling; weak parallel bedding at Section 2, 65 cm. Sharp contact to underlying silty mud at Section 2, 66 cm. Sediment also occurs in CC as greenish gray (5G 5/1). Moderately fractured, with a dark gray (N 4/0) 3-cm-thick layer at the base. Minor lithology: Diatom-bearing sandy mud in Section 1, 65-95 cm, dark greenish gray (5G 4/1) turbidite layer. Silty mud, gray (5Y 6/1), 6-cm-thick layer at base of Section 2. SMEAR SLIDE SUMMARY (%): TEXTURE: <table><tr><td></td><td>1, 62 D</td><td>1, 90 M</td><td>2, 12 M</td><td>2, 64 M</td><td>CC, 14 M</td></tr><tr><td>Sand</td><td>2</td><td>45</td><td>Tr</td><td>2</td><td>—</td></tr><tr><td>Silt</td><td>64</td><td>35</td><td>90</td><td>68</td><td>80</td></tr><tr><td>Clay</td><td>34</td><td>20</td><td>10</td><td>30</td><td>20</td></tr></table> COMPOSITION: <table><tr><td>Quartz</td><td>17</td><td>45</td><td>70</td><td>47</td><td>36</td></tr><tr><td>Feldspar</td><td>—</td><td>5</td><td>—</td><td>4</td><td>—</td></tr><tr><td>Rock fragments</td><td>—</td><td>3</td><td>—</td><td>—</td><td>—</td></tr><tr><td>Mica</td><td>4</td><td>—</td><td>—</td><td>—</td><td>—</td></tr><tr><td>Clay</td><td>34</td><td>20</td><td>10</td><td>30</td><td>20</td></tr><tr><td>Volcanic glass</td><td>—</td><td>3</td><td>—</td><td>—</td><td>2</td></tr><tr><td>Accessory minerals</td><td>8</td><td>3</td><td>12</td><td>15</td><td>4</td></tr><tr><td>Opaque minerals</td><td>2</td><td>3</td><td>4</td><td>2</td><td>2</td></tr><tr><td>Amphiboles</td><td>—</td><td>1</td><td>—</td><td>2</td><td>—</td></tr><tr><td>Diatoms</td><td>35</td><td>15</td><td>4</td><td>Tr</td><td>35</td></tr><tr><td>Radiolarians</td><td>Tr</td><td>—</td><td>Tr</td><td>—</td><td>Tr</td></tr><tr><td>Sponge spicules</td><td>—</td><td>2</td><td>—</td><td>—</td><td>—</td></tr><tr><td>Silicoflagellates</td><td>—</td><td>—</td><td>—</td><td>—</td><td>1</td></tr></table>		1, 62 D	1, 90 M	2, 12 M	2, 64 M	CC, 14 M	Sand	2	45	Tr	2	—	Silt	64	35	90	68	80	Clay	34	20	10	30	20	Quartz	17	45	70	47	36	Feldspar	—	5	—	4	—	Rock fragments	—	3	—	—	—	Mica	4	—	—	—	—	Clay	34	20	10	30	20	Volcanic glass	—	3	—	—	2	Accessory minerals	8	3	12	15	4	Opaque minerals	2	3	4	2	2	Amphiboles	—	1	—	2	—	Diatoms	35	15	4	Tr	35	Radiolarians	Tr	—	Tr	—	Tr	Sponge spicules	—	2	—	—	—	Silicoflagellates	—	—	—	—	1
		1, 62 D	1, 90 M	2, 12 M										2, 64 M	CC, 14 M																																																																																																				
	Sand	2	45	Tr										2	—																																																																																																				
	Silt	64	35	90										68	80																																																																																																				
Clay	34	20	10	30	20																																																																																																														
Quartz	17	45	70	47	36																																																																																																														
Feldspar	—	5	—	4	—																																																																																																														
Rock fragments	—	3	—	—	—																																																																																																														
Mica	4	—	—	—	—																																																																																																														
Clay	34	20	10	30	20																																																																																																														
Volcanic glass	—	3	—	—	2																																																																																																														
Accessory minerals	8	3	12	15	4																																																																																																														
Opaque minerals	2	3	4	2	2																																																																																																														
Amphiboles	—	1	—	2	—																																																																																																														
Diatoms	35	15	4	Tr	35																																																																																																														
Radiolarians	Tr	—	Tr	—	Tr																																																																																																														
Sponge spicules	—	2	—	—	—																																																																																																														
Silicoflagellates	—	—	—	—	1																																																																																																														
	F.P.P.						2																																																																																																												
	<i>D. hustedtii</i> / <i>D. lauta</i> - <i>N. denticuloides</i> C.P.						CC																																																																																																												
	B																																																																																																																		

CORE 113-694C-16X NO RECOVERY

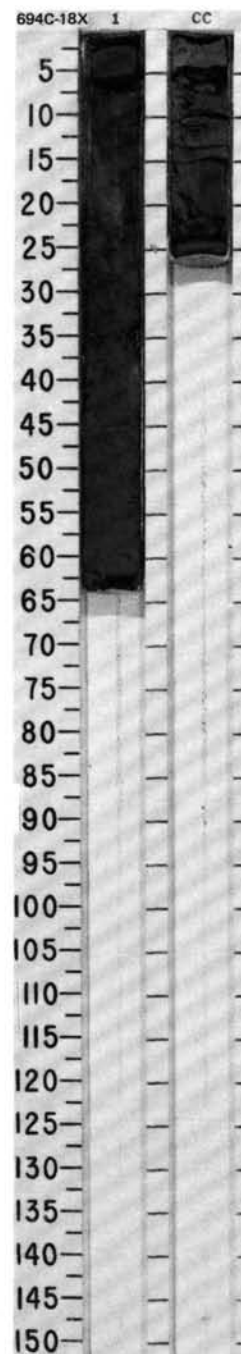
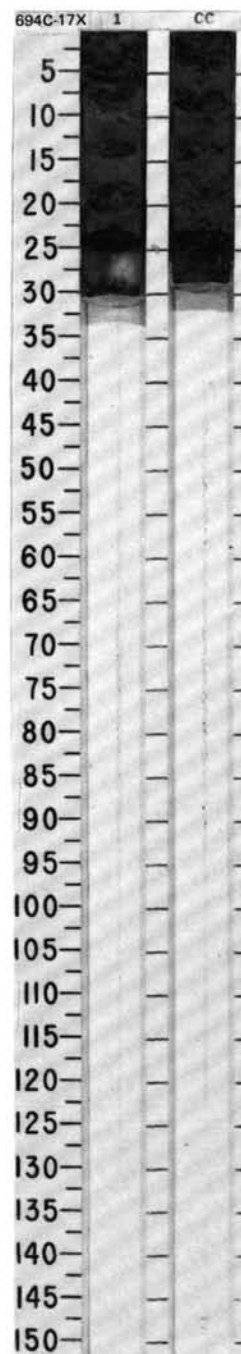


SITE 694 HOLE C CORE 17X CORED INTERVAL 4977.0-4986.7 mbsl; 323.6-333.3 mbsf

TIME-ROCK UNIT	BIOSTRAT. ZONE/ FOSSIL CHARACTER	PHYS. PROPERTIES	CHEMISTRY	SECTION	METERS	GRAPHIC LITHOLOGY	DRILLING DISTURB.	SED. STRUCTURES	SAMPLES	LITHOLOGIC DESCRIPTION
	FORAMINIFERS B	PALEOMAGNETICS V-1.86 0-5.4		1					*	DIATOM CLAYEY MUD
	NAUPOSSILLS B			CC	0.5					Major lithology: Diatom clayey mud, dark bluish gray (5B 4/1), firm sediment, partly biscuitized by drilling.
	RADIOLARIANS B									SMEAR SLIDE SUMMARY (%):
	DIATOMS B F.M.P									1, 11 D
	PALYNOMORPHS B									TEXTURE:
										Silt 45 Clay 55
										COMPOSITION:
										Quartz 4 Mica 2 Clay 55 Accessory minerals 2 Opaque minerals 2 Diatoms 35 Radiolarians Tr

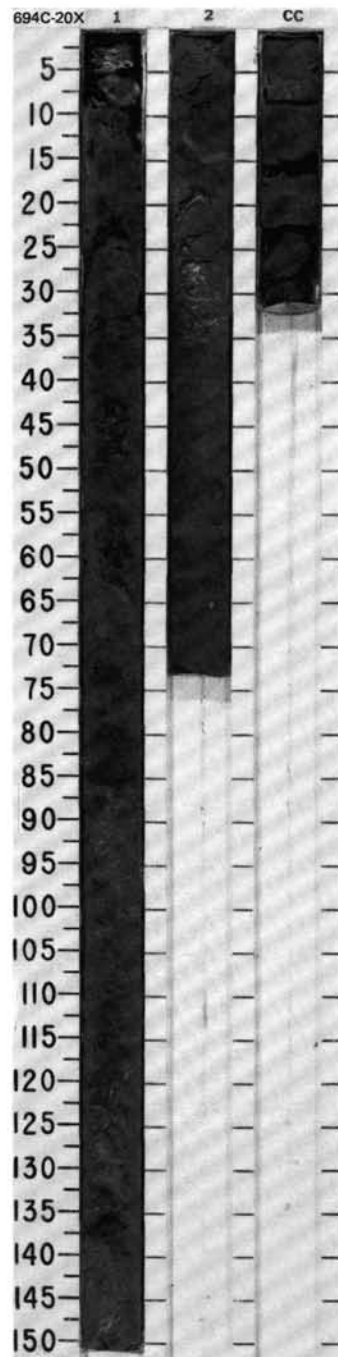
SITE 694 HOLE C CORE 18X CORED INTERVAL 4986.7-4996.4 mbsl; 333.3-343.0 mbsf

TIME-ROCK UNIT	BIOSTRAT. ZONE/ FOSSIL CHARACTER	PHYS. PROPERTIES	CHEMISTRY	SECTION	METERS	GRAPHIC LITHOLOGY	DRILLING DISTURB.	SED. STRUCTURES	SAMPLES	LITHOLOGIC DESCRIPTION
? MIDDLE MIOCENE	FORAMINIFERS B	V-1.39 0-6.0		1					***	DIATOM CLAYEY MUD, DIATOM-BEARING SILTY MUD, and MUDDY DIATOM OOOZE/DIATOMITE
	NAUPOSSILLS R.P			CC	0.5				*	
	RADIOLARIANS C.M.P									
	DIATOMS B									
	PALYNOMORPHS B									Major lithologies: Diatom clayey mud, dark greenish gray (5GY 4/1), laminated, in Section 1, 9-21 cm. Diatom-bearing silty mud, dark gray (5Y 4/1), massive; becomes dark gray (N 4/0) and more silty below Section 1, 35 cm. Muddy diatom ooze/diatomite, dark greenish gray (5GY 4/1), in base of Section 1 and CC; finely laminated. Laminar at base are dark gray (N 4/0) and clayey, without diatoms. Tiny normal faults cut the lamination in the CC, 19 cm.
										Dropstone, ~ 7 cm, dolomite sandstone, at top of core. Drilling has carved enough sand off of it to form a loose sand bed 2 cm thick.
										SMEAR SLIDE SUMMARY (%):
										1, 14 1, 25 1, 38 CC, 10 D D D D
										TEXTURE:
										Sand — — 25 — Silt 59 70 60 — Clay 41 30 15 —
										COMPOSITION:
										Quartz 10 33 42 15 Feldspar Tr 5 3 — Mica 2 1 1 2 Clay 41 30 15 24
										Accessory minerals:
										Heavy minerals 1 2 2 1 Opaque minerals 2 2 3 1 Hornblende — 2 2 1 Garnet Tr — 2 —
										Diatoms 40 20 25 50 Radiolarians 1 2 2 3 Sponge spicules 3 3 3 3 Silicoflagellates Tr — — —

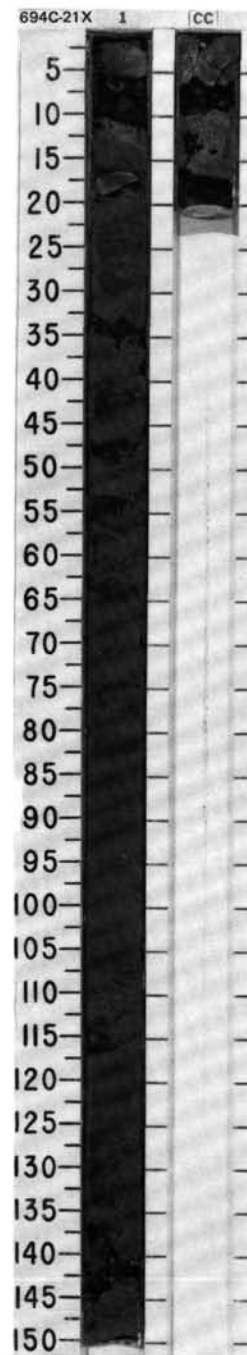


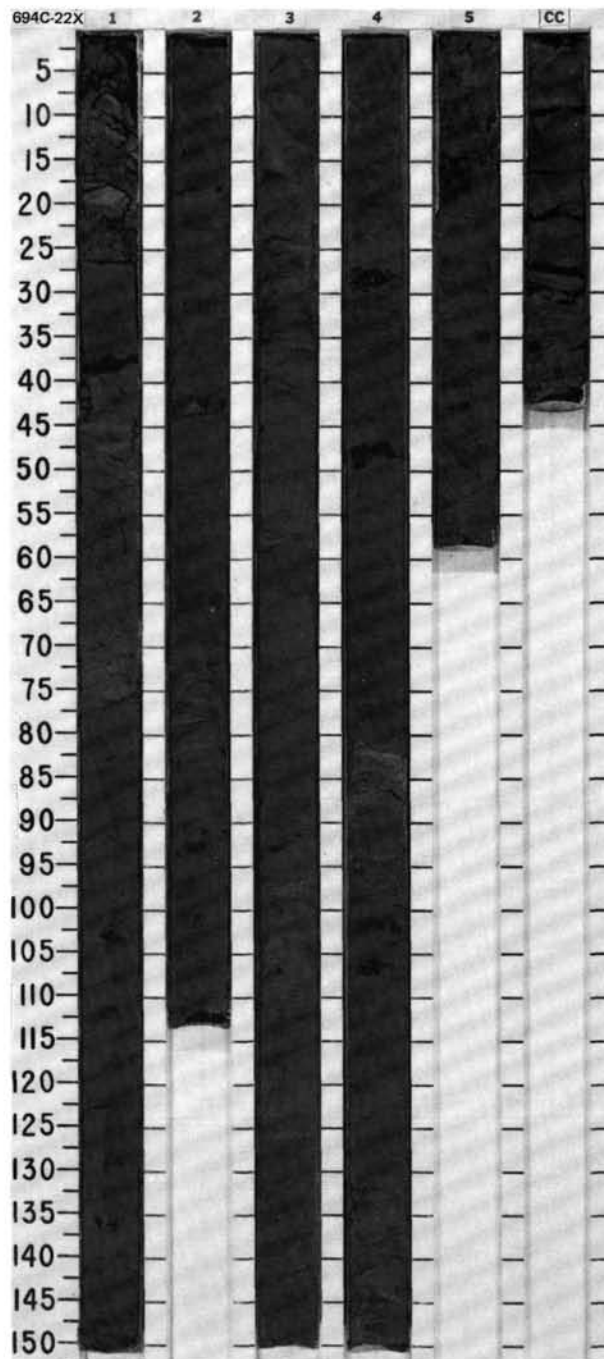


TIME-ROCK UNIT	BIOSTRAT. ZONE/ FOSSIL CHARACTER							SECTION	METERS	GRAPHIC LITHOLOGY	DRILLING DISTURB.	SED. STRUCTURES	SAMPLES	LITHOLOGIC DESCRIPTION
	FORAMINIFERS	NANNOFOSSILS	RADIOLARIANS	DIAZONIS	PALYNOMORPHS	PALEOMAGNETICS	PHYS. PROPERTIES							
? MIDDLE MIOCENE	B							1				*	DIATOM-BEARING CLAYEY MUDSTONE AND CLAYSTONE	
	B													
	F.M.P													
	B													
							2				*	Major lithologies: Diatom-bearing clayey mudstone and claystone, black (5Y 2.5/1), severely biscuitized. Laminations in some biscuits. In Section 1, 100-130 cm, laminations are tilted to high angles. These are more likely to be drilling deformation than a slump. Some biscuits are coarser-grained (e.g., Section 1, 80 cm, is sandy mud). Scattered sand grains in Section 2, 30-73 cm. Minor lithologies: Diatom-bearing silty mudstone, dark greenish gray (5GY 4/1); occurs as thin laminae and deformed patches in Section 2, 40-50 cm. Diatom-bearing silty mudstone, very dark gray (5Y 3/1), laminated; occurs in the CC, 12-31 cm. Sandy mud in Section 1, 80-85 cm, black (5Y 2.5/1), in biscuitized area.		
							CC				*	SMEAR SLIDE SUMMARY (%): TEXTURE: Sand — 57 — 5 — 5 Silt 39 40 12 75 28 65 Clay 61 3 88 20 72 30 COMPOSITION: Quartz 7 72 5 45 7 38 Feldspar 2 5 — 5 — 5 Mica 2 1 — 3 2 Tr Clay 61 3 88 20 72 30 Accessory minerals: Amphibole 1 7 — 1 Tr 5 Glauconite Tr Tr — — — — Garnet 1 3 — 1 — 2 Opaque minerals 3 3 1 2 2 5 Heavy minerals 2 3 — 1 — — Zeolites — — — — — — Diatoms 20 — 5 20 15 15 Radiolarians — — — — — — Sponge spicules 1 3 — 2 1 — Silicoflagellates — — — — Tr —		



TIME-ROCK UNIT	BIOSTRAT. ZONE/ FOSSIL CHARACTER				PALEOMAGNETICS	PHYS. PROPERTIES	CHEMISTRY	SECTION	METERS	GRAPHIC LITHOLOGY	DRILLING DISTURB.	SED. STRUCTURES	SAMPLES	LITHOLOGIC DESCRIPTION
	FORAMINIFERS	NANNOFOSSILS	RADIOLARIANS	DIATOMS										
? MIDDLE MIOCENE		B	R.P											DIATOM-BEARING CLAYEY MUDSTONE Major lithology: Diatom-bearing clayey mudstone, very dark gray (5Y 3/1), biscuited. Lamination in the form of a few lighter layers 2-10-mm thick, not graded. No other structures. Minor lithology: Diatom clayey mudstone, dark gray (N 4/0); two 3-mm laminae in Section 1, 110 cm, contain a few sand grains. These laminae are folded at the side of the core. SMEAR SLIDE SUMMARY (%): TEXTURE: Sand — 5 Silt 45 51 Clay 55 44 COMPOSITION: Quartz 10 15 Mica 2 3 Clay 55 44 Accessory minerals: Amphibole Tr 1 Garnet — Tr Opaque minerals 3 3 Heavy minerals 3 2 Diatoms 25 30 Sponge spicules 2 2
		B	<i>N. grossepunctata</i>	C.PM		γ = 1.96 δ = 5.5								



[illegible]

[illegible]